Delineating a requirement for Survival of Motor Neuron (SMN) protein in skeletal muscle tissue

Michelle R. Faleiro

DOCTORAL THESIS / 2017

THESIS DIRECTORS:

Dr. Umrao Monani (Department of Pathology and Cell Biology, Columbia University Medical Center)

Dr. Juan Valcarcel (Department of Gene Regulation, Stem Cells and Cancer, Centre for Genomic Regulation)

DEPARTAMENT OF EXPERIMENTAL AND HEALTH SCIENCES

Universitat Pompeu Fabra Barcelona

Declaration

I hereby declare that this Ph.D. thesis entitled "Delineating a requirement for Survival of Motor Neuron (SMN) protein in skeletal muscle tissue" was carried out by me for the degree of Doctor of Philosophy in Biomedicine under the guidance and supervision of Dr. Umrao Monani, Department of Pathology and Cell Biology, Columbia University Medical Center. The interpretations put forth are based on my reading and understanding of the original texts and they are not published anywhere in the form of books, monographs or articles. The other books, articles and websites, which I have made use of are acknowledged at the respective place in the text. For the present thesis, which I am submitting to the University Pompeu Fabra, no degree or diploma or distinction has been conferred on me before, either in this or in any other University.

Place: New York
Date: January 4th, 2017
Signed by: Michelle Faleiro

Dedication

To Francis for his unending love and support.

To our loving daughter Kennedy Reis.

To the memory of my grandmother Juliette, my very first teacher,
and an incredibly smart woman whom I still miss every day.

Acknowledgements

I would like to express my sincere graditude to my advisor Dr. Umrao Monani for the continuous support of my Ph.D study and related research, for his patience, motivation, and knowledge. His guidance helped me in all the time of research and writing of this thesis. I would also like to thank my co-director Dr. Juan Valcarcel, and my committee members, Dr. Francisco Real, Dr. Eduardo Tizzano, and Dr. Adrian Krainer for serving as my committee members even at hardship. I would especially like to the members of the Monani Lab at Columbia University Medical Center for their support and mentorship during my research.

A special thanks to my parents. For their love and support, and always teaching me the importance of education. I would not have been able to get to this stage without them. Words cannot express how grateful I am to my mother-in law and father-in-law for all of the sacrifices that they have made on my behalf. I would also like to thank all of my friends who supported me and incented me to strive towards my goal. At the end I would like express appreciation to my amazing husband Francis who spent sleepless nights with and was always my support in the moments when there was no one to answer my queries.

Abstract

Spinal Muscular Atrophy (SMA) is an autosomal recessive neuromuscular disorder characterized by the degeneration of the lower motor neurons. It is caused by homozygous loss or mutations in the Survival Motor Neuron 1 (*SMN1*) gene, leading to a reduction of the amount of Survival Motor Neuron (SMN) protein. In human patients, an almost identical copy gene, *SMN2*, is unable to fully compensate for the lack of *SMN1*, due to a C to T transition in exon 7. Despite progress in the field, the cellular site of action of the SMN protein remains incomplete. Fully defining it is critical for clinical treatments and to enhance our understading of the basic biology of the disease. These questions have been addressed in large part through the study of SMA model organisms. These studies have shown that SMN is particularly important in motor neurons; additional experiments have explored various other tissues which may also be particularly sensitive to SMN, including skeletal muscle. Still, the role of muscle in SMA continues to be debated and the precise function of SMN in this tissue as it pertains to the pathology of the disease remain far from clear. This is partly because *in vivo* experiments performed to date cannot rule out the possibility that changes observed in muscle are simply occurring as a secondary effect of denervation due to pathology in the innervating motor neurons. As therapies for SMA evolve, these remain important questions to address. Accordingly, the goal of this research project has been to more precisely delineate the contributing role of muscle in the overall pathology/phenotype characteristic of SMA. Our results show that wild-type levels of SMN in muscle are absolutely critical to the maintenance of healthy muscle. Thus we believe that SMN functions cell-autonomously within this tissue to ensure its health and viability. Restoring protein to muscle is therefore expected to constitute a vital aspect of treating SMA in SMN repletion-type therapies.

Table of contents

List of Tables and Figures

Abbreviations

ACh	Acetylcholine
AChR	Acetylcholine receptor
ASO	Antisense oligonucleotide
ChAT	Choline Acetyl Transferase
CTX	Cardiotoxin
DNA	Deoxyribonucleic Acid
EBD	Evans Blue Dye
EDL	Extensor Digitorum Longus
FL-SMN	Full-length Survival Motor Neuron
H&E	Hematoxylin and Eosin
HDAC	Histone deacetylase
MN	Motor neuron
MND	Motor Neuron Disease
MO	Morpholino
MyHC	Myosin Heavy Chain
NMJ	Neuromuscular Junction
PBS	Phosphate buffered saline
PCR	Polymerase chain reaction
PND	Post-natal day
RNA	Ribonucleic acid
SMA	Spinal Muscular Atrophy
SMN	Survival Motor Neuron
SMNΔ7	SMN with exon 7 deletion
snRNA	Small nuclear RNA
snRNP	Small nuclear ribonucleoprotein
WT	Wild-type

Chapter 1

Introduction

1.1 Autosomal recessive spinal muscular atrophy

Motor neuron disease (MND) is a group of progressive neurological disorders that attack motor neurons in the brain and spinal cord, leading to muscle weakness, paralysis, and eventually death (Rezania and Roos, 2013). Autosomal recessive proximal spinal muscular atrophy or 5qSMA, simply known as SMA, is a pediatric form of motor neuron disease with a broad spectrum of onset and severities. It is the most common inherited cause of infantile death, with an incidence of one in every 10,000 live births, and a carrier frequency rate of one in 54 (Pearn, 1978; Prior *et al.*, 2010; Sugarman *et al.*, 2012).

1.1.1 Clinical manifestations

Childhood onset SMA is classified into three different forms, based on the age of onset, severity, and symptom progression (Table 1). Type I SMA described by Werdnig in 1891 and Hoffman in 1893, (also known as Werdnig-Hoffmann disease) is the most severe and common type, characterized by severe hypotonia before 12 months of age (Pearn, 1978; Markowitz *et al.*, 2004). There is a progressive

loss of muscle strength in this disease, with histology showing loss of anterior horn cells of the spinal cord and severely atrophic muscle fibers. These defects are reflected in abnormal electromyogram (EMG) patterns when muscle is electrophysiologically examined (Buchthal and Clemmesen, 1941; Brandt, 1950; Buchthal and Olsen, 1970). Type I SMA patients do not have the ability to sit unassisted and die before the age of 2 years from respiratory distress; although the diaphragm is spared, the intercostal muscles are vulnerable. With respiratory support, Type I patients are able to survive past the 2-year mark (Wang and Lunn, 2008).Type II SMA patients are able to sit independently, but fail to be able to walk. The onset of this type of SMA occurs before the age of 18 months, and patients often develop an abnormal curvature of the spine.

There is a reduction in life expectancy compared to normal individuals, but some SMA Type II patients live into adolescence or young adulthood.

Type III SMA (also known as Kugelberg-Welander disease) patients will have an onset of symptoms after 18 months of age. These patients achieve all major motor milestones, but some might require a wheelchair in childhood, and might also develop scoliosis (Wang and Lunn, 2008). Individuals with SMA Type III are prone to respiratory infections, but with care live a normal lifespan. In addition to these early childhood onset types of SMA, there is also an adult form of the disease called Type IV SMA. Symptoms in these patients appear in the 3rd to 4th decade of life, causing mild symptoms

but leaving patients with a normal life span (Zerres and Rudnik-Schöneborn, 1995).

Table 1. The four classes of spinal muscular atrophy (SMA) patients

Type	**Eponym**	**Onset**	**Characteristics**	**Age at death**	**% of SMA cases**
I	Werdnig–Hoffman	< 6 months	Muscle weakness; never sit independently.	< 2 years	60
II	Dubowitz	6–18 months	Muscle weakness; sit unassisted but become wheelchair-dependent; scoliosis of spine.	> 2 years	27
III	Kugelber–Welander	> 18 months	Muscle weakness in early life; walk unaided.	Normal life expectancy	12
IV	–	Adulthood	Muscle weakness following active life during early adulthood; may require walking aid.	Normal life expectancy	1

1.1.2 Genetics

Irrespective of type, SMA is caused by mutations in the Survival Motor Neuron 1 gene (*SMN1* gene). Indeed, linkage analysis mapped all SMA lesions to chromosome 5q11.1-13.3 (Brzustowicz *et al.*, 1990; Melki *et al.*, 1990). There are two almost identical genes, *SMN1* and *SMN2*, present on chromosome 5q13. The *SMN2* gene differs from the *SMN1* gene by five nucleotides (Lefebvre *et al.*, 1995). One of the nucleotide differences between the *SMN1* and *SMN2* gene is a C-T transition in an exonic splicing enhancer (ESE) located in exon 7 of the *SMN2* gene (Lorson *et al.*, 1999; Monani *et al.*, 1999). This transition affects splicing, leading to the exclusion of exon 7 from the *SMN2* messenger RNA (mRNA), resulting in the production of a partially functional and rapidly degrading form of the SMN protein (Cartegni *et al.*, 2006; Kashima *et al*., 2007). About 10% of the transcripts from *SMN2* remain full-length and are translated into the normal full-length, functional SMN protein (Lefebvre *et al.*, 1995). However, this is unable to compensate for loss of full-length SMN normally derived from *SMN1*.

In SMA patients, the *SMN1* gene is mutated or deleted altogether, or at a much lower frequency, carries a point mutation. However, SMA patients invariably retain at least one copy of the *SMN2* gene. The number of *SMN2* gene copies varies between patients, and generally corresponds to the severity of the SMA phenotype. The greater the

number of copies of the *SMN2* gene present in a patient, the less severe the SMA phenotype.

1.1.3 Role of SMN protein

The 38 kDa SMN protein is ubiquitously expressed and known to interact with a large number of factors, indicative of its involvement in multiple biochemical pathways. It is found in both the cytoplasm and the nucleus. In the nucleus, it concentrates in subnuclear structures that lie adjacent to or colocalize with foci containing coilin, a marker of Cajal bodies (Liu and Dreyfuss, 1996). The SMN protein belongs to a large macromolecular complex in combination with other proteins known as Gemins (2 to 8) and Unrip (Chari *et al*., 2009; Cauchi, 2010). It has been deduced that SMN, Gemin2, and Gemin8 come together to form the backbone of the entire complex, and the peripheral building blocks Gemin3/4, Gemin6/7, and Unrip bind the backbone to create the functional unit (Otter *et al.*, 2007).

In SMA patients, SMN protein levels are depleted in all cell types, and individuals with loss of both SMN genes have never been reported. This suggests that SMN is ubiquitously required. In other words, it has an important house-keeping function. The most widely accepted function of the SMN complex is its role in the biogenesis of spliceosomal snRNP particles (Fischer *et al*., 1997), which are major elements of the spliceosome, the nuclear pre-mRNAs processing machinery. Studies in SMN-deficient mouse models show altered stoichiometry of snRNAs, causing widespread tissue-specific splicing defects (Gabanella *et al.*, 2007; Zhang *et al.*, 2008). Other

studies have also shown that low SMN leads to differential splicing defects and alterations in splicing of several genes (Zhang *et al.*, 2008; Lotti *et al.*, 2012; Doktor *et al.*, 2016). These results have supported the view that the SMA phenotype might arise from inefficient splicing of pre-mRNAs coding for proteins required for motor neuron function. Still, there is an intense debate as to whether these splicing defects are a direct result of low SMN or a secondary response to a cellular dysfunction (Bäumer *et al.*, 2009; Garcia *et al.*, 2013).

SMN protein broadly functions in the assembly of ribonucleoprotein (RNP). The protein accomplishes this by bringing together several RNA-binding proteins with several "substrate" RNAs, facilitating the assembly of a specific protein on the target RNAs.

Many studies have also suggested a specific role of SMN in motor neurons since these cells seem to be primarily affected in SMA patients. This view is consistent with previous reports of the existence of axonal SMN complexes which lack the spliceosomal Sm proteins but contain some or all of the Gemins (Zhang *et al.*, 2003, 2006). SMN has also been shown to be associated in axons with distinct RNA binding proteins such as hnRNP R and Q (Rossoll *et al.*, 2002; Dombert *et al.*, 2014), HuD, FMRP (Piazzon *et al.*, 2008; Fallini *et al.*, 2011; Hubers *et al.*, 2011), TDP-43 and FUS (Yamazaki *et al.*, 2012; Tsuiji *et al.*, 2013). These studies support the notion that SMN has an important role in the assembly and function of ribonucleoproteins involved in the regulation of mRNA transport, stability, and translation (Jablonka and Sendtner, 2003; Rossoll *et al.*,

2003; Fallini *et al.*, 2011; Hubers *et al.*, 2011; Fallini *et al*., 2012; Rage *et al.*, 2013; Sanchez *et al.*, 2013).

Moreover, SMN interacts with proteins associated with cytoskeletal dynamics (Bowerman *et al.*, 2009; Fallini *et al.,* 2012). Several studies have indicated that cytoskeletal dynamics are likely to be impaired in SMA. For instance, neurotransmission, which relies on an intact cytoskeletal architecture at the nerve terminals, is compromised in SMA. On this note, SMN has shown to interact and co-localize in motor neurons with the small actin-binding proteins profiling I and II (Giesemann *et al.*, 1999; Bowerman *et al.*, 2007), and SMN deficient cells exhibit a defective microtubule network (Wen *et al.*, 2010). Other studies have revealed that the actin-bundling protein Plastin3 is associated with SMN and acts as a protective modifier of SMA in humans. Thus, in several families, daughters who lack *SMN1* and do not display an overt SMA phenotype, exhibit higher expression of Plastin3 than SMA-affected counterparts (Oprea *et al.*, 2008; Stratigopoulos *et al.*, 2010; Bernal *et al.*, 2011). Plastin3, a conserved calcium binding, actin-bundling and stabilizing protein, is expressed in various tissues. It has been shown that Plastin3 overexpression rescues axon outgrowth defects in SMN deficient zebrafish embryos and cultured motor neurons from SMA mouse models (Hao *et al.*, 2012; Ackermann *et al.*, 2013). Also, invertebrate Plastin3 orthologs act as modifiers in *C. Elegans* and *Drosophila* models of SMA, indicating that plastin-associated pathways are directly connected to SMN function (Dimitriadi *et al.*, 2010). Recent studies have also stated that Plastin3 overexpression restored endocytosis and rescued the SMA phenotype of a SMA

mouse model (Hosseinibarkooie *et al.*, 2016). This is particularly intriguing given the recently described defects in endosomal trafficking in motor neurons synapses observed upon SMN depletion in *C. Elegans* (Dimitriadi *et al.*, 2016). The putative functions of the SMN protein in motor neurons might explain the selective vulnerability of spinal cord motor neurons to low levels of the protein.

1.2 Neuromuscular pathology in SMA

1.2.1 Motor Neuron Defects

One of the most remarkable neuropathological features of SMA is the degeneration of the α-motor neurons of the spinal cord and the lower brain stem. The loss of motor neuron function results in paralysis of muscles and respiratory insufficiency (Crawford and Pardo, 1996). This motor neuron loss is apparent in the Electromyography (EMG) of SMA patients.

In Type I SMA, patients exhibit spontaneous activity in relaxed muscle, even while asleep. (Buchthal and Clemmesen, 1941; Buchthal and Olsen, 1970). Additional signs of neuromuscular pathology include an increase in the mean amplitude of motor unit potentials (MUPs). The level of abnormality in EMGs correlates with the severity of the disease phenotype in patients (Buchthal and Olsen, 1970).

1.2.2 Muscle Atrophy

A second characteristic pathological feature of SMA patients is the presence of atrophic muscle fibers. Before the discovery that *SMN1* mutations are responsible for SMA, muscle histology and electrophysiology were used as diagnostic tools for SMA. In all SMA cases, patients were found to exhibit atrophic muscle fibers, with varying proportions of normal, atrophic, and hypertrophic fibers. In SMA Type 1 and Type 2, the atrophic fibers are intermittently angulated (Dubowitz *et al.*, 1985). The extent of atrophy varies based on each specific muscle, with some muscles being more vulnerable than others. In severe SMA cases, group atrophy of the same fiber type can be seen, which implies a loss of the innervating motor neuron (Dubowitz *et al.*, 1985).

1.2.3 Neuromuscular Junction Defects

Numerous studies performed in the different mouse models of SMA have uncovered morphological abnormalities at the neuromuscular junction (NMJ). The NMJ is a chemical synapse formed between a motor neuron and a muscle fiber, allowing for reciprocal signaling between them. Such signaling is critical to muscle contraction. The NMJ morphological abnormalities in SMA have been shown to occur before axonal degeneration and motor neuron death (Kariya *et al.*, 2008a; Kong *et al.*, 2009; Dachs *et al.*, 2011).

In SMA mouse pups, the number of lumbar motor neurons were not significantly reduced early on (~PND2), and only showed moderate progressive loss in late stages of the disease. However, NMJ defects were observed in newborn SMA mice (Kariya *et al.*, 2008a). These

defects are characterized by loss of presynaptic motor nerve terminals, neurofilament accumulation in the terminals, and immature plaque-like acetylcholine receptor (AChRs) clusters containing the embryonic γ-subunit form of the receptor (Kariya *et al.*, 2008a; Wyatt and Keirstead, 2010).

The morphological abnormalities of the NMJ are reflected in functional abnormalities. Studies of the NMJs of severe SMA mice have shown more than a fifty percent reduction of overall synaptic vesicle density and significant neurotransmission defects (Kariya *et al.*, 2008; Kong *et al.*, 2009). These collective NMJ results in SMA mice led researchers to look at NMJ abnormalities in human SMA patients. Kariya *et al*. found consistent NMJ defects in SMA human patients. Abnormal neurofilament accumulation in nerve terminals was seen in the diaphragm of Type I SMA patients (under 6 months of age). The study also found motor endplates that were smaller in size and structurally under-developed compared to control (Harding *et al.*, 2015; Kariya *et al.*, 2008). Remarkably, defects were also detected during development of the diaphragm and in limb muscles in SMA fetuses (Martínez-Hernández *et al.*, 2013). This study reported changes in AChR clustering, abnormal ultrastructure of nerve terminals prenatally, and unusual pre-terminal accumulation of vesicles (Martínez-Hernández *et al.*, 2013). Martinez-Hernandez also confirmed in type I SMA patients, the results of Kariya *et al* with respect to the delay in maturation of postnatal muscle. This suggests that the NMJ is amongst the very first structures of the neuromuscular system to be affected in SMA.

Remarkably, NMJs in different muscles show differences in vulnerability due to low levels of SMN. Also, the same muscles can be differentially affected among mouse models of SMA (Murray *et al.*, 2007; Ling *et al.*, 2012; Thomson *et al.*, 2012). Studies have investigated which factors contribute to this specific synapse vulnerability, including motor neuron pools, muscle location and fiber type (Murray *et al.*, 2007; Ling *et al.*, 2012; Thomson *et al.*, 2012). Axial muscles are generally more vulnerable, but both distal and proximal regions contain a mix of both resistant and vulnerable muscles in the SMA Δ7 mice (Ling *et al.*, 2012). This study found that most vulnerable muscles were innervated by motor neurons in the cervical and thoracic spinal cord segments. A difference in muscle fiber type has been proposed to influence synapse vulnerability in neuromuscular degenerative diseases. Muscle fibers can be classified into two main types: slow twitch (Type I) muscle fibers, and fast twitch (Type II) muscle fibers. Fast twitch fibers are further classified into Type IIa and Type IIb. Slow twitch fibers use oxygen to generate energy; they fire slowly and are used in continuously extended muscle contractions over an extended period (i.e. muscles involved in posture). In contrast, fast-twitch fibers are anaerobic and are more efficient in creating short bursts of strength or speed (e.g. periocular muscles) than slow fibers. However, they also fatigue faster. In amyotrophic lateral sclerosis (ALS), the fast-twitch muscle fibers are more vulnerable than slow-twitch muscle fibers (Hegedus, Putman and Gordon, 2007). This may be the case in SMA as well. However, two independent studies using two different mouse models of SMA (severe and SMA Δ7 mice), have shown no

linkage between muscle fiber type and NMJ pathology (Murray *et al.*, 2007; Ling *et al.*, 2012).

1.3 Spinal Muscular Atrophy Models

Following the delineation of the molecular genetics of SMA, it became possible to generate transgenic animals that recapitulate the disease. The well characterized genomes and nervous systems of *C. elegans* and *D. melanogaster* make them good invertebrate model systems to study SMA pathology, the tissues involved in the disease and the developmental aspects of the disease. The *C. elegans* ortholog of SMN, CeSMN, is expressed uniformly throughout larval development and detected in the nuclei of every cell (Miguel-Aliaga *et al.*, 1999). Expression however becomes heterogeneous in adulthood, with higher concentrations observed in neurons. Knock-down of CeSMN produces a variety of phenotypes, from decreased embryonic viability to neuronal, muscular and reproductive defects (Miguel-Aliaga *et al.*, 1999). Various mutant SMN alleles and point-mutations have been studied in *D. melanogaster* models of SMA due to the ease of conducting genetic crosses in the fly. Developmental studies show that dSMN is highly expressed in embryogenesis and the levels decrease in adulthood (Rajendra *et al.*, 2007). Homozygous deletion of *D. melanogaster Smn* (dSMN) causes death at various stages of larval development, concomitant with the inexorable depletion of maternally-derived full-length SMN (Chan *et al.*, 2003; Rajendra *et al.*, 2007; Chang *et al.*, 2008). As in the human patient, *D. melanogaster* larvae with SMN depletion exhibit decreases in

motor rhythm, muscle size and locomotion, and aberrant neuromuscular junction transmission (Imlach *et al.*, 2012).

SMA has also been modeled in the zebrafish (*D. rerio*). This was carried out by knocking down the single zebrafish *Smn* gene using antisense morpholino-oligonucleotides (MOs) (McWhorter *et al.*, 2003). Knockdown of the SMN protein led to defects of motor axon length and branching. The lower the level of SMN, the greater was the incidence of these defects. Additionally, high doses of morpholino and thus low levels of SMN compromised the survival of embryos. The axonal defects in mutant fish were further confirmed by visualization of single motor axons following iontophoresis-mediated knock down of SMN in motor neurons (McWhorter *et al.*, 2003). The aforementioned phenotypes confirm that the less the SMN, the more severe is the phenotype. However, development and organization of skeletal muscle remained unaffected in mutant fish, which is not reflective of the human SMA disease phenotype (McWhorter *et al.*, 2003).

Some of the inconsistencies noted above may derive from species-specific effects, and therefore do not allow for firm conclusions to be drawn about the biology of SMA. Additionally, it may be argued that none of the above models harbors the *SMN2* gene, which ensures constant low levels of the SMN protein in SMA patients and is a fundamental hallmark of the human disease. These caveats, along with the advantages rodents offer in modeling human disease, provided a convincing argument to model SMA in mice (Park *et al.*, 2010).

Given the drawbacks of modeling SMA in lower organisms, it became necessary to develop a mammalian model of the disease. With the identification of the *Smn* gene in mice (Mus musculus), the first mouse model of SMA was made in 1997 (Schrank *et al.*, 1997). Mouse *Smn* shares 83% amino acid homology with hSMN, and like its human counterpart is ubiquitously expressed (Schrank *et al.*, 1997). In mice, a homozygous knockout of the single murine *Smn* gene results in early embryonic lethality following massive cell death (Schrank *et al.*, 1997). To create viable SMA mice, mutants had to be transgenically endowed with the human *SMN2* gene. Two groups used this approach (Li *et al.*, 2000; Monani *et al*., 2000). Despite having comparable *SMN2* copies, the mouse developed by Monani *et al.* in the Burghes Laboratory (Tg(*SMN2*)89Ahmbtg/tg;$Smn^{-/-}$, Strain 5024, commonly referred to as "severe SMA mice") survived up to 5 days postnatally, while the mouse developed by Hsieh-Li *et al* in the Li Laboratory (Tg(*SMN2*)2Hungtg/o; $Smn^{\Delta 7/\Delta 7}$, commonly referred to as the "Taiwanese mice") survived until 14 days of age (Li *et al.*, 2000; Gogliotti *et al.*, 2010). Co-expressing an $Smn^{\Delta 7}$ cDNA transgene on the severe 5024 background partially rescues the mutant mice enhancing survival to ~14 days. Still, this model commonly referred to as the *Smn*Δ7 mouse model of SMA exhibits many of the signature features of human SMA and has become the standard model of choice in preclinical development studies for SMA (Le *et al.*, 2005).

1.4 Strategies for treating SMA

Notwithstanding the FDA approval of a recently tested treatment for the disease, there is no cure for SMA. Most therapeutic approaches are based on attempts to increase the amount of SMN protein produced by the *SMN2* gene or by using gene replacement approaches (Bebee *et al.*, 2012). SMN protein levels can be increased by a variety of approaches, including increasing inclusion of exon7 into the *SMN2* transcript, increasing *SMN2* transcription, or increasing the stability of SMN protein generated by *SMN2* (Chang *et al.*, 2001; Sumner *et al.*, 2003, 2009; Avila *et al.*, 2007; Tiziano *et al.*, 2010a; Farooq *et al.*, 2011). Potential therapies also include reintroducing healthy cells to replace the loss of diseased motor neurons. These approaches have been tested *in vitro*, in mouse models of SMA and some have already been tested in clinical trials (Brahe *et al.*, 2005; Wirth, Brichta and Hahnen, 2006; Mercuri *et al.*, 2007; Swoboda *et al.*, 2010; Tiziano *et al.*, 2010b; Abbara *et al.*, 2011; Darbar *et al.*, 2011). However, despite the recent approval by the FDA of Spinraza, an ASO therapeutic approach for SMA, there is no permanent cure for the disease. Some of the therapeutic approaches alluded to above are further described below.

1.4.1 *SMN2* gene activation

One of the first drugs tested as an SMA therapeutic was hydroxyurea (HU), which is a ribonucleotide reductase inhibitor. HU treatment resulted in increased levels of full length SMN mRNA in lymphoblastoid cells from SMA patients by promoting inclusion of

exon 7 during *SMN2* transcription (Grzeschik *et al.*, 2005). In adult SMA carrier mice *($Smn^{+/-}$;SMN2*, (Monani at al., 2000), HU increased the expression of human *SMN2* derived protein in spinal cord after a single intra-peritoneal injection (Mattis *et al.*, 2008). HU has also been tested in clinical trials, where it has been proven to be safe, can be administered orally and has a high bioavailability in children. However, it failed to improve outcome measures such as motor function, strength, lung function, or levels of full length SMN mRNA (Chang *et al.*, 2001; Chen *et al.*, 2010).

Another class of drugs that has been shown to be effective in SMA is histone deacytelase inhibitors (HDACi) (Andreassi *et al.*, 2004; Hahnen *et al.*, 2006; Riessland *et al.*, 2006, 2010; Avila *et al.*, 2007; Narver *et al.*, 2008; Tsai *et al.*, 2008; Garbes *et al.*, 2009). Histones are basic proteins and their positive charge allows them to associate with DNA to form condensed chromatin. Histones undergo post-translational modifications, including acetylation, phosphorylation, methylation, ubiquitination and ADP-ribosylation (Strahl and Allis, 2000), which regulates the conformation of chromatin and partially controls the access of the transcriptional machinery to DNA. Acetylation of specific Lysine residues in the amino termini of the core histones plays a fundamental role in transcriptional regulation (Grunstein, 1997). Levels of acetylation of histones result from the balance of the enzymes histone acetyltransferases (HATs) and histone deacetylases (HDACs). Transcriptional activity is associated with increased levels of acetylation, whereas decreased levels of acetylation are associated with gene repression. There are four classes of histone deacetylases based on their homology to yeast

deacetylase proteins: Class I-III and HDAC11 (de Ruijter *et al.*, 2003). HDAC inhibitors (HDACi) have been shown to increase SMN levels by driving endogenous *SMN2* promoter activity. Most HDACi that are effective in increasing SMN levels target both class I and II HDACs (Evans, Cherry and Androphy, 2011). One unfortunate side effect of HDACi is that these drugs are not gene-specific and therefore might have detrimental off-target effects.

1.4.2 Stabilization of SMNΔ7 transcript

Another approach to treating SMA is to stabilize the SMN protein lacking exon 7 (SMNΔ7). SMNΔ7 has a shorter half-life compared to full-length SMN. However, it has been shown to be more stable when it forms heterotypic complexes with full-length SMN (Burnett *et al.,* 2009). A class of antibiotics, known as aminoglycosides, has been shown to increase SMNΔ7 stability. Aminoglycosides have the ability to suppress efficient recognition of stop codons. When the first stop codon of SMNΔ7 (in exon eight) is not recognized this will allow the translational machinery to elongate the protein with an additional five amino acids. Studies have shown that this protein is more stable, can promote neurite outgrowth and can increase the assembly of the spliceosome (a macromolecule complex containing snRNPs) *in vitro* (Mattis *et al.*, 2008). Forcing translational readthrough results in an increased level of SMN protein in fibroblasts from SMA patients. A significant elongation of lifespan and an increased number of cells in the ventral horn of the spinal cord in SMA Δ7 mice have also been observed following such treatment (Heier and DiDonato, 2009; Rose *et al.*, 2009).

1.4.3 *SMN2* alternative splicing modulation

A third potential treatment strategy is to modulate *SMN2* alternative splicing to restore the expression of the full-length SMN transcript and protein. Several drugs have been shown to be effective, including tetracycline,quinazoline (Thurmond *et al.*, 2008; Hastings *et al.*, 2009; Butchbach *et al.*, 2010). Splice modulation can be effected by using antisense oligonucleotides (ASOs), such as Spinraza (Finkel, 2016), a drug developed by Biogen and Ionis Pharmaceutical. ASOs are single-stranded RNA molecules that are complementary to a certain mRNA sequence and block access to specific sites on the RNA. An antisense oligonucleotide which is directed toward the intron 7 and exon 8 junction in the *SMN2* pre-mRNA, decreases the identification of the exon 8 3′ splice site. As a consequence, the splice site pairing competition between exons 7 and 8 is altered to favor exon 7 inclusions and leads to a 2-fold increase of *SMN2* exon 7 inclusions *in vitro* (Lim and Hertel, 2001). Several studies have shown that injections of such ASOs into the intracerebral ventricular (ICV) space to administer the ASO into the cerebrospinal fluid (CSF) increased exon 7 inclusion and subsequently increased SMN levels in brain and spinal cord (Williams *et al.*, 2009; Hua *et al.*, 2010, 2011; Passini *et al.*, 2011). This resulted in improved motor function and modestly extended survival. Interestingly, when the ASOs are delivered systemically via a subcutaneous injection, exon 7 inclusion and SMN levels were also increased in heart and liver, leading to a more robust rescue in the Taiwanese SMA mice (Hua *et al.*, 2011). This suggests that SMN plays an important role not only in motor

neurons, but also in peripheral tissues. Recently the ASO developed by Biogen and Ionis Pharmaceuticals, and marketed under the name Spinraza, was approved by the FDA as a therapy for SMA.

1.4.4 Neuroprotective agents

Unlike various other drugs in clinical trial, neuroprotective agents are not intended to increase SMN levels and could be an effective intervention to delay or limit motor neuron loss and disease progression in SMA (Rose *et al.*, 2009). Using such agents might be beneficial, especially for patients with a milder form of SMA (Swoboda *et al.*, 2007). An example of such an agent is riluzole, which acts on voltage-dependent sodium channels to limit the release of the neurotransmitter glutamate. In this way, it reduces excitotoxicity (Haddad *et al.*, 2003). Also, it has been shown to exhibit neurotrophic activity, and it enhances expression of brain-derived neurotrophic factor (BDNF) (Katoh-Semba *et al.*, 2002). Riluzole-dependent blockage of sodium channels results in a reduction of ATP release followed by depletion of ectoadenosine, which is thought to increase BDNF synthesis. Increased levels of BDNF have been shown to promote neuronal survival and participate in activity-dependent synaptic plasticity (Katoh-Semba *et al.*, 2002). A study in a mouse model of mild SMA showed that riluzole treatment initiated at postnatal day 21 improved neuromuscular junction organization (i.e. there was less neurofilament accumulation in nerve terminals) and increased median survival (Haddad *et al.*, 2003). Additionally, a neuroprotectant referred to as Olesoxime has been successful in stabilizing motor functions in non-ambulant SMN

Type II and III patients in Europe. Roche has started to direct the production and future development of this compound in clinical trials in the United States (Calder, Androphy and Hodgetts, 2016).

1.4.5 Gene therapy

The first gene therapy attempt to enhance SMN protein levels in motor neurons was accomplished by an intra-muscular injection with a lentiviral vector encoding the full-length SMN protein (Azzouz *et al.*, 2004). The rationale behind this study was that intramuscular injection would result in infection of the presynaptic termini of motor neurons and subsequent retrograde axonal transport of the viral vector to the motor neuron cell soma. The treated mice showed a reduction in motor neuron death; however, the effect on survival was modest (Azzouz *et al.*, 2004). Subsequent approaches used systemic delivery via the temporal facial vein using a self-complementary adeno-associated vector serotype 9 (scAAV9). Three individual studies showed that this approach rescued characteristic SMA phenotypes such as muscle atrophy, immobility and weight loss. In addition, the therapy substantially improved survival of the SMA mice (Foust *et al.*, 2010; Valori *et al.*, 2010; Dominguez *et al.*, 2011). Foust *et al* also showed that the scAAV9 vector traverses the blood-brain barrier in a non-human primate, which supports the possibility of translating this treatment to human patients (Foust *et al.*, 2010). An alternative to systemic delivery is to deliver the vector directly into the CNS (Passini *et al.*, 2010). This strategy showed improvement of motor behavior, body weight, and overall survival, although the model mice involved in this experiment still died

prematurely. This suggests that rescue of tissue, other than the motor neurons, is needed for the complete rescue of the mice.

1.4.6 Stem cell therapy

Neural stem cell therapy was first shown to be effective in a mouse model of ALS. These mice showed a modified disease progression via neurogenesis and also via growth factor release (Corti *et al.*, 2007). The beneficial effect was not only mediated by cell replacement but also by the neuroprotective effect of factors released by the donor cells. The first attempt of stem cell therapy in a mouse model of SMA used primary murine neural stem cells (Corti *et al.*, 2008). The same group also showed *in vivo* that embryonic stem cell-derived neural stem cells could differentiate into motor neurons, and can migrate along the spinal cord when transplanted into the cerebrospinal fluid (Corti *et al.*, 2010). Approximately 15% of these cells engrafted in the spinal cord where most exhibited astrocyte-like characteristics, and to a lesser extent, motor neuron characteristics. Surprisingly, this nevertheless resulted in an increase in survival, body weight and an improvement in muscle morphology (Corti *et al.*, 2010).

1.5 Evidence for the importance of SMN in other (non-neuromuscular) organ systems

The main pathological feature of SMA is a specific loss of motor neurons in the ventral horn of the spinal cord; however as discussed previously SMN is required in all tissues at least at some level. There

has been some debate as to which tissues are primarily affected by the decrease in SMN expression that occurs in SMA. From the studies described earlier, there is evidence that muscle tissue might also be a pathological target in SMA. Recent work has identified a range of additional cell and tissue types that exhibit vulnerability to low levels of SMN (Hamilton and Gillingwater, 2013). Since defects in nonneuronal tissue have been shown to develop in parallel with neuromuscular pathology, this could be suggestive of severe SMA being a multi-system disorder rather than a pure motor neuron disease. In mild SMA on the other hand, the disease almost exclusively affects the neuromuscular system. Instances of peripheral (non-neuromuscular) abnormalities in severe SMA are highlighted below.

1.5.1 Heart defects

One of the most frequently observed abnormalities in SMA outside of the neuromuscular system are congenital heart defects. In a study with a type I SMA patient cohort, three out of four patients were observed with major cardiac septal defects (Rudnik-Schoneborn *et al.*, 2008). Electrocardiography (ECG) studies in a mouse model of SMA (*Smn*$^{-/-}$*;SMN2; SMN*$^{\Delta 7}$) (Le *et al.*, 2005) revealed severe bradycardia characterized by progressive heart block and impaired ventricular conduction throughout development (Heier *et al.*, 2010). Heart failure, characterized by septum thinning, begins at different time depending on disease severity. In the severe SMA mice (*Smn*$^{-/-}$*;SMN2*) (Monani *et al.*, 2000) this was observed at embryonic stages whereas it is observed between postnatal day two and postnatal day

five in the SMA Δ7 mice (Shababi *et al.*, 2010). This indicates an important role for SMN in cardiac development and maintenance.

1.5.2 Vascular defects

Vascular defects, such as those triggering digital necrosis, and capillary bed defects have been observed in both patients and animal models of SMA. These defects became apparent when survival was prolonged in patients with the aid of invasive ventilation or in mice after drug treatment (Foust *et al.*, 2010; Valori *et al.*, 2010). Two studies showed that capillary defects did not precede NMJ pathology, but rather developed in parallel. It is possible that there is an essential role for SMN in these tissues and the corresponding defects are not developing secondarily to neuromuscular pathology (Schreml *et al.*, 2013; Somers *et al.*, 2016).

1.5.3 Metabolic abnormalities

Metabolic abnormalities have been found in SMA mouse models. Glucose metabolism defects have been observed as a result of the loss of the insulin producing β-cells and an equivalent increase in the number of the glucagon producing α-cells in the pancreas (Bowerman *et al.*, 2012). Muscle has a key role here as well, as it is a vital player in glucose metabolism through its role in insulin-dependent glucose uptake. In addition, low levels of SMN have recently been shown to have an effect on the liver (Hua *et al.*, 2011). SMA mice had decreased hepatic insulin-like growth factor binding protein, acid labile subunit (Igfals) expression, which led to a

reduction in circulating insulin-like growth factor 1 (IGF1). IGF1 is a neurotrophic factor and is important for normal postnatal growth (Wu *et al.*, 2009). Interestingly, IGF1 levels were rescued by restoring SMN levels systemically (Hua *et al.*, 2011).

1.6 Investigating the contributing role of muscle in SMA

The survival of motor neurons and the development of muscle rely on communication and contact between the two (Greensmith and Vrbová, 1997; Vrbova, 2008). There is a clear pathology in both motor neuron and muscle in SMA patients. Whether the pathology seen in muscle is a secondary effect of the degeneration taking place in the lower motor neurons, and whether it is a direct consequence of low protein in muscle has been a matter of debate in the field. Many studies have suggested that the survival of motor neurons depends on the motor neuron receiving signals from muscle, and this could be relevant in the context of SMA as well.

In 1987, Henderson described a potential role for muscle in SMA for the first time (Henderson *et al.*, 1987). The study reported that muscle from SMA patients contained substances that caused inhibition of normal neurite outgrowth of chick spinal motor neurons. These inhibitory substances were not seen in control tissue from other diseases and were unique to muscles of SMA patients. A co-culture of SMA patient cells (muscle stem cells) and rat spinal cord degenerated after three weeks in culture, defined by large electron-lucent vacuoles, and sarcomeric disorganization (Braun *et al.*, 1995,

1997). The degeneration was not observed after innervation occurred in mixed co-cultures (where half of cloned satellite cells were from SMA patients and the other half were from healthy donors) (Guettier-Sigrist *et al.*, 1998). The discovery of SMN protein in muscle, in sarcomeres of *D. melanogaster* (Walker *et al.*, 2008), supports these results, suggestive of a role for muscle in SMA. Likewise, myoblast cultures from SMA patients show defects in the formation of myotubes and aggregation of AChRs (Arnold *et al.*, 2004). A recent study showing that satellite cells isolated from severe SMA mice differentiate faster has, in part, confirmed this. Remarkably, it has also been reported that these cells failed to form myotubes (Hayhurst *et al.*, 2012).

To investigate whether a defect of SMN in skeletal muscle might have a direct role in the pathology observed in SMA *in vivo*, Cifuentes-Diaz *et al*, developed a mouse model in which deletion of SMN exon7 was restricted to skeletal muscle. The presumed ablation of SMN led to a severe phenotype characterized by the onset of muscle paralysis after three weeks of age. This culminated in death at a mean age of 33 days. Mononuclear cell infiltration, regenerating myocytes, and necrotic muscle fibers were also observed (Cifuentes-Diaz *et al.*, 2001). In this specific mouse model, the absence of *SMN2* resulted in a *complete* knockout of skeletal muscle SMN protein, a situation that does not accurately represent human SMA, which is a disease of low SMN.

To investigate the cellular site of action of the SMN protein, protein levels were selectively restored in severe model mice by the Burghes

lab using the severe SMA mice. One study restored SMN levels specifically in skeletal muscle under the human skeletal actin (HSA) promoter, and the other attempted to restore SMN levels specifically in motor neurons under the prion promoter (PrP). Both studies concluded that replacement of SMN in neurons rescues the SMA phenotype and increases the survival of the mice, whereas replacement of SMN levels specifically in muscle fibers had no significant effect on the SMA phenotype or in the survival of the mice (Gavrilina *et al.*, 2008). However, this study did not rule out the possibility that expression of SMN protein in both neurons and muscles is needed for the rescue since the PrP promoter was not completely specific for motor neurons and also showed low levels of expression in muscle. Additionally, studies have used MyoD and Myf5 (both myogenic regulatory factors) promoters to restore SMN levels specifically in muscle precursor cells and myofibers. The restoration of SMN levels in both satellite cells and myofibers completely rescued myofiber growth, followed by an increase in survival and improved motor behavior. Nevertheless, there was no improvement observed in NMJ morphology (Martinez *et al.*, 2012).

In a related study, Bosche-Marce attempted to rescue the SMA muscle phenotype by overexpressing muscle specific insulin-like growth factor 1 (IGF-1) (Bosch-Marce *et al.*, 2011). IGF-1 is a small polypeptidic hormone that plays a major role during muscle development, and muscle regeneration after injury. An increase in muscle mass and survival was reported following IGF-1 overexpression. However, this was not accompanied by a significant improvement in motor function (Bosch-Marce *et al.*, 2011). Despite

the above studies, the role of muscle in SMA is still not fully understood and requires further investigation. This is partly because the experiments performed to date cannot rule out the possibility that changes observed in muscle are simply occurring as a secondary effect of denervation due to pathology in the innervating motor neurons. As therapies for SMA move forward, this remains an important question to address. Accordingly, the goal of this research project has been to more precisely delineate the contributing role of muscle in the overall pathology/phenotype characteristic of SMA. Our results show that wild-type levels of SMN in muscle are absolutely critical to the maintenance of healthy muscle. Thus we believe that SMN functions cell-autonomously within this tissue to ensure its health and viability. Restoring protein to muscle is therefore expected to constitute a vital aspect of treating SMA in SMN repletion-type therapies.

Chapter 2

Materials and Methods

2.1 Mice

To generate inducible *Smn* mice harboring 0, 1, or 2 *SMN2* copies, we initially bred homozygous $SMN2^{+/+}$;$Smn^{+/-}$ animals (Jax stock no. 005024; The Jackson Laboratory) with a line ($Smn^{F7/+}$) harboring an allele of the murine *Smn* gene that contains loxP sites flanking exon 7 (Jax stock no. 006138; The Jackson Laboratory). Upon Cre expression, the loxP sites recombine irreversibly, thereby deleting exon 7 and inactivating the allele. Progeny mice ($SMN2^{+/+}$; $Smn^{F7/-}$) were crossed with heterozygous MyoD-icre mice (Jax stock no. 014140; The Jackson Laboratory). Heterozygous MyoD-icre mice are viable, fertile, and normal in size, while homozygous mice exhibit reduced fitness and survival prior to weaning. MyoD is a muscle regulatory factor and a marker of committed myogenic cells. When MyoD-icre mice are bred with mice containing loxP-flanked sequences, Cre-mediated recombination will result in deletion of the floxed sequences in the MyoD-expressing cells of the offspring. This cross generated *MyoD-icre;*$Smn^{F7/-}$ mutants harboring variable copies of the *SMN2* gene. All experiments described in this study included both male and female mice. To preclude strain background

effects, littermate controls were used in the experiment. Study approval; All experiments were conducted in accordance with the protocols described in the Guide for the Care and Use of Laboratory Animals (NIH. Revised 2011) and were approved by Columbia University's Institutional Laboratory Animal Care and Use Committees.

2.2 Molecular Analysis

2.2.1 Genotyping

Mouse genomic DNA was isolated from tail biopsies following overnight digestion at 55°C in buffer containing 50 mM Tris-HCl (pH 8.0), 10 mM EDTA, 100 mM NaCl, 0.1% SDS and 1mg/ml proteinase K, followed by heat inactivation. PCR was performed using the following primers for the various alleles:

Allele	Forward	Reverse
MyoDicre knockin	5′-GCG GAT CCG AAT TCG AAG TTC C-3′	5′-GGA AAA TGC TTC TGT CCG TTT G-3′
***Smn*F7**	5′-GCT AAG TGC CTT CTC TAC ACC TGC-3′	5′-TGG GTC TCC AAA GCG ACT CC-3′
m*Smn* knock out (NEO insert)	5′-CTT GGG TGG AGA GGC TAT TC-3′	5′-AGG TGA GAT GAC AGG AGA TC-3′
SMN2	5′-CTC CGG GAT ATT GGG ATT-3′	5′-GGT AAC GCC AGG GTT TTC C-3′ **&** 5′-CAA GGG AGT TGT GGC ATT CTT C-3'

Products were separated by gel electrophoresis and genotype assigned by presence or absence of a band of appropriate size.

2.2.2 Analysis of Cre Recombinase Transgene Activity

To characterize the pattern of Cre recombinase activity, *ROSA26* (Jax stock no. 003474; The Jackson Laboratory) reporter mice were used. Homozygous *ROSA26* mice have a loxP-flanked DNA STOP sequence preventing expression of the downstream lacZ gene. When crossed with a cre transgenic strain, the STOP sequence is removed and lacZ is expressed in cells/tissues where cre is expressed. These mice are often used as a Cre-reporter strain to test the tissue/cellular expression pattern of cre transgenic mice. The specificity and efficiency of MyoDicre mediated recombination was tested in PND7 *MyoDicre;ROSA26* mice and relevant controls as described in the results section. Mice were transcardially perfused with 4% paraformaldehyde in phosphate buffer (pH 7.4). Spinal cords and gastrocnemius and triceps muscles were dissected. Cervical, thoracic, and lumbar spinal cords were cryo-sectioned in 20 μm sections. Prior to treatment with antibodies, sections were post-fixed in 4% PFA (10 mins), washed in 1× PBS, permeabilized (0.5% Triton X-100 in PBS) and finally incubated in blocking medium (10% FBS, 0.2% Triton X-100 in PBS). To detect YFP expressing cells, cryosections were stained with primary antibodies specific for green fluorescent protein (GFP) (1:1000, Invitrogen) and ChAT (1:200, Millipore) respectively followed by corresponding secondary antibodies: donkey anti-rabbit Alexa-488 (1:2,000, Invitrogen) and donkey anti-goat Alexa-594 (1:2000, Invitrogen). Fluorescent images were

acquired using either an E80i Nikon microscope equipped with a 20× objective and Spot Flex digital camera (Diagnostic Instruments) or a Leica TCS SP5 II confocal microscope equipped with a 63× objective.

2.2.3 Quantitative PCR

To quantify levels of α and γ subunit of the AChR, RNA was isolated with Trizol (Invitrogen, CA, USA) according to the manufacturer's instructions. GAPDH was used as a normalizer to account for differences in cDNA input. Relative quantification of AChRα and AChRγ mRNA, corrected for the quantity of GAPDH mRNA was divided by a calibrator value (wild-type value) to calculate transcript levels. Primers used were:

	Forward Primer	**Reverse Primer**
AChRα	5'-ACG GCG ACT TTG CCA TTG TC-3′	5'-CAG GCG CTG CAT GAC GAA GT-3′
AChRγ	5′-GAC CAA CCT CAT CTC CCT GA-3′	5′-GAG AGC CAC CTC GAA GAC AC-3′
GAPDH	5’-TGA AGG TCG GTG TGA ACG GAT TTG GC-3′	5'-CAT GTA GGC CAT GAG GTC CAC CAC-3′

2.2.4 Protein Extraction and Western Blotting

Muscle tissue samples were homogenized in lysis buffer (50 mmol/L Tris-HCl pH 7.5, 150 mmol/L NaCl, 1 mmol/L EDTA, 1% NP-40, 5 mmol/L DTT, 1 mmol/L PMSF). Total protein concentration was determined using BCA Protein Assay Kit–Reducing Agent

Compatible (Pierce, Thermo Scientific). Protein lysates (20 μg) were resolved on a 12.5% polyacrylamide gel and transferred to polyvinylidene fluoride membrane Immobilion-P (Millipore Corporation, Billerica, MA). The membrane was probed sequentially, first with a mouse anti-mSMN antibody (1:5,000; BD Transduction Laboratories, San Jose, CA) followed by goat anti–mouse IgG secondary antibody (1:10,000; Jackson Immunoresearch Laboratories, West Grove, PA). Chemiluminescent signals were developed using Amersham ECL Plus western blotting kit (GE Healthcare).

2.3 Neuromuscular Pathology

2.3.1 Motor Neuron Analysis

To determine spinal motor neuron and gem counts and to assess motor neuron morphology, spinal cord tissue was extracted from mice following transcardial perfusion with 1× PBS and then 4% PFA. Following postfixation in 4% PFA (4°C for 4 hours), tissue was cryoprotected (sucrose gradient for 3 days at 4°C), embedded in Tissue-Tek OCT, and then frozen in liquid N_2–cooled isopentane for sectioning. 20-μm transverse sections from cervical, thoracic, and lumbar spinal cord were sectioned. They were then washed with PBS to remove Tissue-Tek OCT, and then blocked with blocking buffer (3% BSA, 2% Triton-X 100) for 30 minutes (room temperature), and then incubated with an anti-SMN antibody, (1:100) and an antibody against choline acetyltransferase (ChAT) (1:100; Millipore) dissolved in blocking buffer (24 hours at 4°C).

After washing, the sections were incubated with appropriate fluorescently conjugated secondary antibodies (24 hours at 4°C), overlaid with a mixture of DAPI and mounting media (Vectashield), and imaged on a Leica SP3 confocal microscope. Motor neuron numbers were assessed in segments and the raw number extrapolated to the entire region based on the length and thickness of each section. Gem numbers were determined by counting intranuclear SMN-positive dot-like structures within ChAT-expressing motor neurons. Motor neuronal cytoplasmic SMN levels were determined by assessing the fluorescence intensity of the entire motor neuron and subtracting from it the fluorescence of the nucleus.

2.3.2 Neuromuscular Junction Analysis

NMJs were analyzed in the gastrocnemius, triceps, and intercostal muscles. Prior to tissue extraction, mice were perfused with 1× PBS and then specific dissected muscles were incubated in ice-cold methanol (5 mins), and teased to remove the fascia before being rinsed in ice-cold 1× PBS (10 mins). Samples were then incubated in blocking solution [3% bovine serum albumin (FBS), 1% Triton X-100 in PBS] overnight at 4°C to reduce non-specific binding of antibodies and treated with an anti-neurofilament (NF) antibody (1:1000, Millipore) for 2 days (4°C). After washing, the samples were incubated with Alexa 488-conjugated secondary antibody (1:500, Invitrogen) and Alexa-594 conjugated α-bungarotoxin (1:1000, Invitrogen). Excess antibody was washed off with PBS-T, samples mounted in Vectashield (Vector Labs) and NMJs imaged on a Leica TCS SP5 II confocal microscope (Leica Microsystems).

Pre-synaptic defects were quantified by determining the nerve terminal branch diameter. Specifically, the axon terminal was followed until it branched in the NMJ for the first time, and the widest portion of the branch in the distal half measured to determine levels of NF accumulation. Post-synaptic complexity was determined by the number of perforations per motor end-plate. Only *en face* endplates were included in the quantification. Perforations were defined as "holes," areas devoid of staining circumscribed by regions that either stained intensely or diffusely with labeled α-bungarotoxin. The number of acetylcholine receptor clusters exhibiting fragmentation was quantified. All of the NMJ analyses were performed on 300 or more NMJs from each mouse ($n \geq 4$).

2.3.3 Muscle Analysis

Animals were euthanized and whole muscle dissected, and flash-frozen in liquid nitrogen–cooled (N2) isopentane. Transverse sections (8-μm thick) from the belly of the muscle were cut on a cryostat (Leica) and the sections were stained with hematoxylin and eosin (H&E) as follows. Sections were fixed sequentially in 50%, 70%, 90% and 100% ethanol, rinsed in tap water (3x) and stained in Harris' Hematoxylin 53 (Sigma) for 30 s. The slides were then washed in tap water (3x), stained in Eosin (Sigma) for 20 s and rinsed in tap water (3x). This was followed by a step-wise dehydration in 50% (4x), 70% (4x), 90% (7x) and 100% (10x) ethanol, and clearing in Histoclear (Sigma) twice (10x each). The slides were mounted with Permount (Sigma). The myofiber cross-

sections were viewed with a Nikon Eclipse 800 microscope (Nikon Corporation, Japan) and imaged using a Nikon FDX-35 digital camera. Cardiac muscle pathology was similarly assessed from transverse sections cut at the level of the ventricles. Immunostains on muscle were performed on 8-μm–thick sections of tissue that were flash frozen as described above. The sections were blocked in blocking solution (3% BSA, 2% Triton-X 100) for 30 minutes (room temperature), and then incubated with muscle fiber specific antibodies dissolved in blocking solution. After washing, the sections were incubated in appropriate fluorescently conjugated secondary antibodies (24 hours at 4°C), overlaid with a mixture of DAPI and mounting media (Vectashield), and imaged. All of the muscle analyses were performed on 100 or more NMJs from each mouse ($n \geq 4$).

2.3.3.1 Myosin Heavy Chain antibodies

For contractile fiber type determination, and in order to detect slow and fast MyHC isoforms, the following antibodies were used:

Antibody Name	Antigen	Company	Concentration
BA-D5	MyHC I	DSHB, Iowa	1:10
SC-71	MyHC IIa	DSHB, Iowa	1:10
BF-F3	MyHC IIb	DSHB, Iowa	1:10
S5-8H2	MyHC I, IIx and IIb	DSHB, Iowa	1:10

Muscle immunostaining protocol was followed as described above.

2.3.3.2 Evans Blue Dye

Mice were intraperitoneal injected with a solution of 1% Evans Blue Dye (EBD) at a volume of 1% of body mass (BM) 1 mg EBD/0.1 mL PBS/10 gBM (Matsuda, 1995), referred to subsequently as the standard 1% EBD. Mice were sacrificed 24 hrs after injection. Muscles were prepared from frozen sections, and sectioned following the protocol previously described under "muscle analysis." The number of myofibers stained with EBD was observed by fluorescence microscopy and quantified.

2.3.3.3 Cardiotoxin

To determine how SMN-depleted muscle responded to traumatic injury, mice were anesthetized with 1%–2% Isoflurane, and myonecrosis was induced with cardiotoxin (CTX). A 30-gauge needle was used to inject 20 µl of a 10 µM solution of cardiotoxin (CTX), in PBS, into the belly of the gastrocnemius. Cardiotoxin was delivered uniformly into the muscles of the right hind limb. The left hind limb was injected with identical volumes of PBS. Mice were assessed at baseline point (no injections) and at various time points following CTX and PBS injections (*days 6*, *14*, *26*, $n = 4$/time point), and muscles of the hindlimb were removed, weighed, and immediately used to prepare tissue lysates and cryosections.

2.3.4 Morpholino antisense oligonucleotide treatment

The Morpholino sequence, numbered from the *SMN2* exon 7 donor site (shown below), was 5' ATTCACTTTCATAATGCTGG 3' (MWT = 8564, Gene Tools). The Scramble Morpholino sequence was 5' CCTCTTACCTCAGTTACAATTTATA 3' (MWT = 8328, Gene Tools). Morpholino antisense oligonucleotides were resuspended in sterile water, and aliquoted to a final concentration 0.5 mM. Stock solutions were stored at −20°C, and working solutions were stored at 4°C. Mutants and controls treated at PND210 with morpholino and scramble morpholino (injected IP) were analyzed 7 weeks post injections (12.5 mg oligo/kg of mouse) (n = 3).

Figure: Illustration of *SMN2* exon and intron 7 with highlighted ISS-N1 and the target site for morpholino (Porensky, 2012)

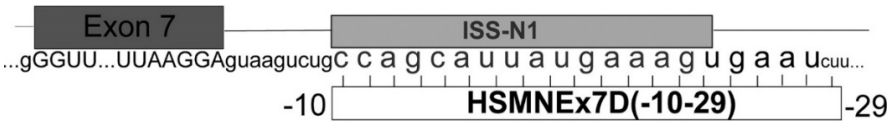

2.4 Behavioral Assays

2.4.1 Motor Behavior Assays

2.4.1.1 Forelimb and hindlimb strength

Forelimb and hindlimb strength were measured using the BIOSEB Grip Strength Tester BIO-GS3. Mice were allowed to grasp the bar by either just the forearms or with all limbs and then pulled by the

tail away from it until their grip was broken. The force applied at the moment of release was recorded by the machine as the maximal grip strength. Each mouse was subjected to 6 trials and the mean reported for the analysis ($n \geq 4$).

2.4.1.2 Righting ability

Righting reflex was used to estimate muscle strength in mutants and control littermates. Mice were placed on their backs, and latency to turn over and place all four paws on the bench top was recorded. The procedure was repeated thrice for each subject, and the best performance recorded as the righting ability score ($n \geq 4$).

2.4.2 Weight/survival

Survival of mice was determined by noting the day on which a mouse succumbed to the disease or had to be euthanized due to disease conditions, such as poor response to touch, a failure to eat/drink, inability to groom, or 20% or greater loss of body weight. Survival data were plotted as Kaplan-Meier curves. Mice were weighed as required ($n \geq 4$).

2.5 Statistical analysis

Muscle fiber type distribution and cross-sectional areas are expressed as means and standard error of the mean. Statistical significance of the differences between means was assessed by analysis of variance (ANOVA). Statistics for Kaplan-Meier survival curves were compared and assessed for differences using the log-rank test

equivalent to the Mantel-Haenszel test. The unpaired 2-tailed Student's t test or 1-way ANOVA followed by Tukey's post hoc comparison, where indicated, was used to compare means for statistical differences. Data in the manuscript are represented as mean ± SEM unless otherwise indicated. $P < 0.05$ was considered significant. Statistical analyses were performed with GraphPad Prism v4.0 (GraphPad Software).

Chapter 3

Results

3.1 Model mice to examine effects of low SMN specifically in muscle.

The *SMN2* gene is unique to humans and always present in at least one copy in SMA patients. Rodents possess a single *Smn* gene, which is the equivalent of human *SMN1*. To genetically mimic human SMA in rodents, we crossed previously reported Smn^{F7} mice, which harbor a floxed exon 7 allele (Miniou *et al.*, 1999) with animals heterozygous for an *Smn* null allele (disrupted in exon 2A - Smn^{KO} or Smn^{-}). This resulted in $Smn^{F7/-}$ mice (Figure 3.1A). $Smn^{F7/-}$ animals were subsequently crossed with mice carrying the *SMN2* transgene (Monani *et al.*, 2000) (Figure 3.1B). The *SMN2*; $Smn^{F7/-}$ were then crossed with heterozygous MyoDiCre mice (Chen *et al.*, 2005), resulting in *MyoDiCre; SMN2;* $Smn^{F7/-}$ animals (Figure 3.1C). In this manner, we generated mice without *SMN2*, with 1 copy of *SMN2*, and with two copies of *SMN2* for analysis (*MyoDiCre;* $SMN2^{-/-}$*;* $Smn^{F7/-}$, *MyoDiCre;* $SMN2^{+/-}$*;* $Smn^{F7/-}$ and *MyoDiCre;* $SMN2^{+/+}$*;* $Smn^{F7/-}$ respectively). As shown in Figure 3.1D, upon activation of Cre, exon 7 of the floxed allele gets deleted resulting in the $Smn^{\Delta 7}$ state. $Smn^{\Delta 7}$ produces an unstable protein. Thus, in the presence of

SMN2, this situation mimics the low levels of SMN protein in tissues (skeletal muscle) where the Cre is expressed.

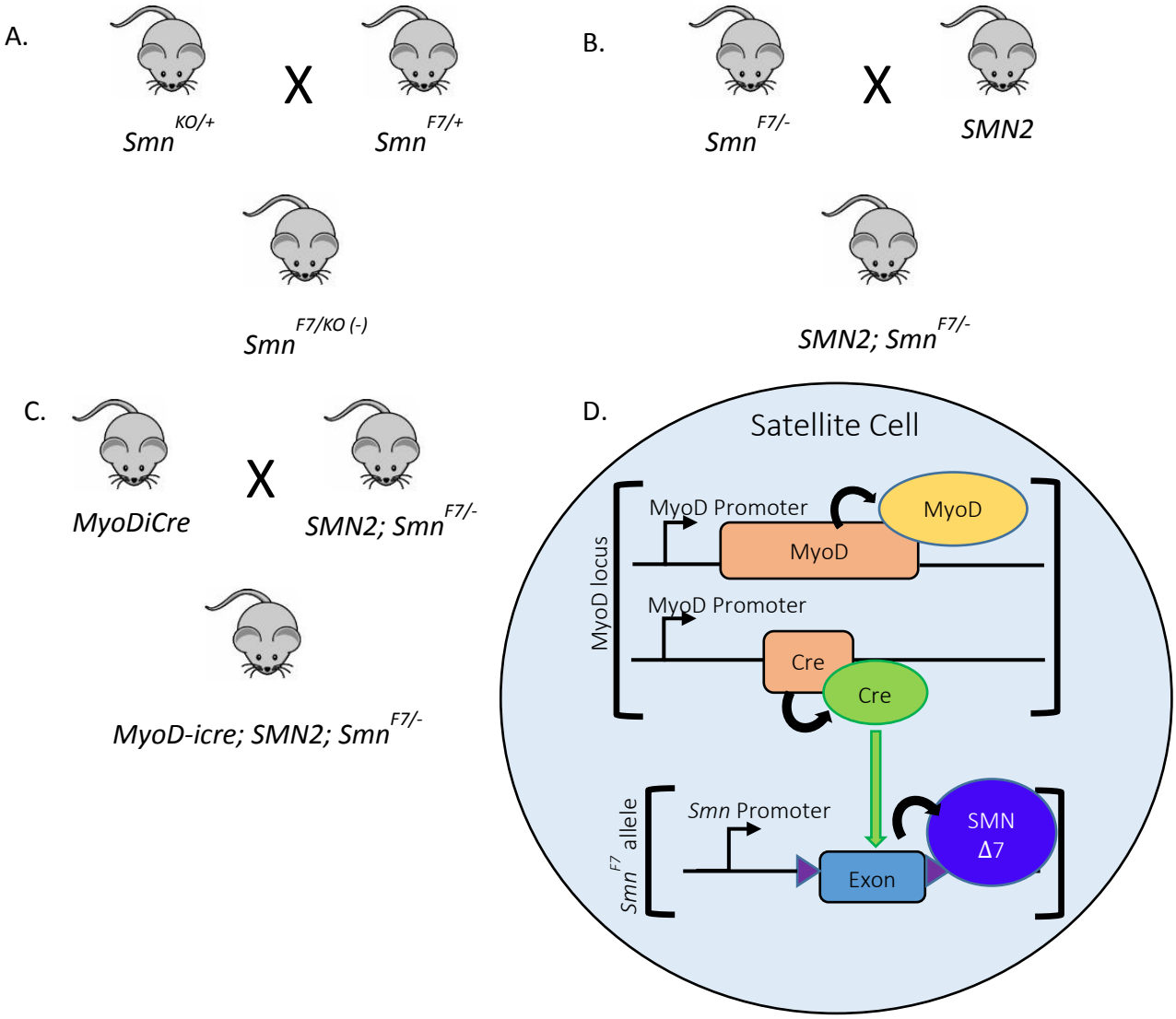

Figure 3.1 Model mice to examine effects of low SMN specifically in muscle. **(A)** Diagram of cross made in order to

generate $Smn^{F7/-}$ mice. **(B)** Diagram depicting the addition of the *SMN*2 transgene to the $Smn^{F7/-}$ line. **(C)** The *SMN2*; $Smn^{F7/-}$ mice were then crossed with heterozygous MyoDiCre mice, resulting in *MyoDiCre; SMN2;* $Smn^{F7/-}$ animals. **(D)** Upon activation of Cre, exon 7 gets deleted resulting in $Smn^{\Delta 7}$ in tissues expressing the Cre.

3.1.1 MyoDiCre driver leads to recombination specifically in skeletal muscle.

In order to investigate the role of the SMN protein specifically in skeletal muscle tissue, we took advantage of a previously reported Cre knock-in allele at the MyoD locus (Yamamoto *et al*., 2009). We chose MyoD because it is one of the earliest markers of myogenic commitment, expressed by embryonic day E10.5 (Wood *et al*., 2013). Therefore, SMN protein will be reduced in skeletal muscle at the earliest stages of muscle development. Mice carrying *Smn* exon 7 flanked by two loxP sites (Smn^{F7}) were crossed with mice harboring the *Cre* recombinase transgene driven by the promoter of the MyoD gene. To detect Cre mediated recombination at the Smn^{F7} locus, primers PHR5 and GS8 (Frugier *et al.*, 2000) were used to amplify a 460bp fragment (Figure 3.1.1A). The efficiency of recombination (~89%) was further determined by quantitative PCR analysis. Cre recombination driven by another skeletal muscle specific promoter, Human Skeletal Actin (HSA), resulted in a much lower recombination frequency of ~62% (Figure 3.1.2B). Leaky Cre expression as assessed by the presence/absence of the $Smn^{\Delta 7}$ band was not observed in any of the MyoDiCre mutant mice. To assay SMN protein levels in MyoDiCre SMA mutants (*MyoDiCre; SMN2;*

Smn$^{F7/-}$) western blot analyses were performed on tissue from mutants (*MyoDiCre; SMN2*$^{+/+}$*; Smn*$^{F7/-}$) and age-matched controls (*SMN2*$^{+/+}$*; Smn*$^{F7/-}$). As expected, there was a dramatic reduction of protein in skeletal muscle, but not in other tissues (Figure 3.1.1B and C). These results confirm the efficiency and specificity with which the MyoDicre line targets the *Smn*^{F7} locus in skeletal muscle.

To further characterize cell-type specify of the MyoDiCre transgenic line, and to determine if the Cre expression is limited to skeletal muscle, we bred our mice with ROSA26-YFP (Jax stock no. 006148; The Jackson Laboratory) reporter mice (Srinivas *et al.*, 2001). In Rosa26-YFP animals, the expression of EYFP (Enhanced Yellow Fluorescent Protein) is blocked by an upstream loxP-flanked STOP sequence. When bred with the MyoDiCre animals, the STOP sequence is deleted in the tissue of interest (skeletal muscle), and EYFP expression is observed. Muscle sections of the gastrocnemius from ROSA26-YFP mice harboring the MyoDiCre transgene were prepared and examined for the presence of fluorescence. MyoDiCre mice harboring the ROSA26-YFP marker expressed robust YFP in their muscle fibers while age-matched controls lacking MyoDiCre did not (Figure 3.1.2A). These findings further demonstrate that MyoDiCre mediated recombination is specific to skeletal muscle tissue.

A.

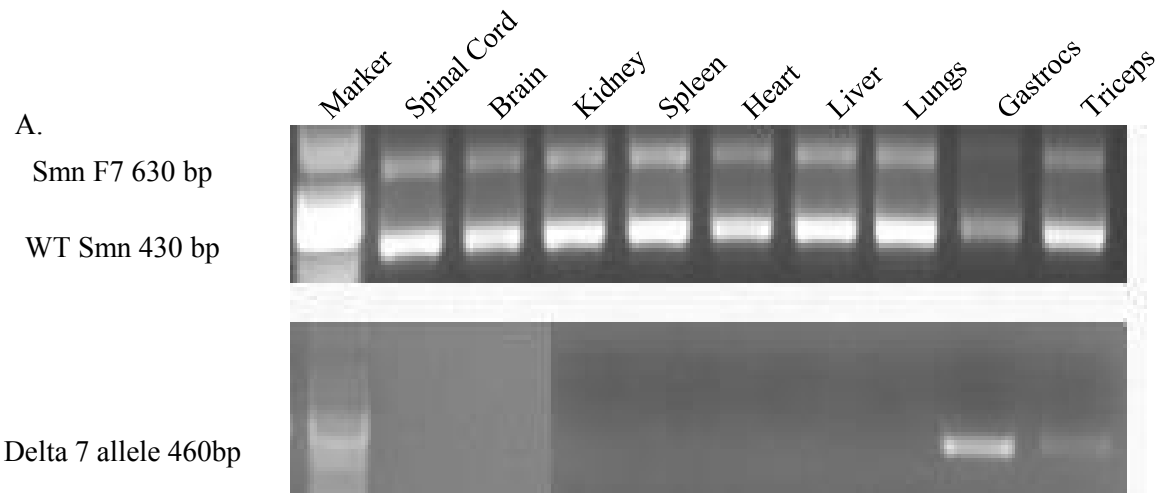
Marker
Spinal Cord
Brain
Kidney
Spleen
Heart
Liver
Lungs
Gastrocs
Triceps
Smn F7 630 bp
WT Smn 430 bp
Delta 7 allele 460bp

B.

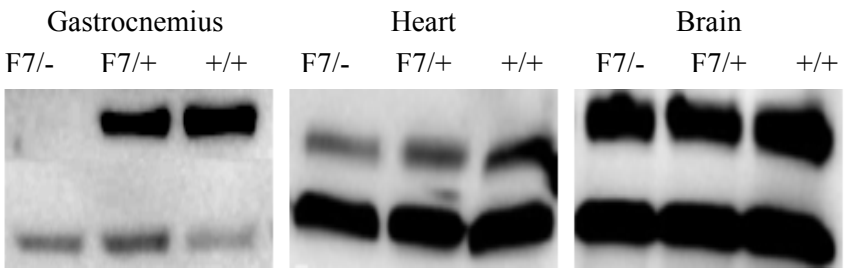
Gastrocnemius
Heart
Brain
F7/-
F7/+
+/+
F7/-
F7/+
+/+
F7/-
F7/+
+/+

C.

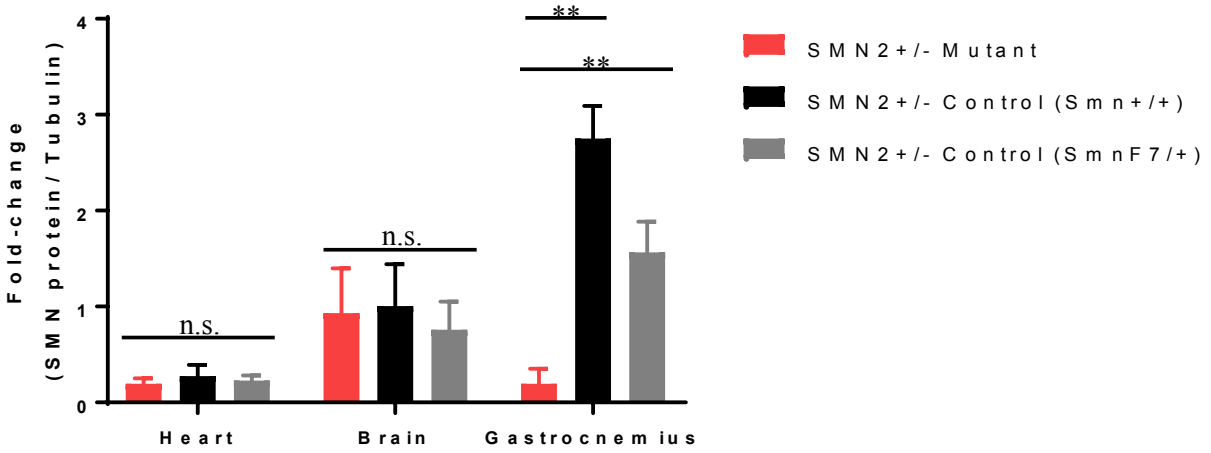
Fold-change (SMN protein/Tubulin)
0
1
2
3
4
n.s.
n.s.
**
**
Heart
Brain
Gastrocnemius
SMN2+/- Mutant
SMN2+/- Control (Smn+/+)
SMN2+/- Control (SmnF7/+)

Figure 3.1.1 MyoDiCre driver induces recombination at the Smn^{F7} locus specifically in skeletal muscle. **(A)** After PCR analysis of spinal cord, brain, kidney, spleen, liver, heart, gastrocnemius and triceps of mutant mice, MyoDiCre expression was confirmed to be specific to skeletal muscle. **(B)** Representative western blot of SMN protein showed heart and brain to express normal levels of SMN protein, while skeletal muscle SMN levels were lower in the mutants. **(C)** Quantified results of western blot of SMN protein ($n \geq 4$, $^{**}p < 0.01$, unpaired 2-tailed Student's t test).

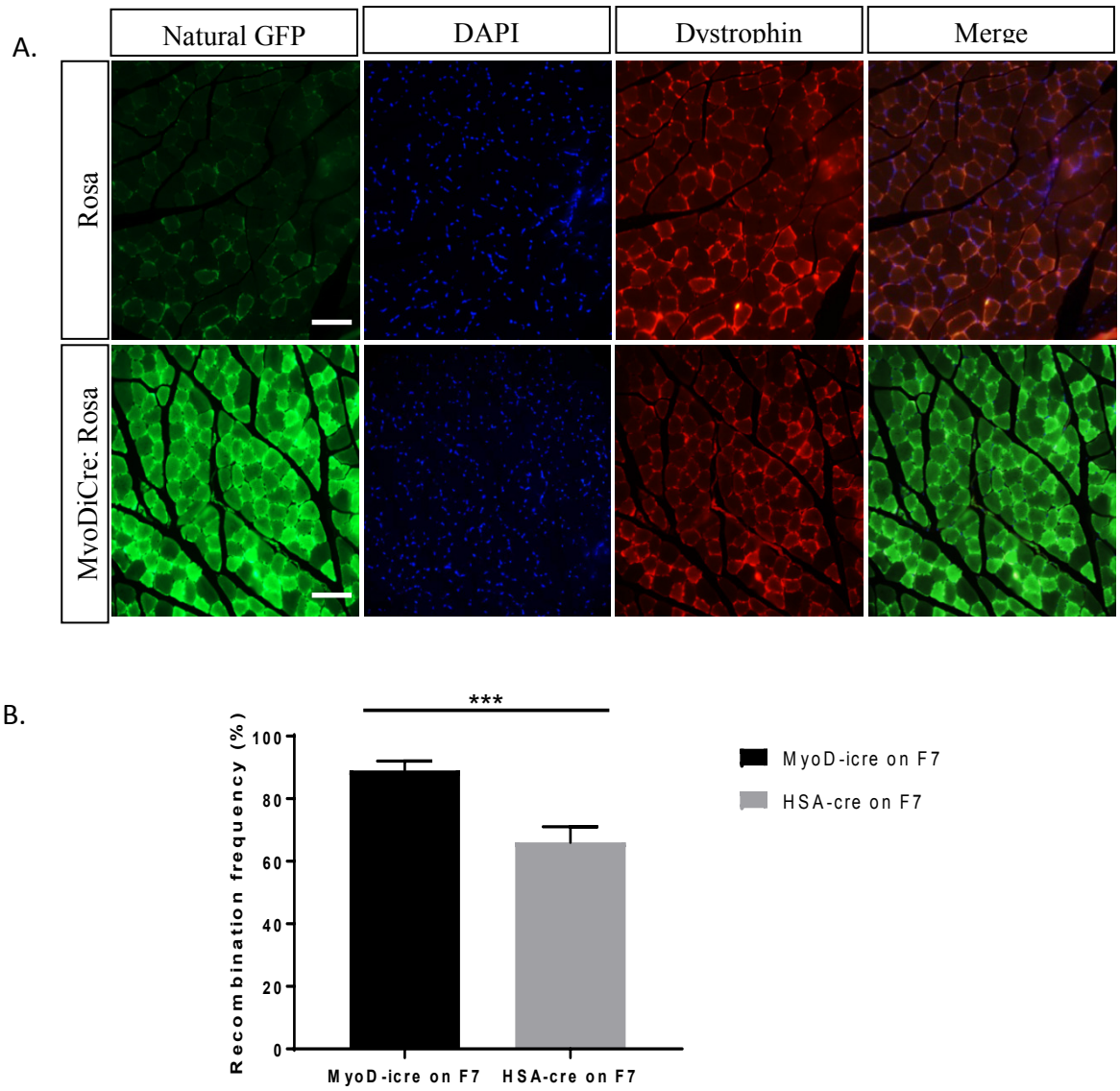

Figure 3.1.2 MyoDiCre driver leads to recombination of floxed alleles specifically in skeletal muscle. **(A)** Muscle sections of the gastrocnemius from ROSA26-YFP mice harboring the MyoDiCre transgene were prepared and examined for the presence of fluorescence. MyoDiCre mice harboring the ROSA26-YFP

marker expressed robust YFP in their muscle fibers while age-matched controls lacking MyoDiCre did not (Scale bar = 85 μm). **(B)** Quantitative PCR performed on skeletal muscle also revealed a Cre-mediated recombination rate at the Smn^{F7} locus of ~89%. In contrast, Cre recombination driven by another skeletal muscle specific promoter, Human Skeletal Actin (HSA), resulted in a recombination frequency of ~62% ($n \geq 4$, ***$p < 0.001$, unpaired 2-tailed Student's t test).

3.2 Selective depletion of SMN in skeletal muscle triggers an overt SMA phenotype.

We found that the MyoDiCre driver selectively depleted SMN protein in skeletal muscle. Thus *MyoDiCre;* $SMN2^{-/-}$*;* $Smn^{F7/-}$*,* and *MyoDiCre;* $SMN2^{+/-}$*;* $Smn^{F7/-}$*, MyoDiCre;* $SMN2^{+/+}$*;* $Smm^{F7/-}$ mutants all displayed deletion of exon 7 of the floxed *Smn* allele in the skeletal muscle. In such situations, the muscle becomes reliant on the SMN produced by the *SMN2* gene (and $Smn^{\Delta 7}$). On examining MyoDiCre animals with 2 copies of *SMN2* (hereafter referred to as $SMN2^{+/+}$ mutants and $SMN2^{+/+}$ controls), we found that $SMN2^{+/+}$ mutant mice appeared phenotypically normal, showing no overt signs of necrosis or muscular weakness. They furthermore exhibited normal survival (Figure 3.2A) and weight compared to controls ($SMN2^{+/+}$; $Smn^{F7/-}$) (Figure 3.2B). $SMN2^{+/+}$ mutants (*MyoDiCre;* $SMN2^{+/+}$*;* $Smn^{F7/-}$) also showed no deficit in righting reflex as pups (Figure 3.2C). In contrast, MyoDiCre mutants with 1 copy of *SMN2* (hereafter referred to as $SMN2^{+/-}$ mutants) showed overt signs of muscle weakness and atrophy compared to controls ($SMN2^{+/-}$; $Smn^{F7/-}$). They had a decrease in survival with a mean of PND21 (Figure 3.2A) and a significant

decrease in weight starting at PND1 (Figure 3.2B) compared to *SMN2*$^{+/+}$ mutants (*MyoDiCre; SMN2*$^{+/+}$*; Smn*$^{F7/-}$) and their respective controls (*SMN2*$^{+/+}$; *Smn*$^{F7/-}$). Furthermore, *SMN2*$^{+/-}$ mutants show a deficit in righting reflex between PND4-PND7, which is then most likely rescued by intact levels of SMN protein outside of skeletal muscle (i.e. motor neurons) (Figure 3.2C). MyoDiCre mutants without *SMN2* (hereafter referred to as *SMN2*$^{-/-}$ mutants) were all found dead at PND0 (Figure 3.2A).

A.

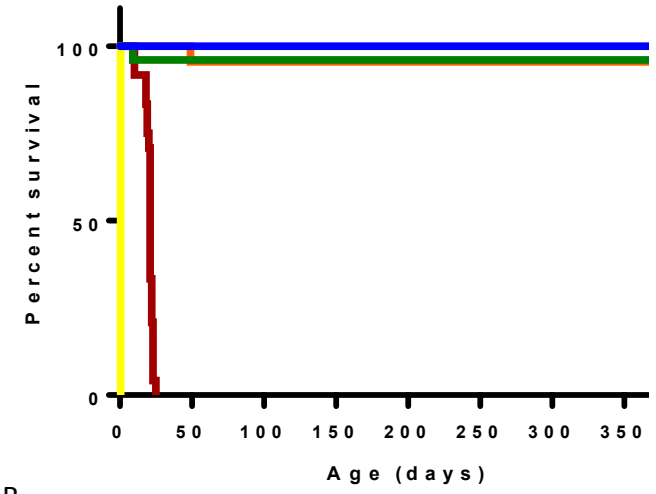
Percent survival
100
50
0
0
50
100
150
200
250
300
350
Age (days)

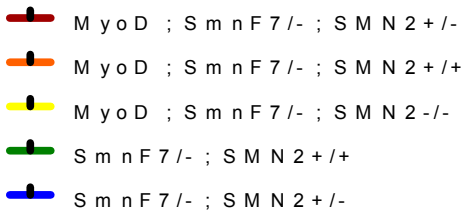
MyoD ; SmnF7/- ; SMN2+/-
MyoD ; SmnF7/- ; SMN2+/+
MyoD ; SmnF7/- ; SMN2-/-
SmnF7/- ; SMN2+/+
SmnF7/- ; SMN2+/-

B.

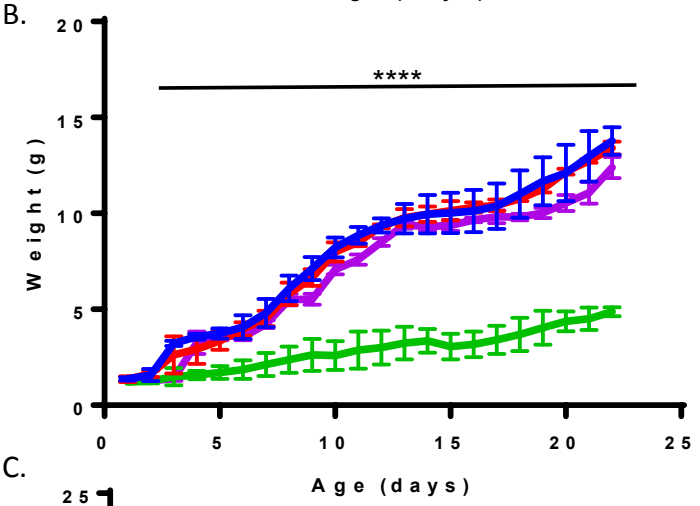
Weight (g)
20
15
10
5
0
****
0
5
10
15
20
25
Age (days)

C.

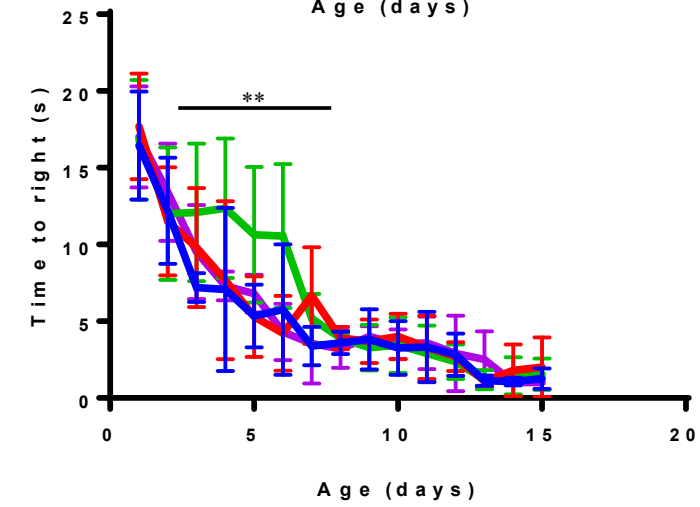
Time to right (s)
25
20
15
10
5
0
**
0
5
10
15
20
Age (days)

Figure 3.2 Selective depletion of SMN in skeletal muscle triggers an overt disease phenotype. **(A)** MyoDiCre mutants with 2 copies of *SMN2* showed normal survival compared to controls (n =18, p>0.05, log-rank test). In contrast, MyoDiCre mutants with 1 copy of *SMN2* showed overt signs of muscle weakness and atrophy. They had a decrease in survival with a mean of PND21 (n=27, ****p<0.0001, log-rank test). MyoDiCre mutants without *SMN2* were all found dead at PND0 (n=19). **(B)** $SMN2^{+/+}$ mutants showed normal weights compared to controls between PND0-PND21 (n=22, p>0.05, unpaired 2-tailed Student's t test). $SMN2^{+/-}$ mutants showed significant decrease in weight starting at PND1 (n=27, ****p<0.0001, unpaired 2-tailed Student's t test) compared to $SMN2^{+/+}$ mutants and their respective controls. **(C)** $SMN2^{+/+}$ mutants also showed no deficit in righting reflex as pups from PND0-PND15 (n=18, p>0.05, unpaired 2-tailed Student's t test). Furthermore, $SMN2^{+/-}$ mutants show a deficit in righting reflex between PND4-PND6, which is then rescued by PND7 (n=18, **p<0.01, unpaired 2-tailed Student's t test).

3.3 Muscle Analysis

3.3.1 Selective depletion of SMN in skeletal muscle decreases fiber size in $SMN2^{+/-}$ mutants.

Considering our attempt to selectively deplete SMN in skeletal muscle, we initiated our neuropathological analysis of the various mutant mice by examining this tissue. We began by studying the muscle fiber size of our $SMN2^{+/-}$ mutants. The muscle morphology was examined by H&E staining of the gastrocnemius, biceps, triceps, and intercostal muscles (Figure 3.3.1A-D) at PND21. The mean fiber

size (Figure 3.3.1E) and fiber size distribution (Figure 3.3.1A-D) was plotted for each group. The fiber size and number of our *SMN2*$^{+/-}$ mutants (*MyoDiCre; SMN2*$^{+/-}$*; Smn*$^{F7/-}$) was determined to be smaller than the control (*SMN2*$^{+/-}$; *Smn*$^{F7/-}$). This suggests that normal levels of SMN protein in skeletal muscle is required for proper muscle morphology.

While we did not expect there to be an effect in the muscle fibers of the heart, as MyoD is specific to skeletal muscle, we nevertheless confirmed that cardiac muscle was left intact. There was no significant difference found in the left ventricle wall thickness or in fiber area distribution between *SMN2*$^{+/-}$ mutant and control mice (Figure 3.3.1.1). This indicates that MyoDiCre driven recombination of the *Smn*^{F7} allele does not occur in smooth muscle of mutants, and does not affect the heart.

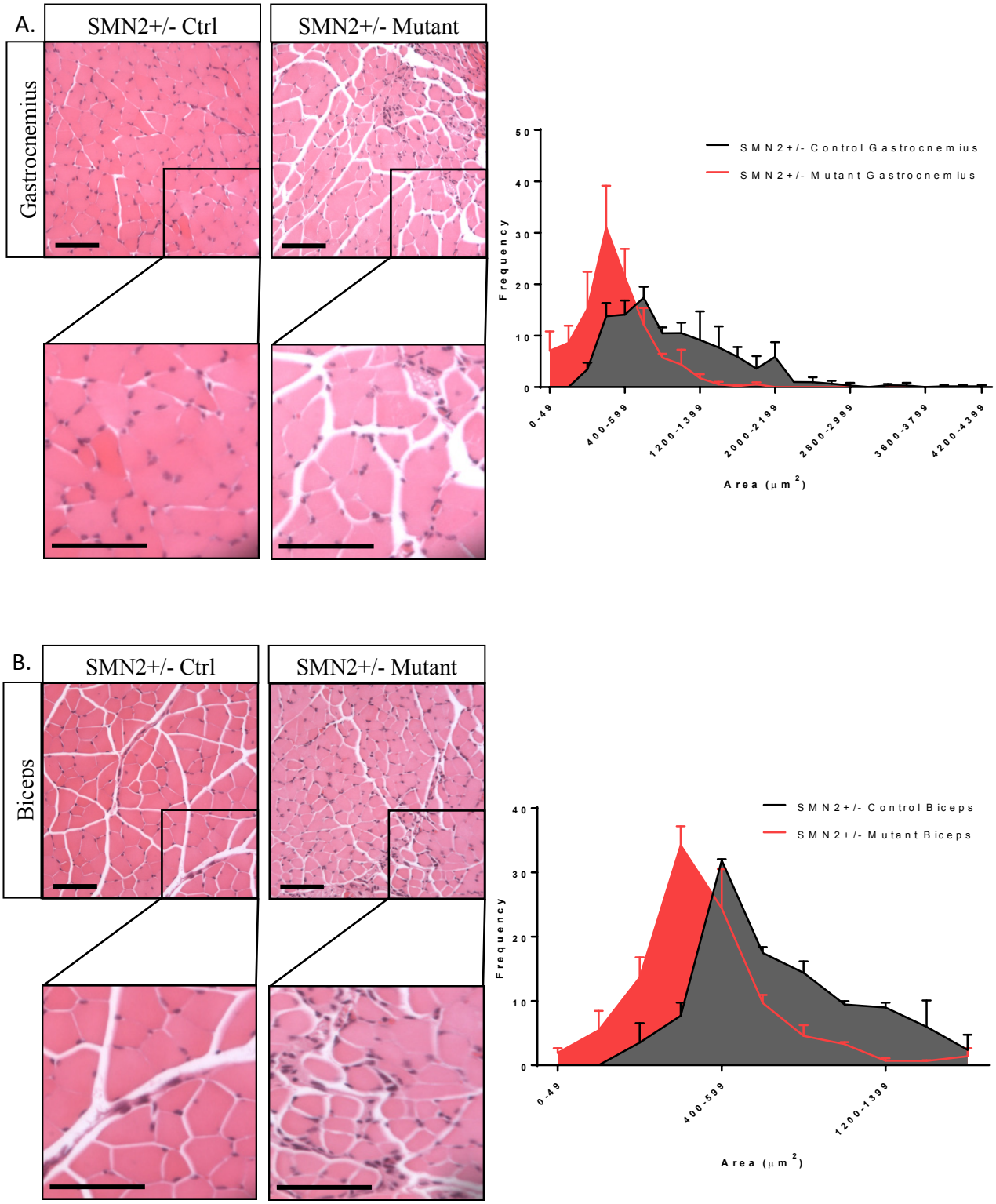
A.
SMN2+/- Ctrl
SMN2+/- Mutant
Gastrocnemius
SMN2+/- Control Gastrocnemius
SMN2+/- Mutant Gastrocnemius
Frequency
0
10
20
30
40
50
0-49
400-599
1200-1399
2000-2199
2800-2999
3600-3799
4200-4399
Area (μm²)
B.
SMN2+/- Ctrl
SMN2+/- Mutant
Biceps
SMN2+/- Control Biceps
SMN2+/- Mutant Biceps
Frequency
0
10
20
30
40
0-49
400-599
1200-1399
Area (μm²)

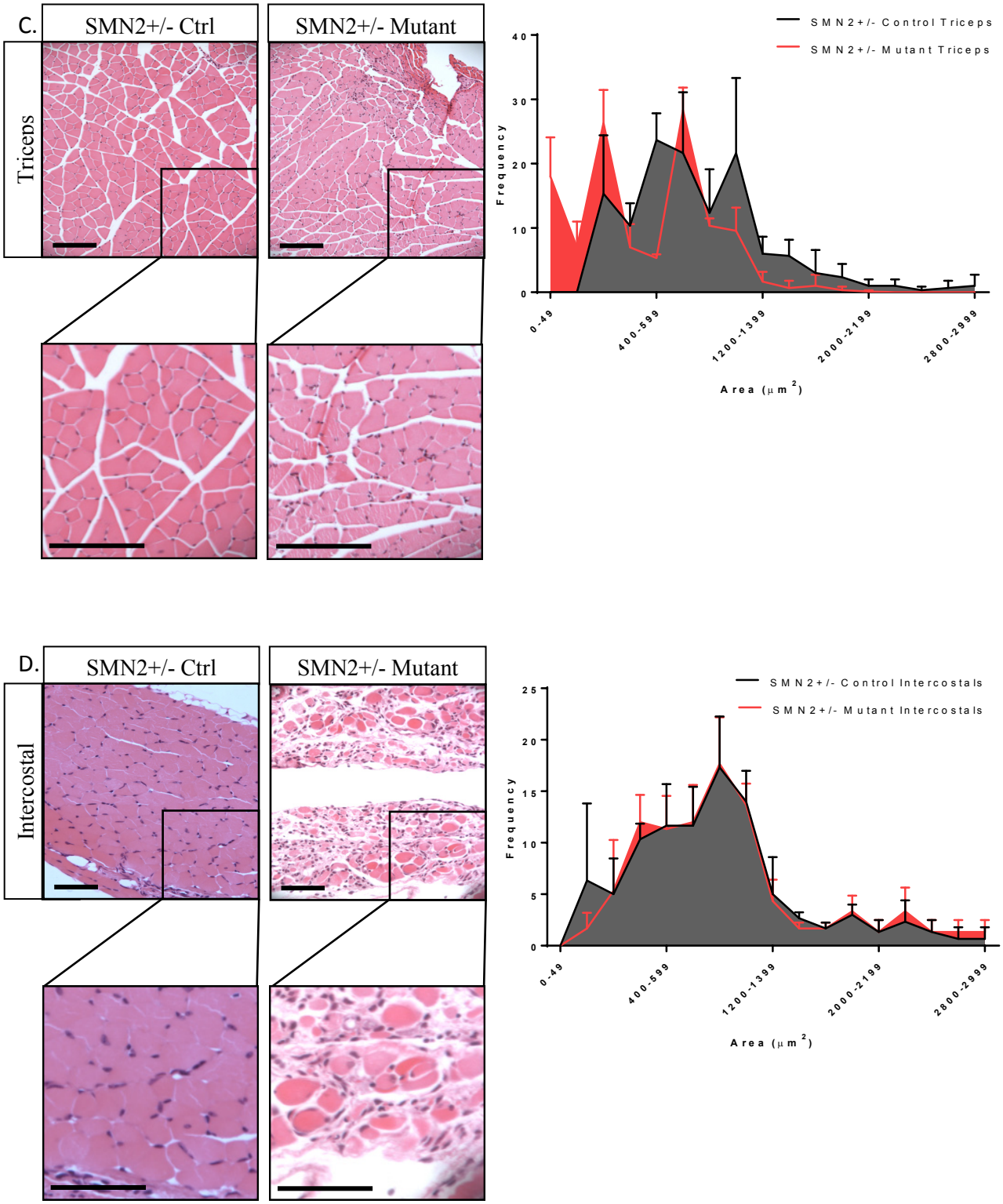
C.
SMN2+/- Ctrl
SMN2+/- Mutant
Triceps
SMN2+/- Control Triceps
SMN2+/- Mutant Triceps
Frequency
40
30
20
10
0
0-49
400-599
1200-1399
2000-2199
2800-2999
Area (μm²)
D.
SMN2+/- Ctrl
SMN2+/- Mutant
Intercostal
SMN2+/- Control Intercostals
SMN2+/- Mutant Intercostals
Frequency
25
20
15
10
5
0
0-49
400-599
1200-1399
2000-2199
2800-2999
Area (μm²)

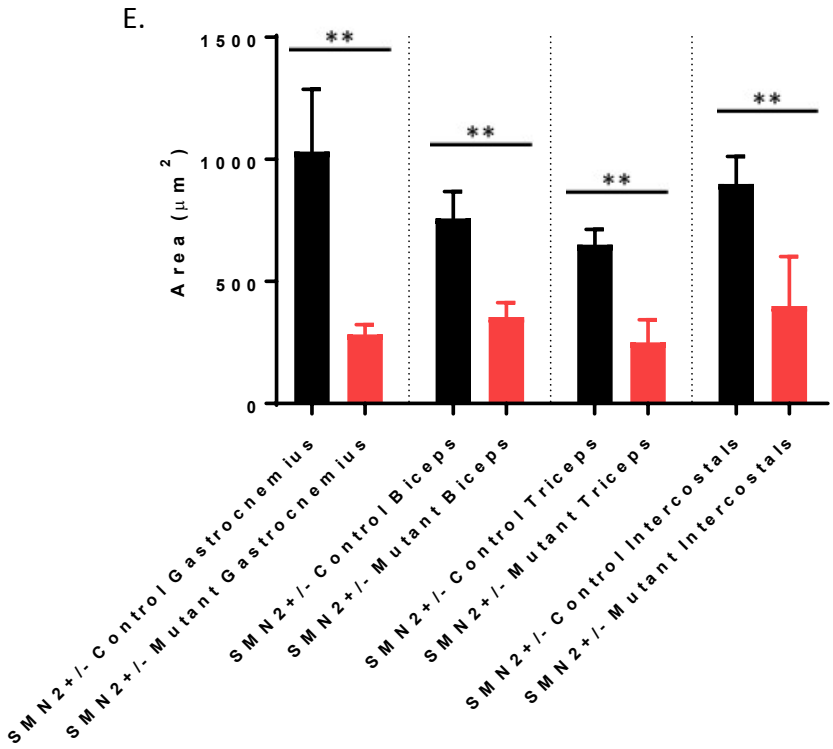

Figure 3.3.1 Selective depletion of SMN in skeletal muscle decreases fiber size in *SMN2*$^{+/-}$ mutants. **(A, B, C, D)** Representative pictures of muscle sections after H&E staining, along with fiber area distribution. Graph of fiber distribution shows that mutant data is skewed to the left, indicative of *SMN2*$^{+/-}$ mutants (red) generally having a greater number of fibers with a smaller area size compared to control (black) **(E)** Average muscle fiber size of the gastrocnemius, biceps, triceps, and intercostal were smaller in the *SMN2*$^{+/-}$ mutants (red) than in controls (black) at PND21 (n=9, **p<0.01, unpaired 2-tailed Student's t test) (Scale bar = 150 μm).

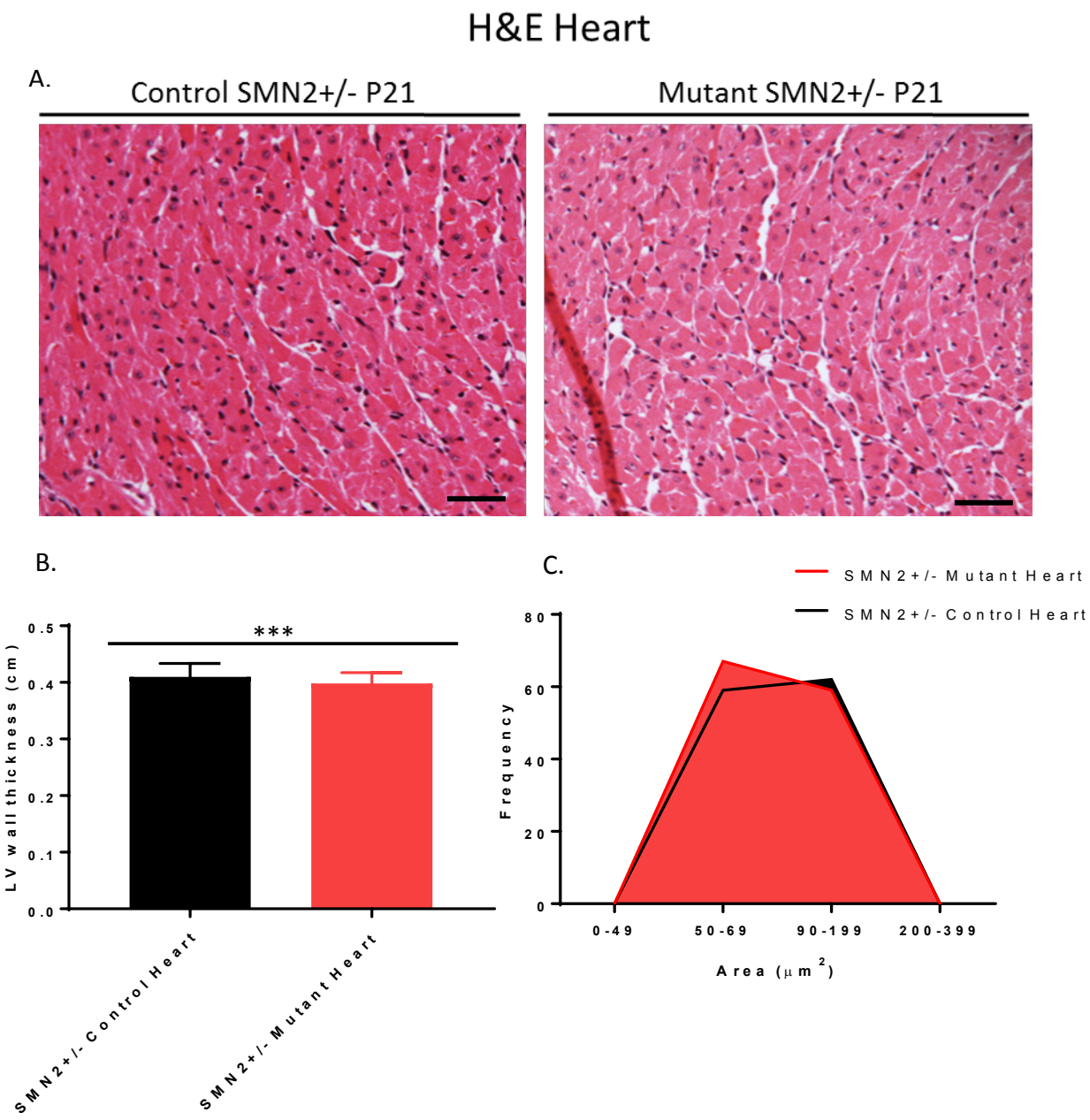
H&E Heart
A.
Control SMN2+/- P21
Mutant SMN2+/- P21
B.
***
LV wall thickness (cm)
0.5
0.4
0.3
0.2
0.1
0.0
SMN2+/- Control Heart
SMN2+/- Mutant Heart
C.
SMN2+/- Mutant Heart
SMN2+/- Control Heart
Frequency
80
60
40
20
0
0-49
50-69
90-199
200-399
Area (μm²)

Figure 3.3.1.1 MyoDiCre driven recombination of the *Smn*$^{F7/-}$ allele does not occur in the heart. **(A)** Representative picture of heart fibers in *SMN2*$^{+/-}$ mutants (*MyoDiCre; SMN2*$^{+/-}$*; Smn*$^{F7/-}$) and controls (*SMN2*$^{+/-}$*; Smn*$^{F7/-}$) at PND21. **(B)** There is no significant difference in left ventricle wall thickness between *SMN2*$^{+/-}$ mutant (red) and control (black) (n=4, $p>0.05$, unpaired 2-tailed Student's t test). **(C)** There is no significant difference between fiber area distribution between *SMN2*$^{+/-}$ mutant (red) and control (black) (n=4, $p>0.05$, unpaired 2-tailed Student's t test) (Scale bar = 118 μm).

3.3.2 *SMN2*$^{+/-}$ mutants do not show signs of muscle fiber regeneration.

In the *SMN2*$^{+/+}$ mutants where the motor neurons are intact, we saw evidence of degeneration and regeneration of skeletal muscle fibers. The regeneration was marked by centralized nuclei (Figure 3.3.2A and B). Surprisingly in the *SMN2*$^{+/-}$ mutants, we did not see evidence of any degeneration and regeneration (Figure 3.3.2A and C). For instance, we observed no central nuclei in muscle tissue of *SMN2*$^{+/-}$ mutants. However, *SMN2*$^{+/-}$ mutants had fewer muscle fibers than controls at PND5, and progressively lost them until their death at around PND21 (Figure 3.3.2D). This suggests that 1 copy of *SMN2* in skeletal muscle is not sufficient for regeneration. In contrast, when we look at aged mutants with two copies of the *SMN2* gene, there is a remarkable increase of fibers containing centralized nuclei compared to the control mice. In addition, the vast majority of fibers present in the *SMN2*$^{+/+}$ mutants have more than one centralized nuclei (mean number of centralized nuclei = 1.56, n=6, $p<0.001$) (Figure

3.3.2B). It should be noted however, that centralized nuclei is not a prominent feature of SMA muscle biopsies (Dubowitz, 1985), although it is seen in mild forms of the disease (mild Type III and IV). This could be explained by the fact that mild SMA patients live longer, and therefore may have enough time to display this phenotype.

A.

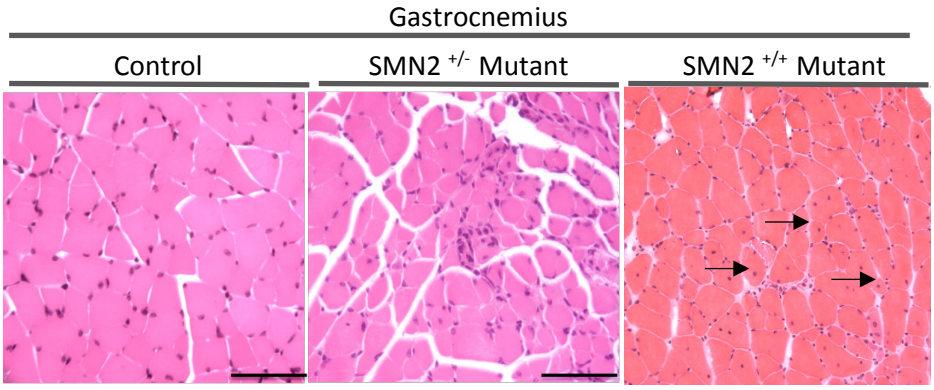
Gastrocnemius
Control
SMN2 +/- Mutant
SMN2 +/+ Mutant

B.

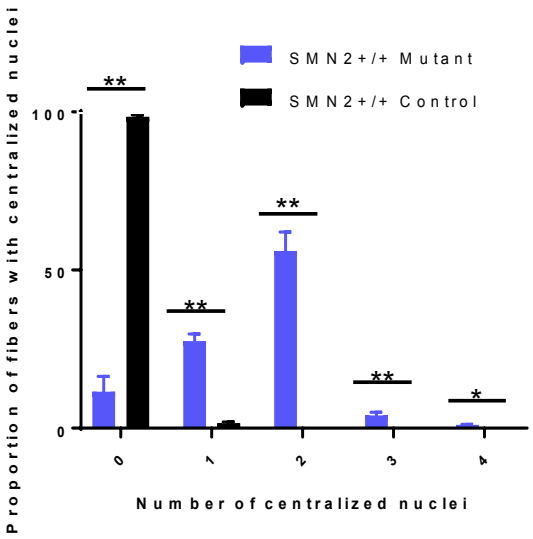
SMN2+/+ Mutant
SMN2+/+ Control
Proportion of fibers with centralized nuclei
Number of centralized nuclei
**
**
**
**
*

C.

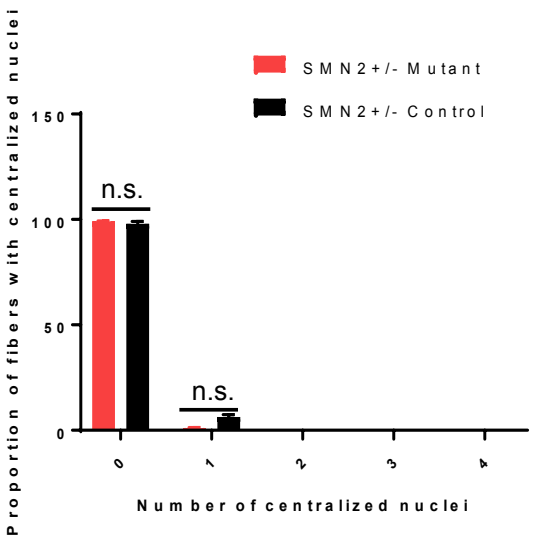
SMN2+/- Mutant
SMN2+/- Control
Proportion of fibers with centralized nuclei
Number of centralized nuclei
n.s.
n.s.

D.

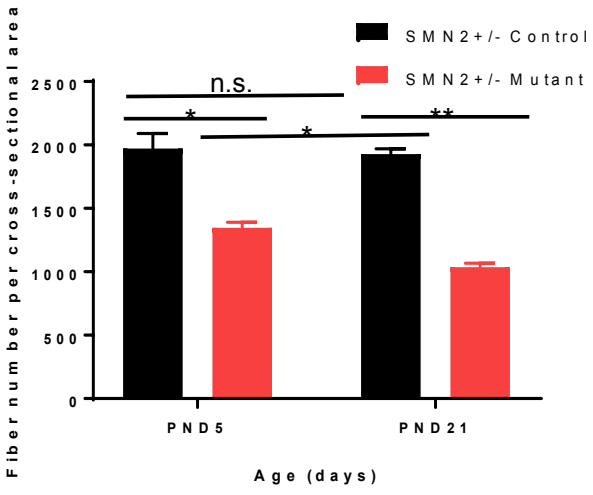
SMN2+/- Control
SMN2+/- Mutant
Fiber number per cross-sectional area
Age (days)
PND5
PND21
n.s.
*
*
**

`

Figure 3.3.2. *SMN2*$^{+/-}$ mutants do not show signs of muscle fiber regeneration. **(A)** Representative pictures of muscle of control and *SMN2*$^{+/-}$ mutant at PND21, and *SMN2*$^{+/+}$ mutant at PND210. **(B)** *SMN2*$^{+/+}$ mutants (blue) start showing centralized nuclei at 6 months of age, with a greater proportion of fibers having multiple centralized nuclei (black arrows); mean number of centralized nuclei = 1.56, n=6, ***p<0.001, **p<0.01, *p<0.05, unpaired 2-tailed Student's t test) **(C)** Even at end stage, *SMN2*$^{+/-}$ mutants (red) show decreased fiber size, but no evidence of centralized nuclei (mean number of centralized nuclei = 0.01, n=6, p>0.05, unpaired 2-tailed Student's t test). **(D)** *SMN2*$^{+/-}$ mutants had fewer muscle fibers than controls at PND5 (n=3, *p<0.05, unpaired 2-tailed Student's t test), and progressively lost them until their death around PND21 (n=3, **p<0.01, unpaired 2-tailed Student's t test) (Scale bar = 150 μm).

3.3.3 Loss of muscle at PND210 following restricted depletion of SMN in the tissue.

SMN2$^{+/+}$ mutant mice clearly undergo muscle regeneration, but they also exhibit a decrease in number of muscle fibers, along with a decrease in weight of skeletal muscle. Thus, the weight of gastrocnemius and tibialis anterior, were significantly lower in *SMN2*$^{+/+}$ mutants compared to controls (Figure 3.3.3A and B). In contrast, the weight of the soleus muscle was significantly higher in *SMN2*$^{+/+}$ mutants compared to controls (Figure 3.3.3C). This phenomenon has been observed in other muscular diseases such as Duchenne Muscular Dystrophy (DMD), where some muscles, especially the calves, are larger due to compensatory hypertrophy of non-affected myofibers and increased fat content of muscle (Papa *et al.*, 2016). It is important to note that the decrease in fiber number and change in muscle weight in the *SMN2*$^{+/+}$ mutant mice is progressive, as there is no significant difference between mutants and controls in either parameter at PND21 (Figure 3.3.3.1).

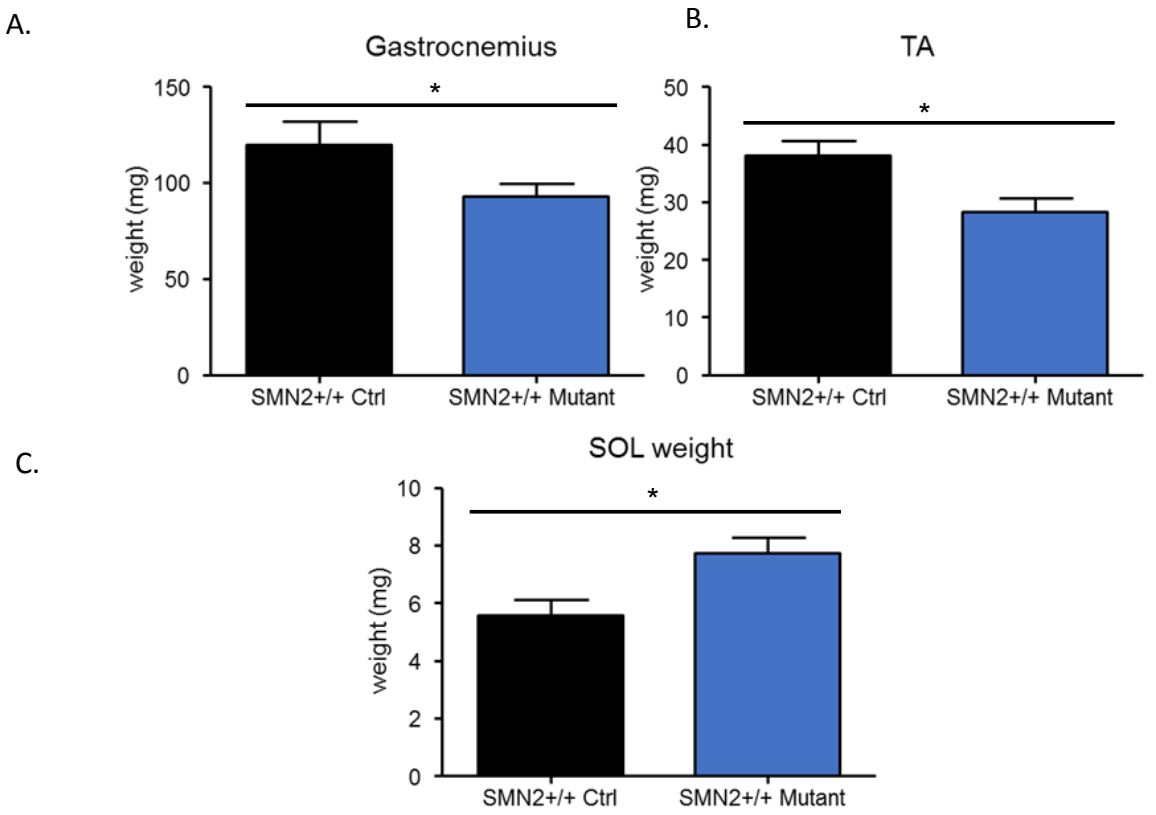

Figure 3.3.3 Loss of muscle at PND210 following restricted depletion of SMN in the tissue. **(A)** Weight of gastrocnemius in *SMN2*$^{+/+}$ mutant (blue) is significantly lower than control (black) (n=4, *p<0.05, unpaired 2-tailed Student's t test). **(B)** Weight of tibialis anterior in *SMN2*$^{+/+}$ mutant (blue) is significantly lower than control (black) (n=4, *p<0.05, unpaired 2-tailed Student's t test). **(C)** Weight of soleus in *SMN2*$^{+/+}$ mutant (blue) is significantly greater than control (black) (n=4, *p<0.05, unpaired 2-tailed Student's t test).

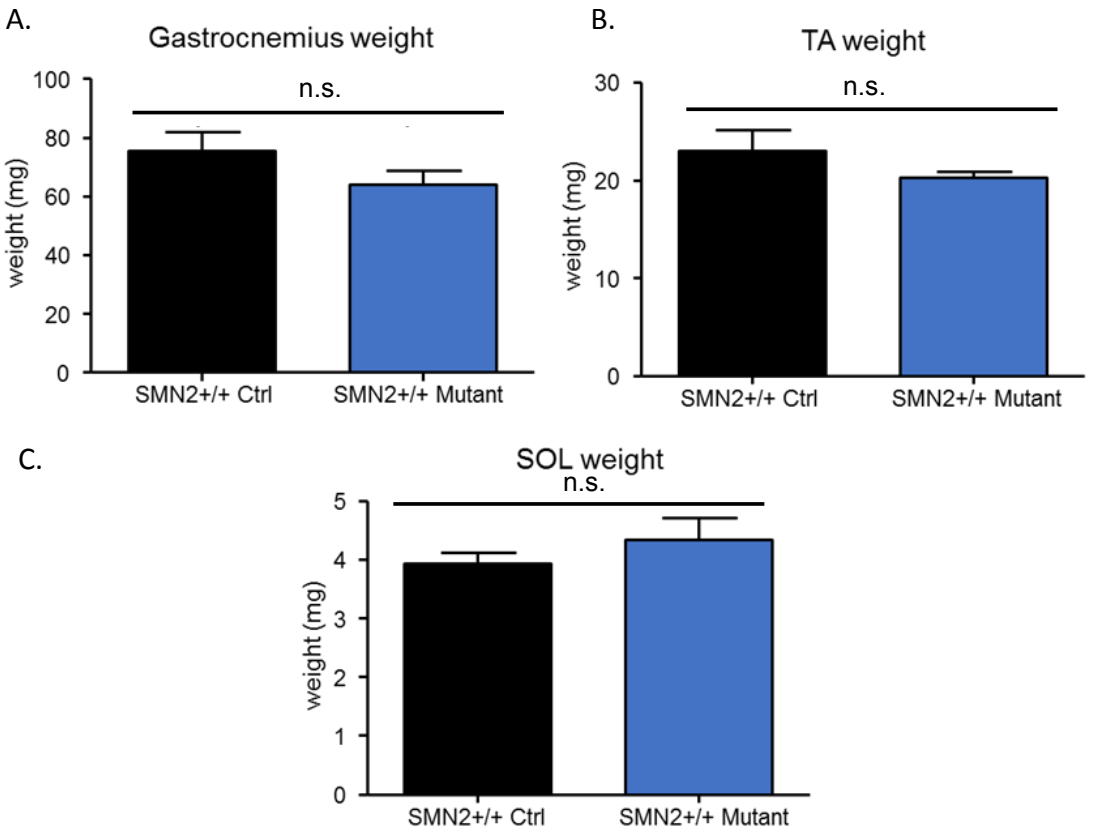

Figure 3.3.3.1 SMN deficiency in muscle does not affect weight of skeletal muscle of *SMN2*$^{+/+}$ mutants at PND21. **(A)** Weight of gastrocnemius in *SMN2*$^{+/+}$ mutant (blue) is not significantly different from control group (black) (n=4, p>0.05, unpaired 2-tailed Student's t test). **(B)** Weight of tibialis anterior in *SMN2*$^{+/+}$ mutant (blue) is not significantly different from control group (black) (n=4, p>0.05, unpaired 2-tailed Student's t test). **(C)** Weight of soleus in *SMN2*$^{+/+}$ mutant (blue) is not significantly different from control group (black) (n=4, p>0.05, unpaired 2-tailed Student's t test).

3.3.4 *SMN2*$^{+/+}$ mutants selectively depleted for SMN in skeletal muscle express fewer Type IIb fibers (fast fibers) than controls at PND21.

Skeletal muscle tissue is composed of a variety of fast-twitch and slow-twitch muscle fibers. There is a differential sensitivity between selective skeletal muscle fiber subtypes, as fast-twitch glycolytic fibers are more vulnerable than slow-twitch oxidative fibers under a variety of atrophic conditions (Wang *et al.*, 2013). These observations have been made in another motor neuron disease, amyotrophic lateral sclerosis (ALS), where fast-twitch muscle fibers innervated by fast fatigable motor neurons are more vulnerable than slow-twitch muscle fibers (Hegedus *et al.,* 2007). Given the decrease in fiber number observed in our *SMN2*$^{+/+}$ mutant mice, we wanted to find out if the degeneration affected all fiber types equally, or if some fiber types exhibited greater vulnerability to low levels of SMN protein. Quantitative PCR on muscle of PND210 *SMN2*$^{+/+}$ mutants showed a decrease in Type IIb fibers (fast twitch fibers) compared to controls. This was confirmed with immunohistochemistry of muscle of *SMN2*$^{+/+}$ mutants (Figure 3.3.4). One explanation for this result could be that given the decrease in fiber number, the fast twitch fibers are the most vulnerable to degeneration irrespective of the motor neuron innervating them.

A.

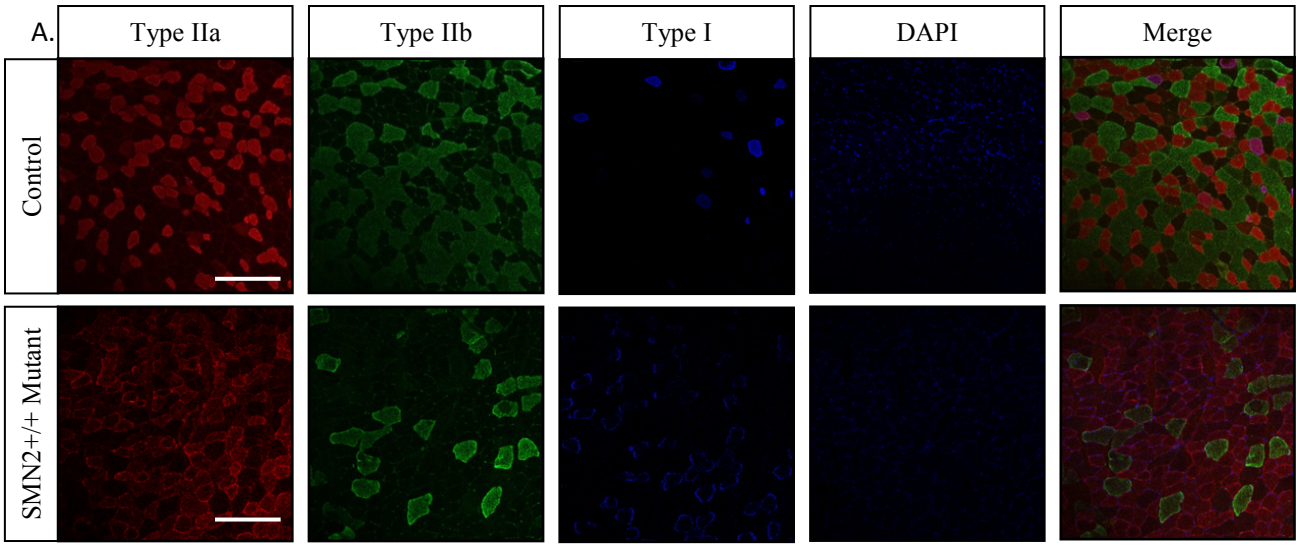
Type IIa
Type IIb
Type I
DAPI
Merge
Control
SMN2+/+ Mutant

B.

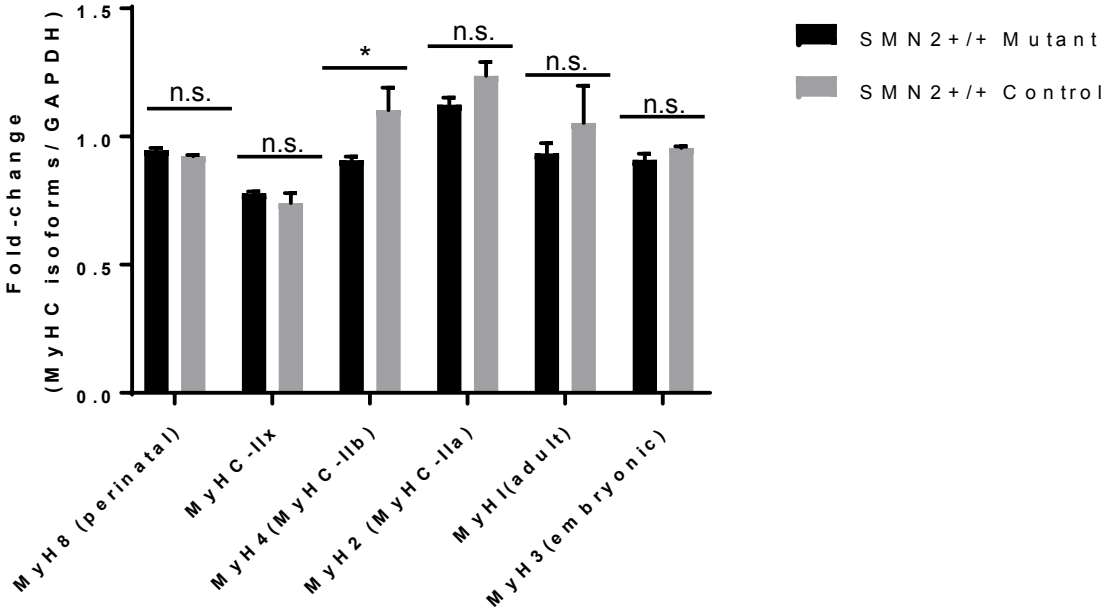
Fold-change (MyHC isoforms/GAPDH)
1.5
1.0
0.5
0.0
n.s.
n.s.
*
n.s.
n.s.
n.s.
MyH8 (perinatal)
MyHC-IIx
MyH4 (MyHC-IIb)
MyH2 (MyHC-IIa)
MyHI (adult)
MyH3 (embryonic)
SMN2+/+ Mutant
SMN2+/+ Control

Figure 3.3.4 *SMN2*$^{+/+}$ mutants selectively depleted for SMN in skeletal muscle express fewer Type IIb fibers (fast fibers) than controls at PND210. **(A)** Representative picture of *SMN2*$^{+/+}$ mutant and controls showing muscle stained for Type IIa, IIb, and Type I fibers. *SMN2*$^{+/+}$ mutants show fewer fibers stained for Type IIb compared to controls. **(B)** This result was confirmed by quantitative PCR, as there is a significant decrease in MyHC-IIb expression in *SMN2*$^{+/+}$ mutants compared to controls (n=4, *$p<0.05$, unpaired 2-tailed Student's t test) (Scale bar = 118).

3.3.5 Further evidence of muscle fiber degeneration and regeneration in *SMN2*$^{+/+}$ mutants.

Evans blue dye (EBD), is an azo dye widely used to study membrane permeability, and is capable of identifying skeletal myofibers that have become damaged as a result of muscular dystrophy, injury, or membrane associated fragility. We utilized EBD in order to confirm that muscle fiber degeneration was occurring in our mouse model. We performed serial sections, staining for H&E in consecutive slides. H&E staining of muscle of *SMN2*$^{+/+}$ mutants, showed centralized nuclei along with evidence of muscle fiber necrosis (black arrows, Figure 3.3.5A and C). *SMN2*$^{+/+}$ mutants exhibited muscle fibers stained in red (EBD), while control showed no evidence of EBD (Figure 3.3.5B and D). It is also important to note that in the *SMN2*$^{+/+}$ mutant, the intercostal showed a greater proportion of fibers stained with EBD than the gastrocnemius (Figure 3.3.5 B and D). This is indicative of more degeneration occurring in the intercostal than in the gastrocnemius, which is suggestive of the greater vulnerability to low SMN of the intercostal muscles compared to the gastrocnemius.

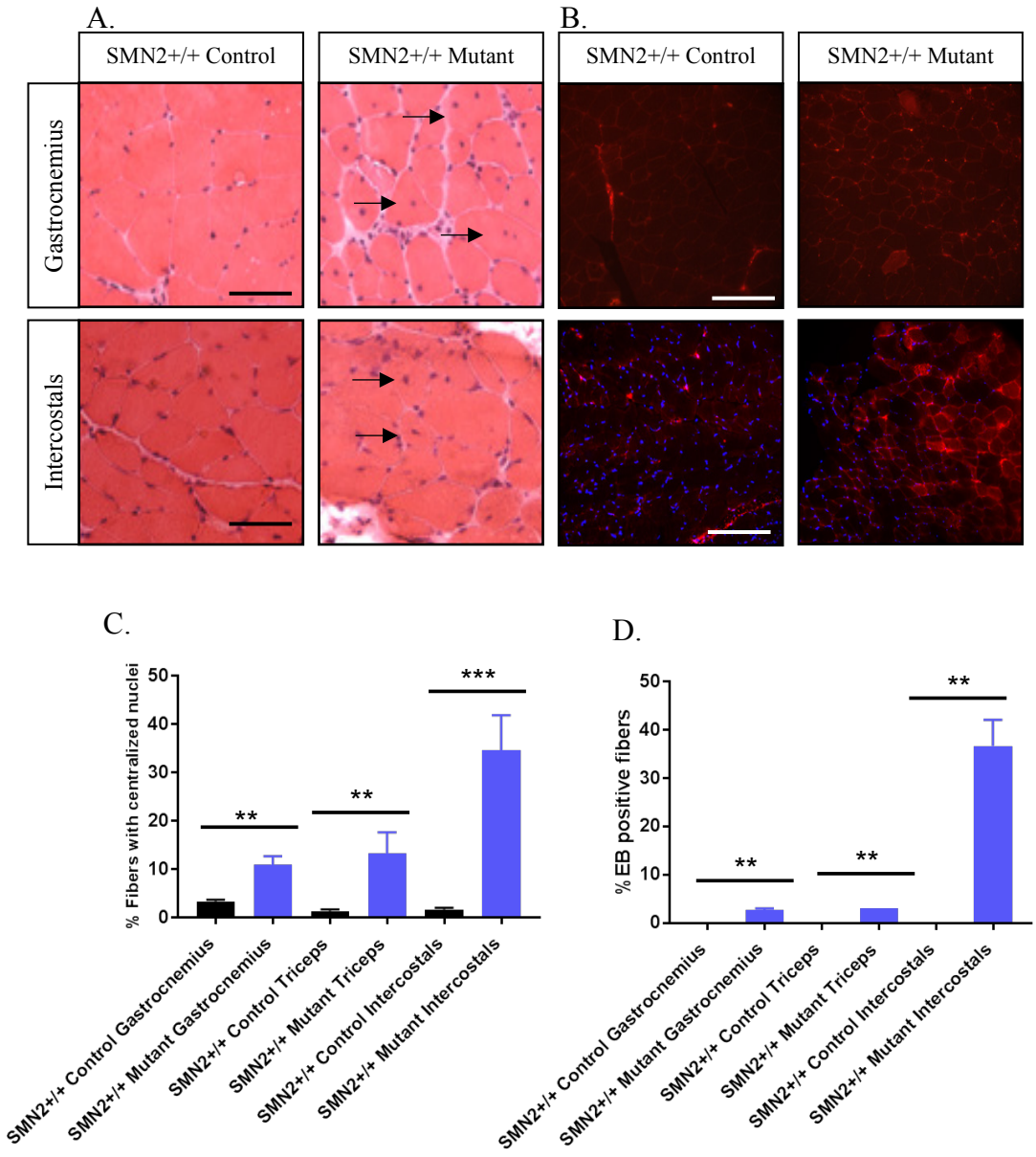
A.
B.
SMN2+/+ Control
SMN2+/+ Mutant
SMN2+/+ Control
SMN2+/+ Mutant
Gastrocnemius
Intercostals
C.
% Fibers with centralized nuclei
50
40
30
20
10
0
**
**
***
SMN2+/+ Control Gastrocnemius
SMN2+/+ Mutant Gastrocnemius
SMN2+/+ Control Triceps
SMN2+/+ Mutant Triceps
SMN2+/+ Control Intercostals
SMN2+/+ Mutant Intercostals
D.
% EB positive fibers
50
40
30
20
10
0
**
**
**
SMN2+/+ Control Gastrocnemius
SMN2+/+ Mutant Gastrocnemius
SMN2+/+ Control Triceps
SMN2+/+ Mutant Triceps
SMN2+/+ Control Intercostals
SMN2+/+ Mutant Intercostals

Figure 3.3.5 *SMN2*$^{+/+}$ mutant shows evidence of muscle fiber degeneration and regeneration. **(A)** Representative H&E sections of gastrocnemius and intercostal in *SMN2*$^{+/+}$ mutant and control. *SMN2*$^{+/+}$ mutants show centralized nuclei and evidence of muscle fiber necrosis (Scale bar = 150 µm). **(B)** Representative images of gastrocnemius and intercostal muscle section after Evans blue dye (EBD) experiment. *SMN2*$^{+/+}$ mutants show muscle fibers stained in red (EBD, while control shows no evidence of EBD staining (Scale bar = 198 µm) **(C)** *SMN2*$^{+/+}$ mutants (blue) show a greater percentage of fibers with centralized nuclei compared to controls (black). Intercostal muscle shows the greatest proportion of centralized nuclei (n=4, ***$p<0.001$, unpaired 2-tailed Student's t test). **(D)** *SMN2*$^{+/+}$ mutants (blue) have a greater proportion of fibers that are positive for EBD staining compared to control (black). Intercostal muscle shows the greatest difference in all analyzed muscles (n=4, **$p<0.01$, unpaired 2-tailed Student's t test).

3.3.6 Compromised regeneration of muscle expressing low levels of the SMN protein

At PND21, there was no evidence of muscle defects in *SMN2*$^{+/+}$ mutants, but at PND210 we found degenerating and regenerating muscle fibers. To determine if muscle defects could be unmasked in young adult *SMN2*$^{+/+}$ mutants, we induced degeneration in the mice at PND21 by injecting them with a myonecrotic agent, cardiotoxin (CTX) derived from snake (*Naja mossambica*) venom. Hematoxylin and eosin (H&E) was then used to determine the integrity of muscle tissue at 6, 14, and 26 days post CTX injection. On day 6, both mutant and control muscle show necrotic fibers resulting from the CTX injection. On day 14 too, there is evidence of regeneration in both *SMN2*$^{+/+}$ mutants and control, although mutants show fibers with multiple centralized nuclei, while controls show fibers with a single centralized nucleus. On day 26, control fibers had fully regenerated, showing fibers with only peripheral nuclei, while *SMN2*$^{+/+}$ mutants still showed fibers with centralized nuclei (Figure 3.3.6). This indicates that even in young *SMN2*$^{+/+}$ mutant mice, there is a potential for the muscular defects seen in older mice. In other words, once the muscle is insulted, a muscular phenotype develops during recovery. This suggests that there is already a difference in skeletal muscle, at the molecular level, of *SMN2*$^{+/+}$ mutant mice compared to controls at PND21.

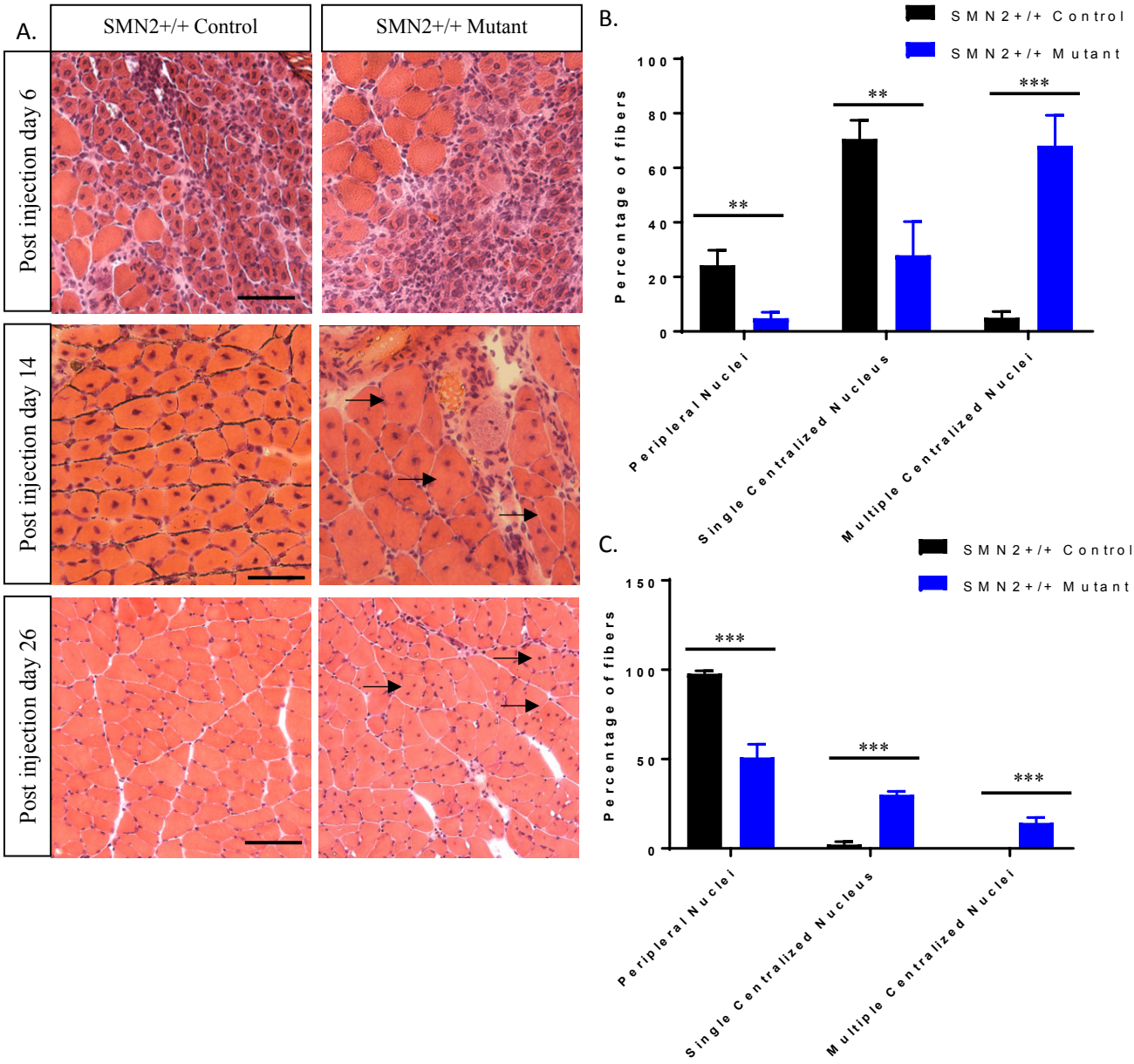

Figure 3.3.6 Compromised regeneration of muscle expressing low levels of the SMN protein **(A)** Representative H&E sections of gastrocnemius of PND21 *SMN2*$^{+/+}$ mutant and control 6, 14, and 26 days after CTX injection. On day 6, both mutant and control display necrotic fibers. On day 14, there is evidence of

regeneration in both *SMN2*$^{+/+}$ mutants and control, although mutants show fibers with multiple centralized nuclei, while controls show fibers with a single centralized nucleus. On day 26, control fibers have fully regenerated, while *SMN2*$^{+/+}$ mutants still show fibers with centralized nuclei. **(B)** Quantification at post injection day 14, showing *SMN2*$^{+/+}$ mutants (blue) have significantly greater number of fibers with multiple centralized nuclei, compared to control (black) (n=3, ***p<0.001, unpaired 2-tailed Student's t test). **(C)** Control mice muscle fibers (black) have fully regenerated by 26 days post CTX injection, exhibiting muscle fibers with peripheral nuclei, while *SMN2*$^{+/+}$ mutants (blue) still exhibit a significant number of fibers with one or multiple centralized nuclei per fiber. (n=3, ***p<0.001, unpaired 2-tailed Student's t test) (Scale bar = 150 μm).

3.4 NMJ Analysis

3.4.1 Selective depletion of SMN in skeletal muscle precludes NMJ remodeling following injury.

It has been reported in both severe- and mild-*SMN2* expressing mouse models of SMA that the earliest structural defects involve the neuromuscular synapse (Kariya *et al.*, 2008). During the postnatal development of the neuromuscular junction, as the acetylcholine receptors (AChRs) becomes localized to the postsynaptic muscle membrane, the embryonic form of the receptor containing the γ subunit (full composition: α2βγδ) is replaced by the ϵ containing adult form of the receptor (full composition: α2βϵδ) (Missias *et al*., 1996). This switch is largely completed by PND14 and is recapitulated in adults during NMJ remodeling after muscle injury

(Lingling *et al.*, 2009). To determine if this process is compromised in skeletal muscle specific SMN-depleted mice, we injured the gastrocnemius muscle of PND21 *SMN2*$^{+/+}$ mutant and control mice with a single CTX injection, and measured the relative expression of both the γ (present in embryonic) and α (present in embryonic and adult) subunits of the NMJs 14 days post injury. Our results showed that the *SMN2*$^{+/+}$ mutants expressed lower levels of both the αAChR as well as an inability to upregulate AChR expression. Together this indicates that reduced SMN protein levels in injured skeletal muscle, precludes NMJ remodeling.

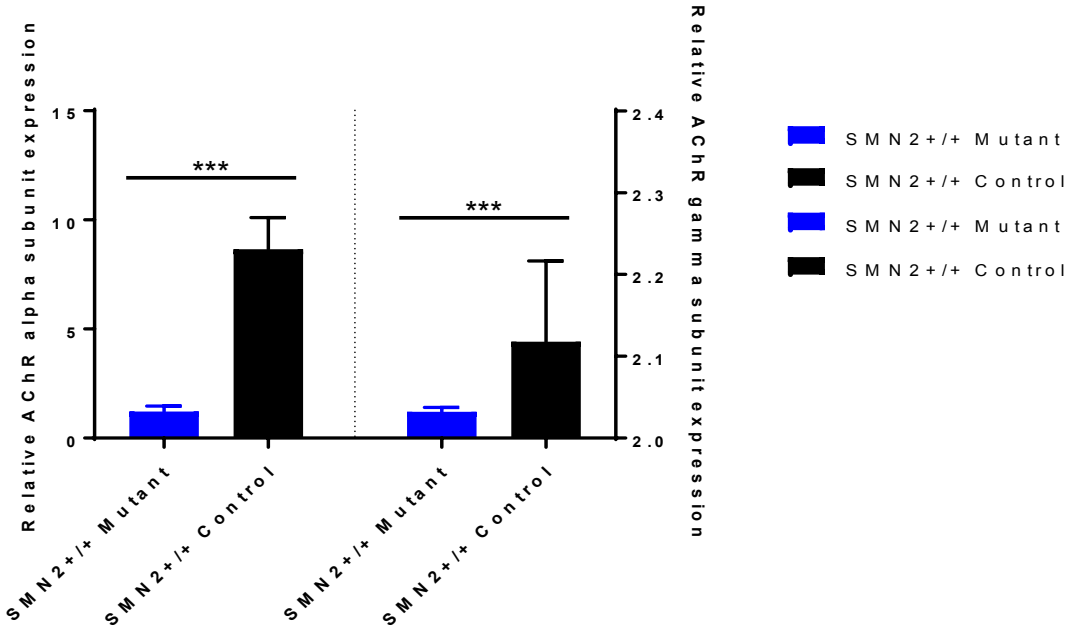

Figure 3.4.1. PND21 *SMN2*$^{+/+}$ mutants fail to go through NMJ remodeling 14 days after CTX injections compared to controls. *SMN2*$^{+/+}$ mutants (blue) show fewer total number of acetylcholine receptor compared to control (black), measured by relative expression of the alpha subunit acetylcholine receptor (n=4, ***p<0.001, unpaired 2-tailed Student's t test). Similarly, *SMN2*$^{+/+}$ mutants do not show an increase in relative expression of the gamma subunit after induced muscle fiber necrosis.

3.4.2 *SMN2*$^{+/-}$ mutants with depleted levels of SMN in skeletal muscle show abnormal neurofilament (NF) accumulation in the nerve terminal.

It has been previously reported that insufficient SMN protein arrests the post-natal development of the neuromuscular junction (NMJ), impairing the maturation of acetylcholine receptor (AChR) clusters into 'pretzels' (Kariya *et al.*, 2008). Pre-synaptic defects such as poor arborization and intermediate filament aggregates are useful biomarkers of the disease, and appear prior to any overt symptoms (Kariya *et al.*, 2008). Based on the striking defects found at the NMJs of SMA mice, we asked if similar abnormalities are also characteristics of skeletal muscle specific SMN-depleted mice.

At PND21, both *SMN2*$^{+/-}$ mutants and *SMN2*$^{+/+}$ mutants have mature and intact acetylcholine receptor clusters in the gastrocnemius and intercostal muscles. Surprisingly, at PND21, *SMN2*$^{+/-}$ mutants display abnormal neurofilament accumulation in the gastrocnemius and intercostal muscles (Figure 3.4.2). The acetylcholine receptor clusters in both groups are comparable in area and complexity to the ones observed in controls (Figure 3.4.2.1). Moreover, *SMN2*$^{+/-}$ mutants have a greater proportion of denervated acetylcholine receptor clusters in intercostal muscles than control, although there is no significant increase in denervation in the gastrocnemius muscle (Figure 3.4.2.2). This again suggests the intercostal is a more vulnerable muscle than the gastrocnemius, and also provides an explanation of respiratory failure for the premature death of the

SMN2$^{+/-}$ mutant mice. *SMN2*$^{+/+}$ mutant mice do not show any evidence of neurofilament accumulation or denervation (Figure 3.4.2.2 and 3.4.2.3). These observations point to the fact that the pre-synaptic defects of SMA do not always precede post-synaptic abnormalities. To reiterate, our mutant mice have normal levels of SMN protein outside of skeletal muscle, and still exhibit a NMJ phenotype. This indicates that depleted SMN protein specifically in skeletal muscle can induce abnormalities at the NMJs.

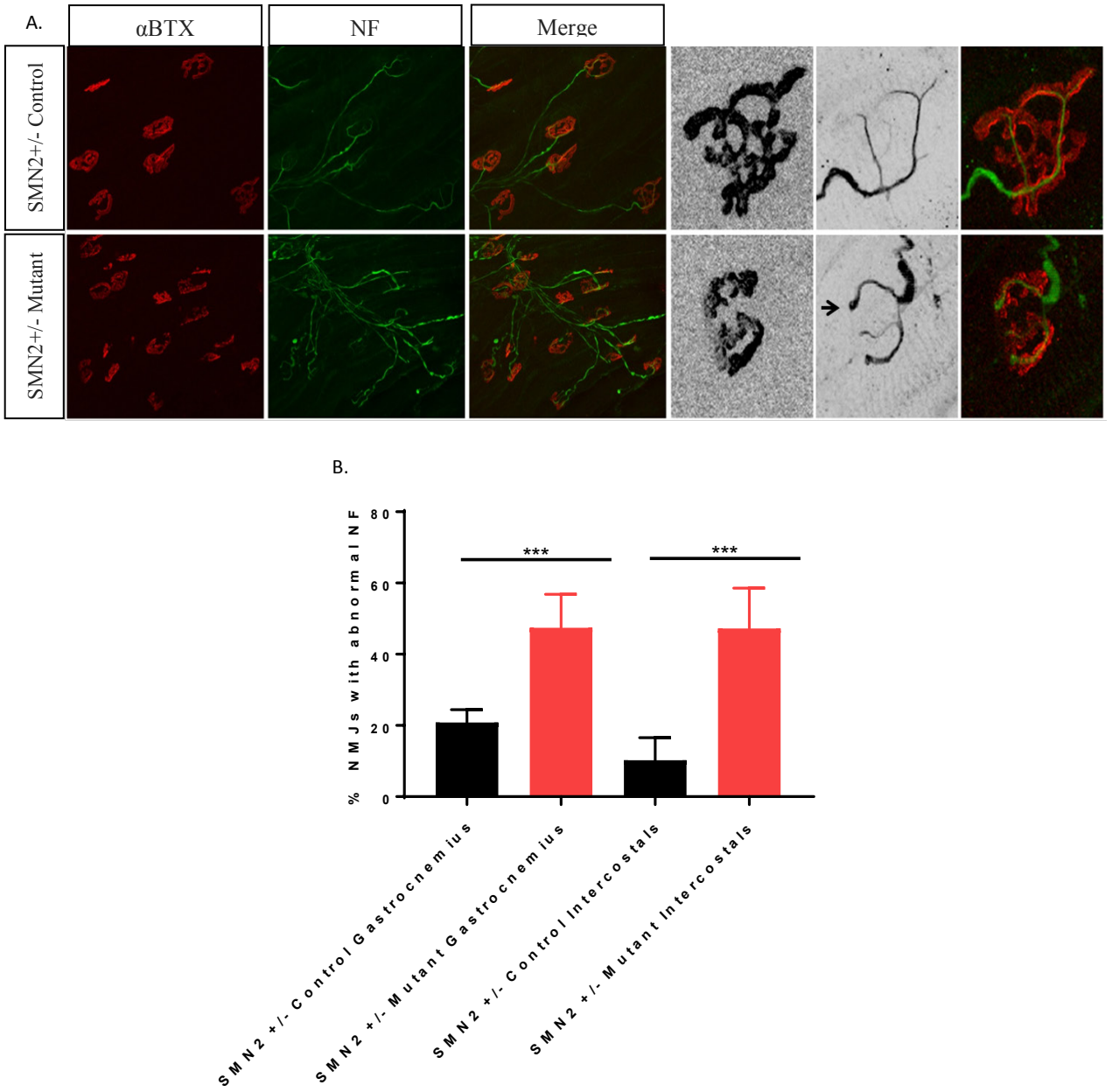

Figure 3.4.2 *SMN2*$^{+/-}$ mutants with depleted levels of SMN in skeletal muscle show abnormal neurofilament (NF) accumulation in the nerve terminal. **(A)** Representative image of neuromuscular

junctions of gastrocnemius of *SMN2*$^{+/-}$ mutants and controls. NF accumulation is shown by black arrow (Scale = 118 µm; 25 µm). **(B)** Quantification of abnormal NF accumulation in the gastrocnemius and intercostal muscles showing *SMN2*$^{+/-}$ mutants (red) have significantly more neurofilament accumulation at the nerve terminal of compared to controls (black) (n=6, ***$p<0.001$, unpaired 2-tailed Student's t test).

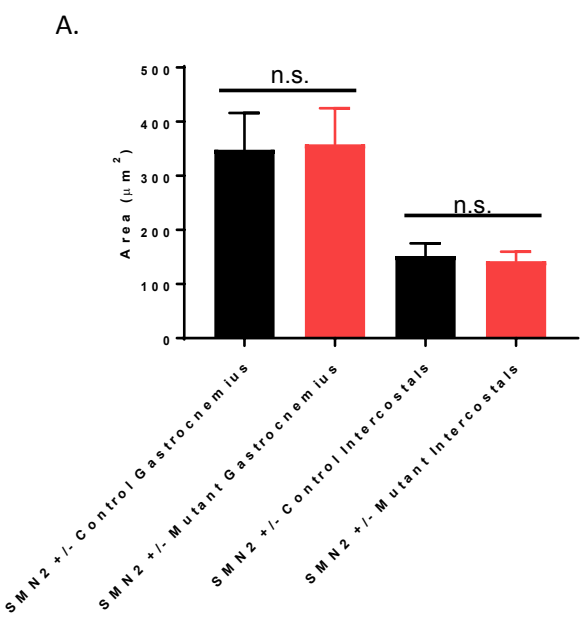
A.
n.s.
n.s.
Area (μm²)
500
400
300
200
100
0
SMN2+/- Control Gastrocnemius
SMN2+/- Mutant Gastrocnemius
SMN2+/- Control Intercostals
SMN2+/- Mutant Intercostals

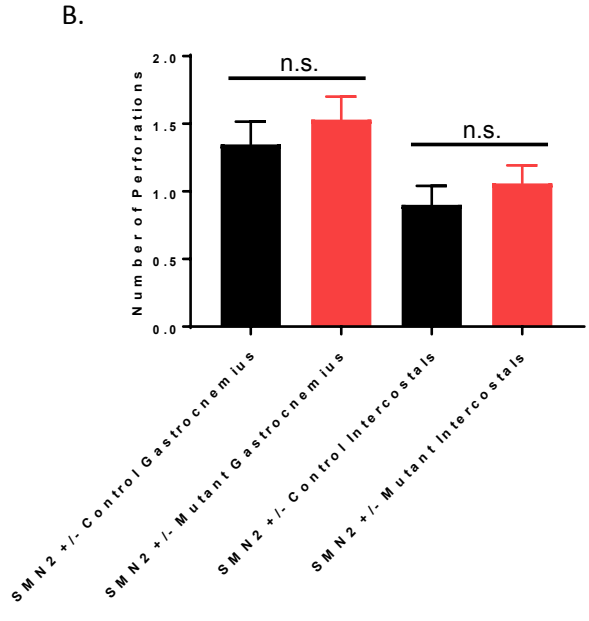
B.
n.s.
n.s.
Number of Perforations
2.0
1.5
1.0
0.5
0.0
SMN2+/- Control Gastrocnemius
SMN2+/- Mutant Gastrocnemius
SMN2+/- Control Intercostals
SMN2+/- Mutant Intercostals

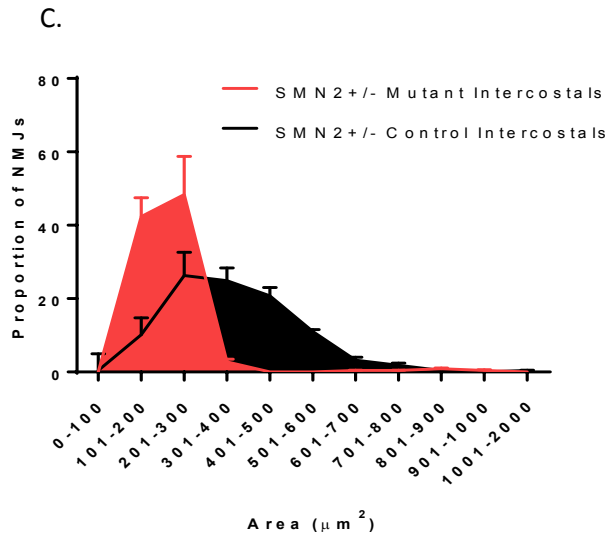
C.
SMN2+/- Mutant Intercostals
SMN2+/- Control Intercostals
Proportion of NMJs
80
60
40
20
0
0-100
101-200
201-300
301-400
401-500
501-600
601-700
701-800
801-900
901-1000
1001-2000
Area (μm²)

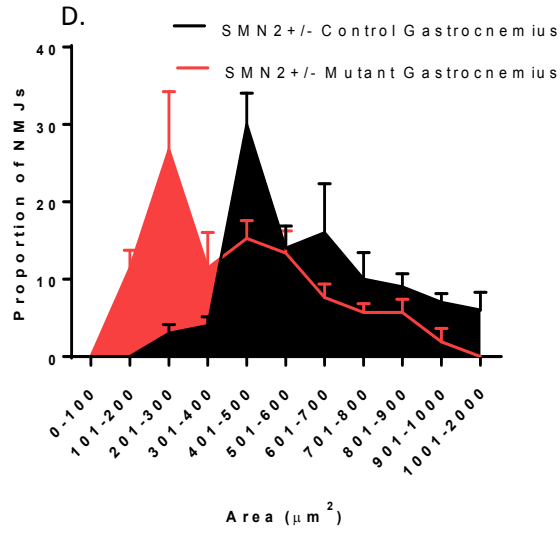
D.
SMN2+/- Control Gastrocnemius
SMN2+/- Mutant Gastrocnemius
Proportion of NMJs
40
30
20
10
0
0-100
101-200
201-300
301-400
401-500
501-600
601-700
701-800
801-900
901-1000
1001-2000
Area (μm²)

Figure 3.4.2.1 Morphology of NMJs in *SMN2*$^{+/-}$ mutants depleted of SMN protein in skeletal muscle. **(A)** Quantification of acetylcholine receptor clusters area size in *SMN2*$^{+/-}$ mutants (red) and controls (black), in gastrocnemius and intercostal showed no statistical difference after being adjusted for the size of the animal (n=6, p>0.05, unpaired 2-tailed Student's t test). **(B)** Quantification of perforations in the acetylcholine receptor clusters of *SMN2*$^{+/-}$ mutants (red) and controls (black) showing no statistical difference in the complexity of the receptors (n=6, p>0.05, unpaired 2-tailed Student's t test). **(C, D)** Frequency distribution of size of NMJs in intercostal and gastrocnemius muscles (respectively) of *SMN2*$^{+/-}$ mutants (red) and controls (black) showing that the distribution curve is skewed to the left, representative of a greater number of fibers with a smaller area in *SMN2*$^{+/-}$ mutants.

A.

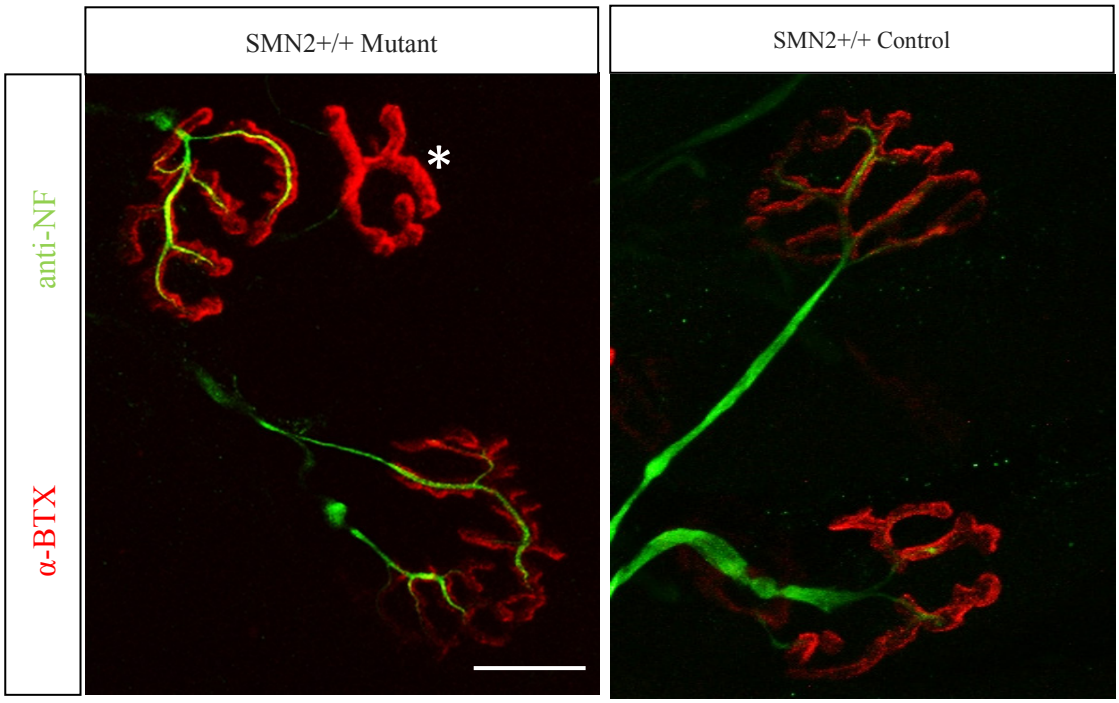
SMN2+/+ Mutant
SMN2+/+ Control
anti-NF
α-BTX
*

B.

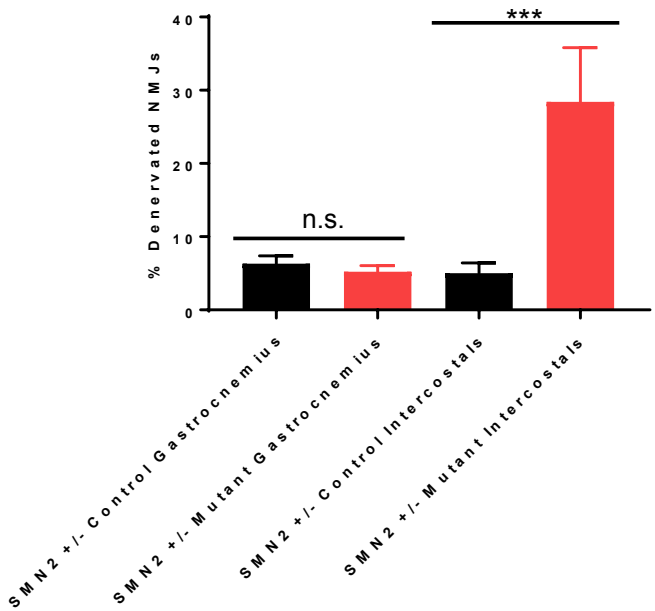
% Denervated NMJs
40
30
20
10
0
n.s.
***
SMN2+/- Control Gastrocnemius
SMN2+/- Mutant Gastrocnemius
SMN2+/- Control Intercostals
SMN2+/- Mutant Intercostals

Figure 3.4.2.2 *SMN2*$^{+/-}$ mutants with depleted levels of SMN protein in skeletal muscle have increased denervation of acetylcholine receptor clusters in intercostals compared to controls (Scale bar = 15 μm) **(A)** Representative image of a denervated acetylcholine receptor (marked by a white asterisk) compared to innervated ones. **(B)** Percent of denervated acetylcholine receptors in both gastrocnemius and intercostal of *SMN2*$^{+/-}$ mutants (red) and controls (black). There is no significant difference in denervation in the gastrocnemius between the two groups (n=6, $p>0.05$, unpaired 2-tailed Student's t test). However, intercostal muscle shows a significant increase in denervation compared to controls (n=6, ***$p<0.001$, unpaired 2-tailed Student's t test).

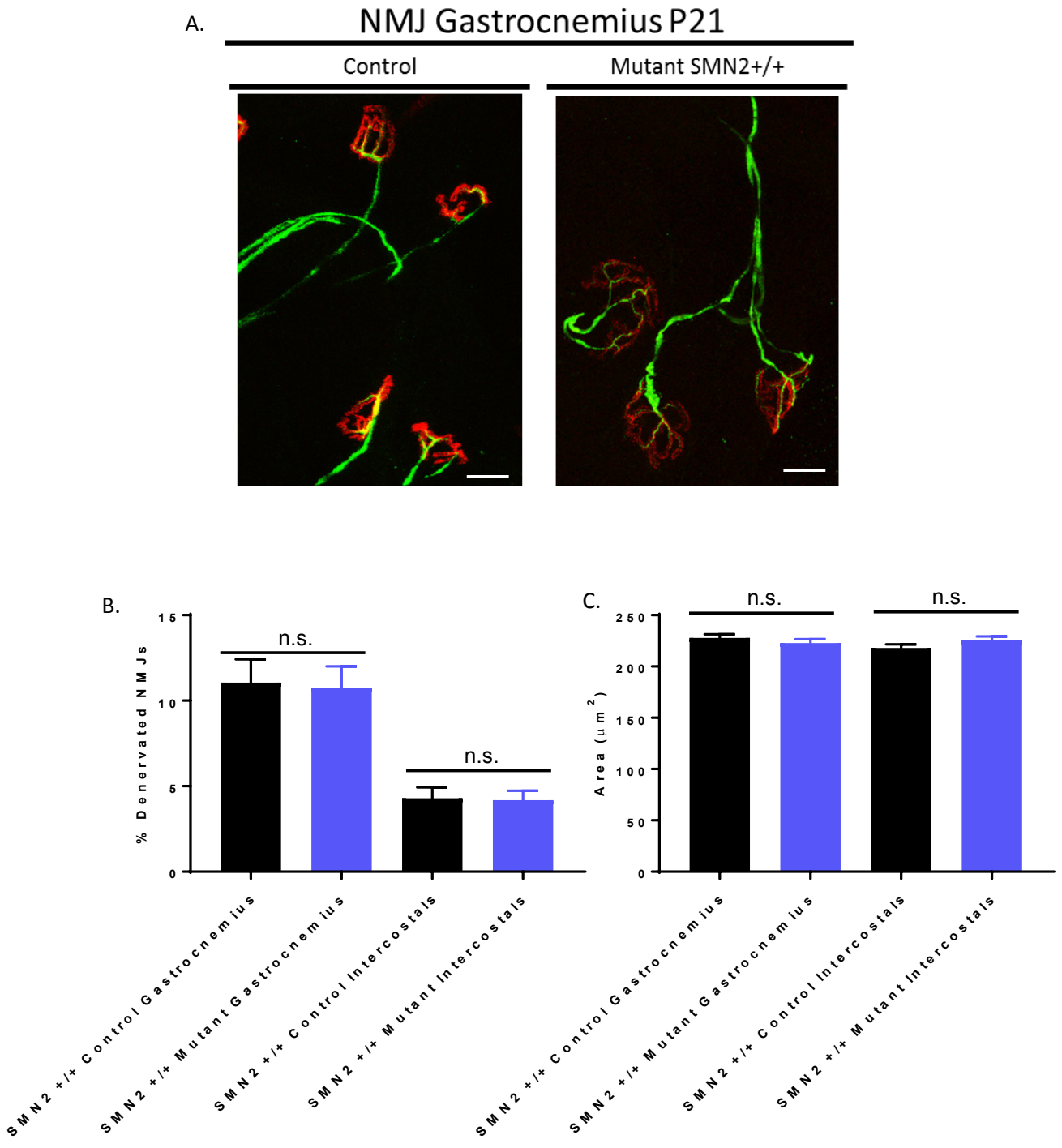
A.
NMJ Gastrocnemius P21
Control
Mutant SMN2+/+
B.
% Denervated NMJs
15
10
5
0
n.s.
n.s.
SMN2+/+ Control Gastrocnemius
SMN2+/+ Mutant Gastrocnemius
SMN2+/+ Control Intercostals
SMN2+/+ Mutant Intercostals
C.
Area (μm²)
250
200
150
100
50
0
n.s.
n.s.
SMN2+/+ Control Gastrocnemius
SMN2+/+ Mutant Gastrocnemius
SMN2+/+ Control Intercostals
SMN2+/+ Mutant Intercostals

Figure 3.4.2.3 *SMN2*$^{+/+}$ mutants with depleted SMN levels in skeletal muscle show no NMJ defects at PND21. **(A)** Representative image of neuromuscular junctions of *SMN2*$^{+/+}$ mutants and controls at PND21 (Scale bar = 25 µm). **(B)** Percent of denervated NMJ in gastrocnemius and intercostal muscles of *SMN2*$^{+/+}$ mutants (blue) and controls (black). There is no significant difference in denervation in the gastrocnemius or intercostal muscles between the two groups (n=6, $p>0.05$, unpaired 2-tailed Student's t test). **(C)** Likewise, there is no difference in area of acetylcholine receptor clusters between *SMN2*$^{+/+}$ mutants (blue) and controls (black) at PND21 (n=6, $p>0.05$, unpaired 2-tailed Student's t test).

3.4.3 *SMN2*$^{+/+}$ mutants with depleted levels of SMN in skeletal muscle show progressive functional NMJ defects.

Striking defects have been reported at SMA junctions in patients as well as SMA mice. These defects have associated alterations in neuromuscular transmission. Therefore, we performed electrophysiological recordings on muscles of our younger *SMN2*$^{+/+}$ mutants and our aged *SMN2*$^{+/+}$ mutants. It appeared likely that any pathology observed at the NMJ of our mutants would be reflected as alterations in neuromuscular transmission.

At PND21, *SMN2*$^{+/+}$ mutants do not exhibit functional NMJ defects in response to selective depletion of muscle SMN. We looked at end plate potentials (Epp) amplitude, miniature end plate potentials (mEpp) amplitude and frequency, and Quantal Content (QC) of extensor digitorum longus (EDL) in *SMN2*$^{+/+}$ mutants and control (ages PND21 and PND210). Epp measured the depolarizations of

fibers caused by neurotransmitters binding to the postsynaptic membrane at the NMJ. mEpp measures small (~0.4mV) depolarizations of the postsynaptic terminal caused by the release of a single vesicle into the synaptic cleft. Neurotransmitter vesicles containing acetylcholine collide spontaneously with the nerve terminal and release acetylcholine into the neuromuscular junction even without a signal from the axon. It represents the smallest possible depolarization which can be induced in a muscle. Furthermore, QC measured the number of effective vesicles released in response to a nerve impulse.

There is no significant difference between *SMN2*$^{+/+}$ mutants and control with respect to Mepp and Epp amplitude, Mepp frequency, or in Quantal content at PND30 (Figure 3.4.3). However, at PND210, *SMN2*$^{+/+}$ mutants exhibit functional NMJ defects in response to selective depletion of SMN in muscle (Figure 3.4.3.1). At PND210, in *SMN2*$^{+/+}$ mutant NMJs, the Quantal Content had significantly increased. This increase in Quantal Content in PND210 *SMN2*$^{+/+}$ mutants may have resulted from an increase in vesicle release probability, or a larger readily releasable pool (RRP) or both (Ling *et al*., 2010). Interestingly, the mean Mepp amplitude at *SMN2*$^{+/+}$ mutant NMJs was lower than that at control junctions. This could be likely caused by a decrease in the input resistance of the SMA muscle fibers caused by the depletion of SMN protein (Park *et al*., 2010). It could also be explained by the increase in fragmentation of the NMJs (Figure 3.4.3.2) (n=4, ***$p<0.001$, unpaired 2-tailed Student's t test), and by the decrease in number of AChRs compared to control, indicated by quantitative PCR of the α subunit acetylcholine receptor

(Figure 3.4.3.3). Alternatively, the amount of acetylcholine per vesicle or the postsynaptic response to a given amount of neurotransmitter might have increased as a homeostatic response to the reduced feedback from skeletal muscle (David and Goodman, 1998; Wang *et al*., 2005). Together, these results suggest that the electrophysiology defects seen at PND210 *SMN2*$^{+/+}$ mutant NMJs are progressive, as they are not present in the *SMN2*$^{+/+}$ mutants at PND21. In addition, the electrophysiology results show that these defects are caused cell-autonomously by the depletion of SMN in the muscle of *SMN2*$^{+/+}$ mutant mice.

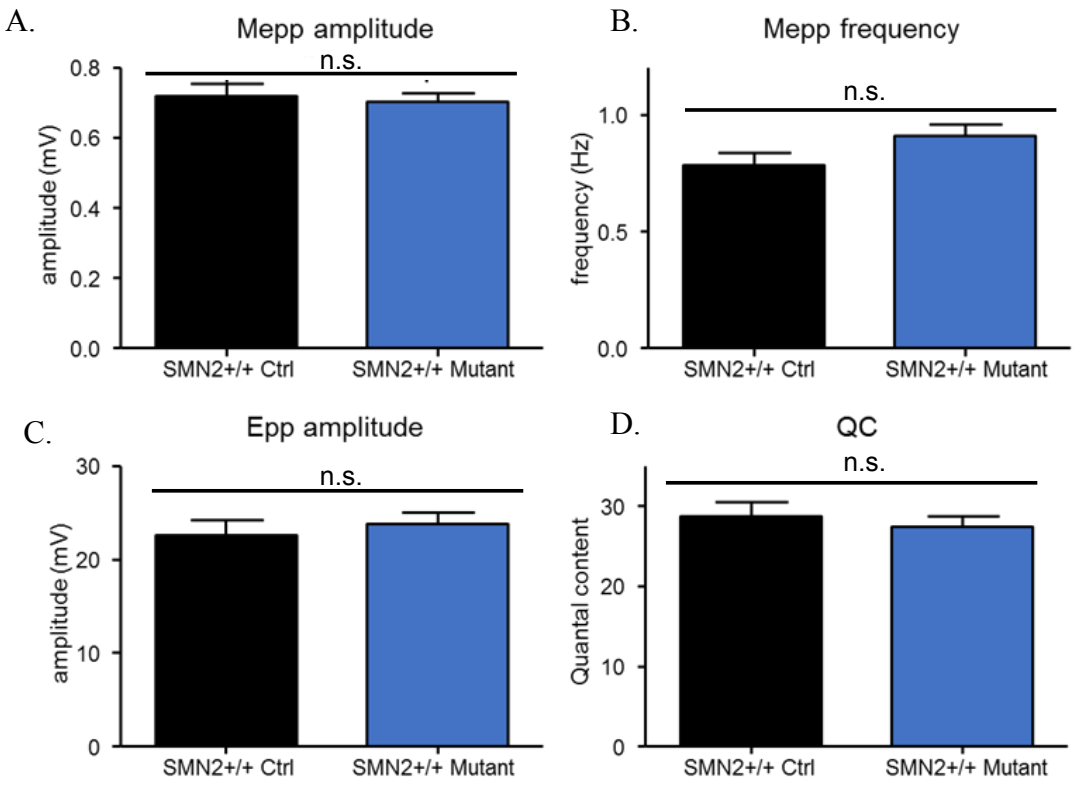

Figure 3.4.3 At PND21, *SMN2*$^{+/+}$ mutants do not exhibit functional NMJ defects in response to selective depletion of muscle *SMN*. **(A, B, C, D)** There is no significant difference between *SMN2*$^{+/+}$ mutants (blue) and control (black) Mepp and Epp amplitude, Mepp frequency, or in Quantal content (n=4, $p>0.05$, unpaired 2-tailed Student's t test).

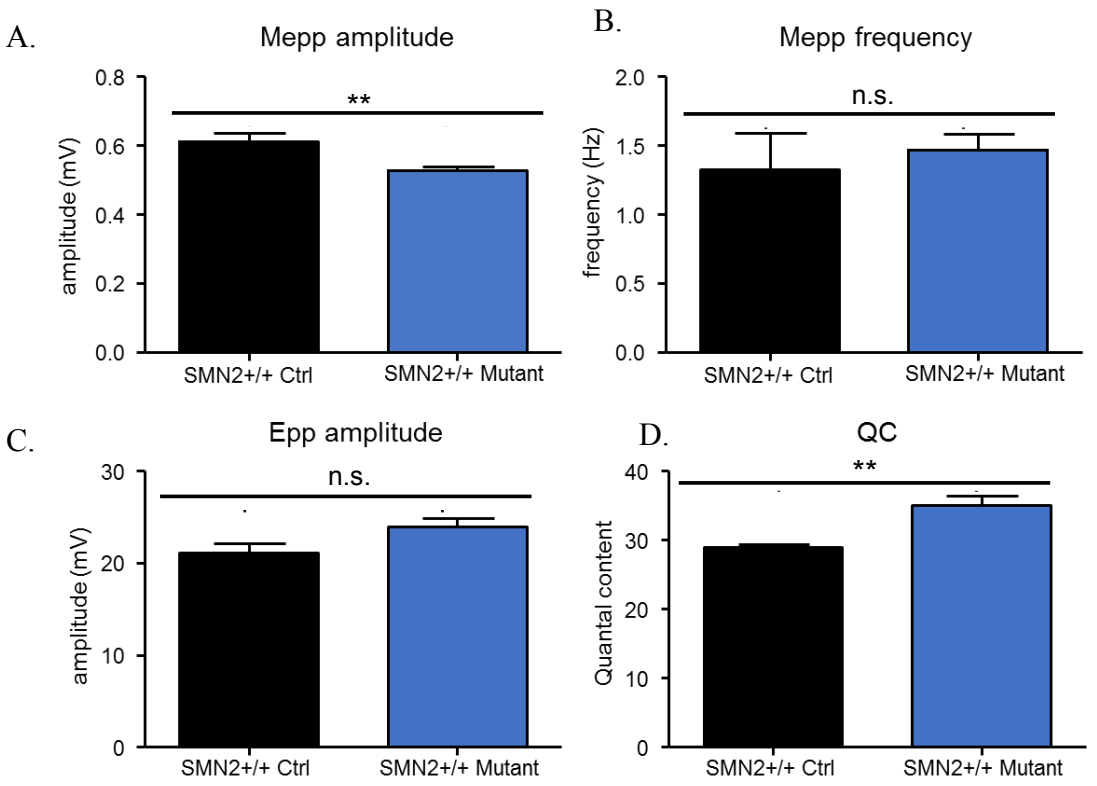

Figure 3.4.3.1 At PND210, *SMN2*$^{+/+}$ mutants exhibit functional NMJ defects in response to selective depletion of muscle *SMN*. **(A)** *SMN2*$^{+/+}$ mutants (blue) show a decrease in Mepp amplitude compared to controls (black) ($p<0.001$, n=4). **(B, C)** However, there is no significant difference in Mepp frequency and Epp amplitude between *SMN2*$^{+/+}$ mutants (blue) and controls (black) (n=4, $p>0.05$, unpaired 2-tailed Student's t test). **(D)** On the other hand, *SMN2*$^{+/+}$ mutants (blue) show an increase in Quantal content compared to controls (black) (n=4, **$p<0.01$, unpaired 2-tailed Student's t test).

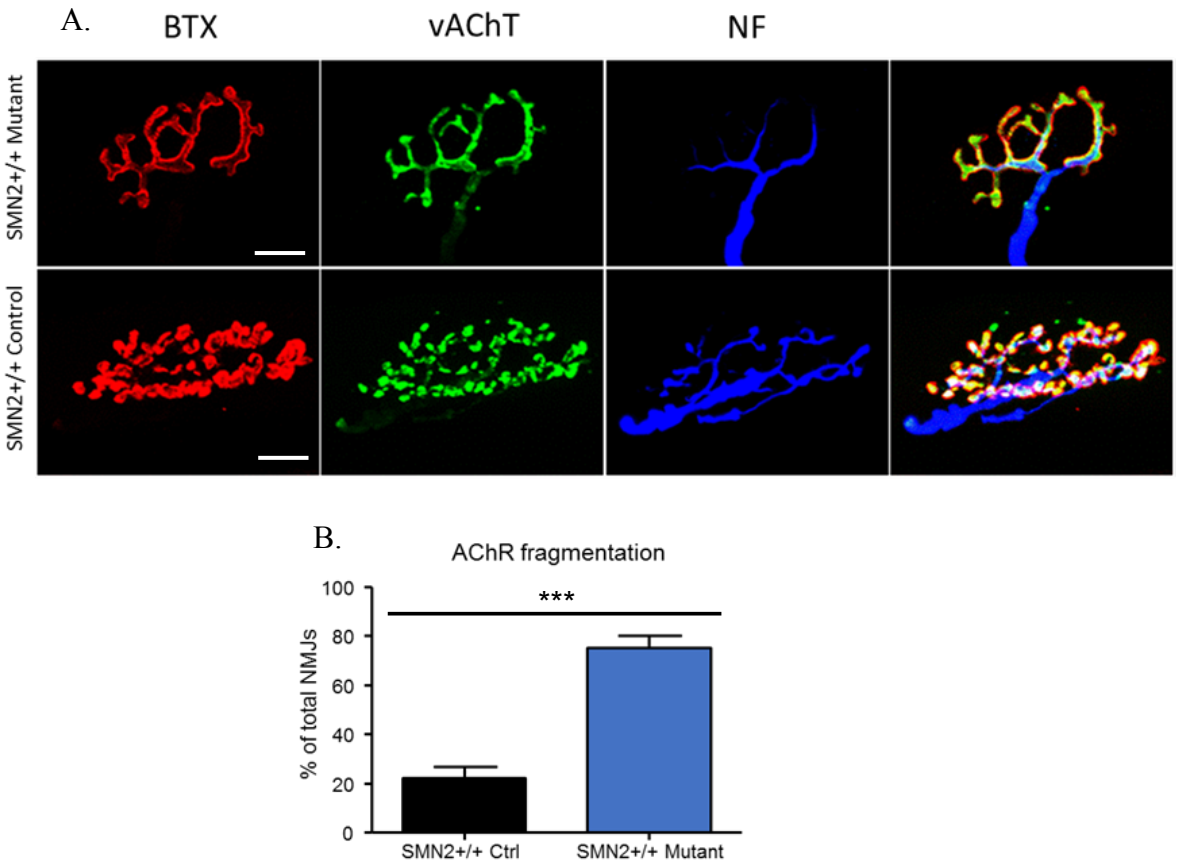

Figure 3.4.3.2 At PND210, *SMN2*$^{+/+}$ mutant mice exhibit fragmentation of NMJs. **(A)** Representative image of fragmentation of the NMJs seen in *SMN2*$^{+/+}$ mutants compared to normal morphology of NMJs in controls (black). **(B)** Quantification of NMJs showing a significant increase in fragmentation in the *SMN2*$^{+/+}$ mutants (blue) compared to control (black) (n=100-130 NMJs from 4 controls and 4 *SMN2*$^{+/+}$ mutants, ***p<0.001, unpaired 2-tailed Student's t test) (Scale bar = 15 μm).

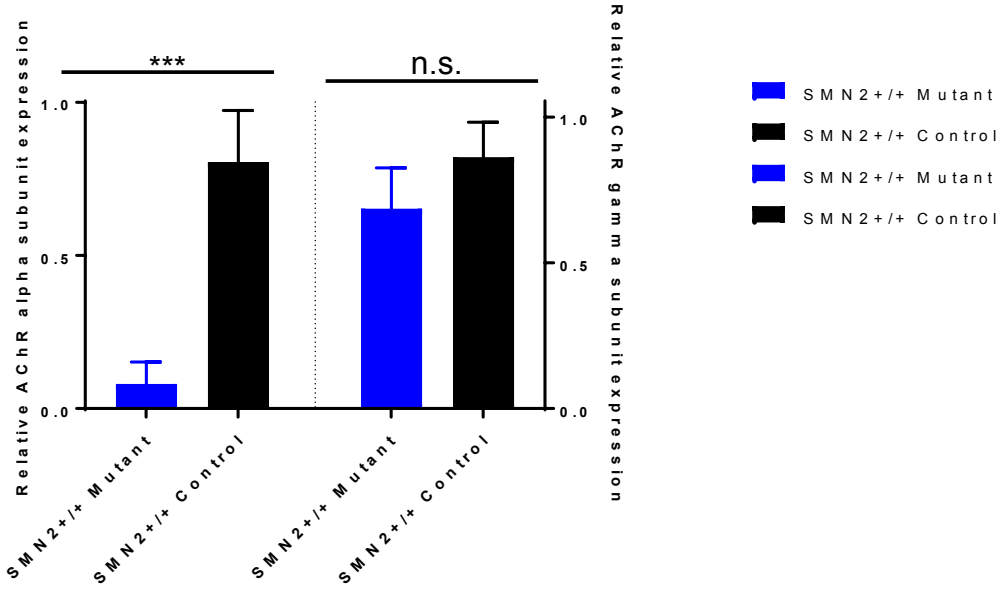

Figure 3.4.3.3 At PND210, *SMN2*$^{+/+}$ mutants (blue) have a decreased expression of the α subunit of the AChR compared to control (black), as assessed by quantitative PCR (n=4, ***p<0.001, unpaired 2-tailed Student's t test). On the other hand, *SMN2*$^{+/+}$ mutants and controls do not show increased expression of the gamma subunit acetylcholine receptor (n=4, p>0.05, unpaired 2-tailed Student's t test).

3.5 Motor Neuron Analysis

3.5.1 Depletion of SMN in skeletal muscle does not affect SMN levels in motor neurons.

Considering the pathological consequences of depleting SMN in muscle on the NMJs, we felt it was important to analyze whether the low levels of SMN in skeletal muscle could also be affecting the motor neurons. Therefore, motor neuron number and size were quantified from cervical, thoracic, and lumbar spinal cord. There was no significant difference between motor neuron numbers in either *SMN2*$^{+/+}$ or *SMN2*$^{+/-}$ mutants relative to control (Figure 3.5.1). We established that the selective depletion of SMN in skeletal muscle did not affect SMN protein levels in motor neurons. Additionally, we observed that gems, sub-nuclear foci that contain the SMN protein were not depleted (Figure 3.5). Together, these results suggest that depleting SMN protein selectively in skeletal muscle does not induce motor neuron degeneration. Yet, our mutant mice still show a disease phenotype, attesting to the cell-autonomous effects of low SMN in muscle.

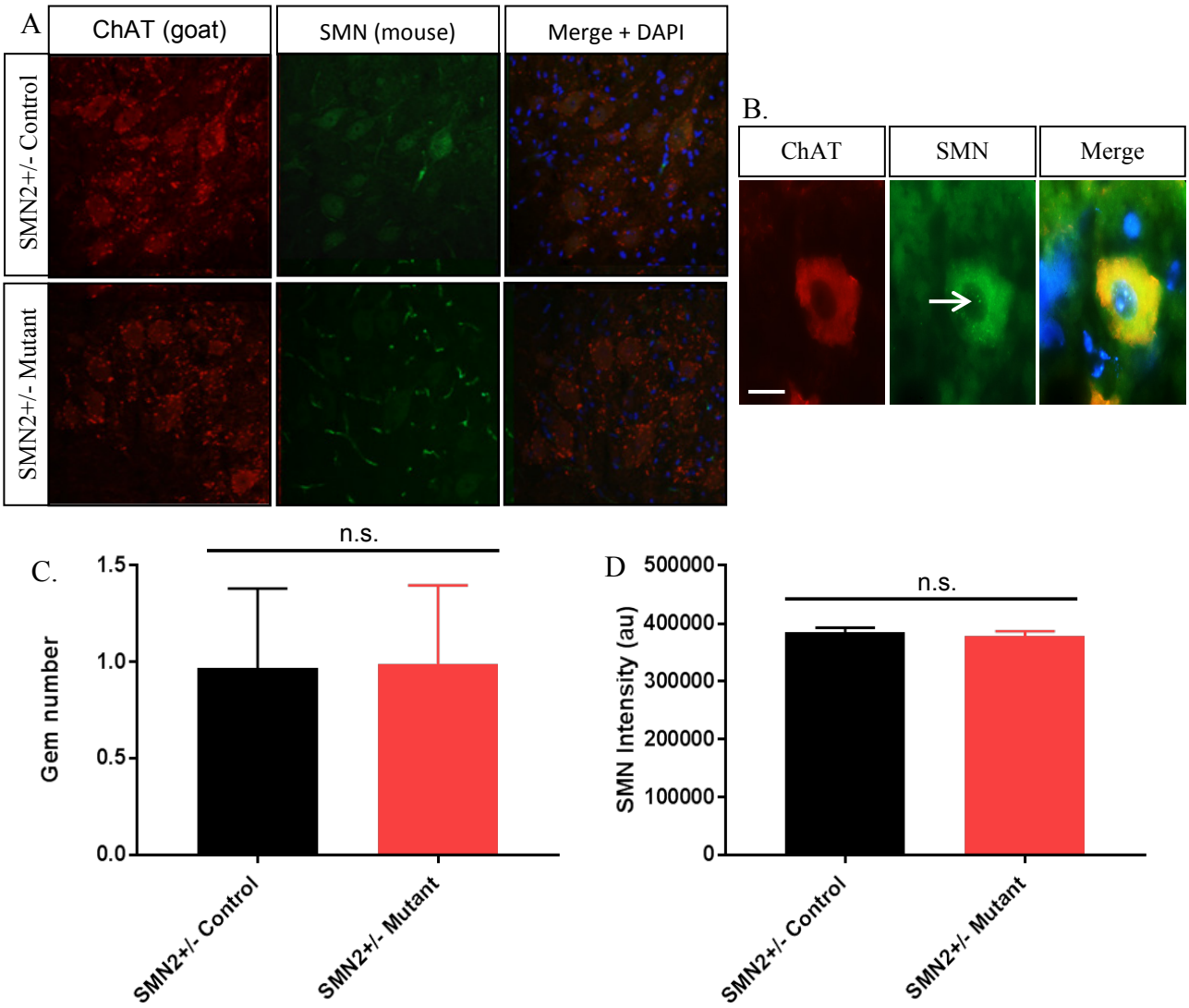

Figure 3.5 Depletion of SMN in skeletal muscle does not affect SMN levels in motor neurons **(A)** Representative image of motor neurons in thoracic spinal cord, along with SMN staining in both *SMN2*$^{+/+}$ mutants and controls. **(B)** Representative image of ChAT stained motor neuron, and *SMN* stain gems present in the nucleus.

(C) Gems were counted and quantified, and found to not be different between *SMN2*$^{+/-}$ mutants and controls. **(D)** Intensity of SMN staining was quantified, and also found to be the same in *SMN2*$^{+/-}$ mutants and controls (n=4, $p>0.05$, unpaired 2-tailed Student's t test).

A.

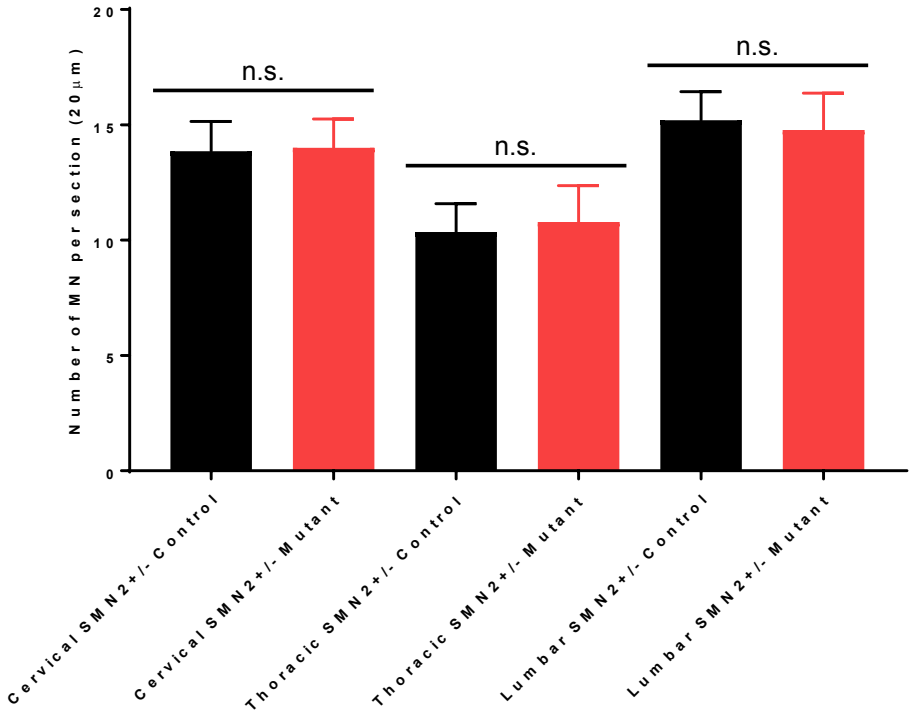
Number of MN per section (20µm)
20
15
10
5
0
n.s.
n.s.
n.s.
Cervical SMN2+/- Control
Cervical SMN2+/- Mutant
Thoracic SMN2+/- Control
Thoracic SMN2+/- Mutant
Lumbar SMN2+/- Control
Lumbar SMN2+/- Mutant

B.

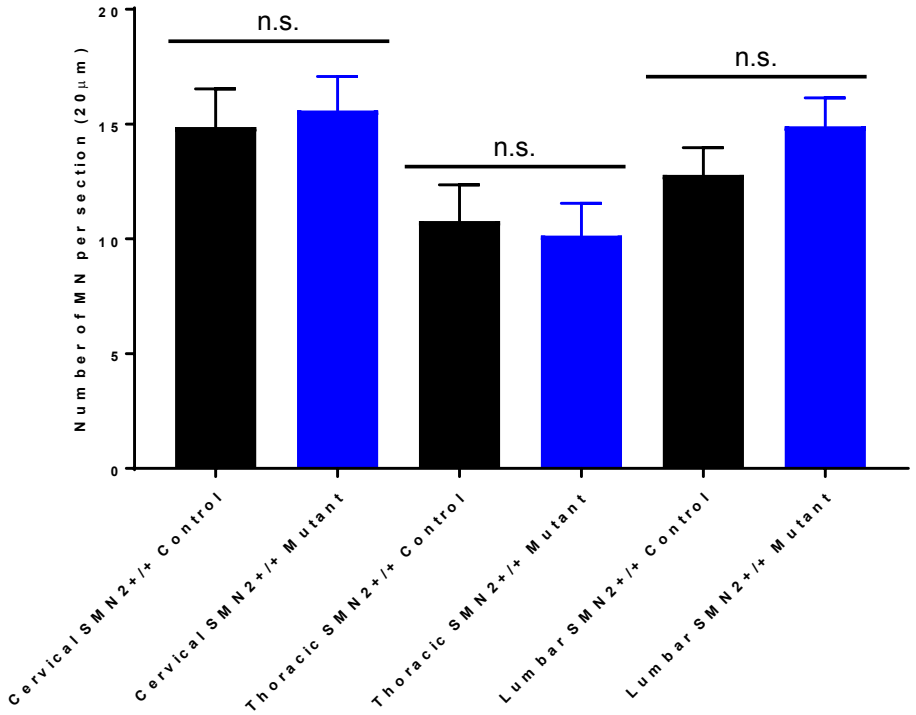
Number of MN per section (20µm)
20
15
10
5
0
n.s.
n.s.
n.s.
Cervical SMN2+/+ Control
Cervical SMN2+/+ Mutant
Thoracic SMN2+/+ Control
Thoracic SMN2+/+ Mutant
Lumbar SMN2+/+ Control
Lumbar SMN2+/+ Mutant

Figure 3.5.1 Reduced SMN levels in skeletal muscle does not induce motor neuron loss. **(A)** Quantification of motor neuron number from cervical, thoracic, and lumbar spinal cord shows no difference in motor neuron number between *SMN2*$^{+/-}$ mutants (red) and control (black) (n=4, p>0.05 unpaired 2-tailed Student's t test). **(B)** Quantification of motor neuron number from cervical, thoracic, and lumbar spinal cord shows no difference in motor neuron number between *SMN2*$^{+/+}$ mutants (blue) and control (black) (n=4, p>0.05, unpaired 2-tailed Student's t test).

3.6 SMN Repletion Analysis

3.6.1 Muscle pathology mitigated following SMN repletion in symptomatic model mice.

As previously stated in the introduction of this thesis, a single nucleotide difference between the *SMN1* and *SMN2* genes results in the exclusion of exon 7 in the majority of *SMN2* transcripts. This causes a decrease in SMN protein levels and leads to the development of SMA. The incorporation of *SMN2* exon 7 is regulated by a series of splice enhancers and silencers. In particular, an element in the 5' proximal intron flanking exon 7 called ISS-N1 is a powerful intronic silencing suppressor to which the factor hnRNP A1 binds, inducing exon skipping. This splice motif can be blocked with antisense oligomers (ASOs) in order to alter *SMN2* transcript splicing. In our concluding set of experiments, we took advantage of this finding and used a previously reported antisense morpholino that binds the element, preventing hnRNP A1 from binding to ISS-N1 to treat our symptomatic mice. Consequently, exon 7 is included in the *SMN2*

transcript, eventually increasing SMN levels. The morpholino was delivered by IP injection to the symptomatic *SMN2*$^{+/+}$ mutant mice at PND210. This was performed in order to determine whether the muscle and NMJ pathologies reported in this study were reversible. Mice were analyzed 7 weeks after morpholino or scramble morpholino were administered.

After the administration of morpholino, the weight of the gastrocnemius was significantly increased in treated *SMN2*$^{+/+}$ mutants compared to untreated *SMN2*$^{+/+}$ mutants. Still, the weight of gastrocnemius was significantly decreased in both untreated *SMN2*$^{+/+}$ mutants and treated *SMN2*$^{+/+}$ mutants, compared to control mice (Figure 3.6.1B). Furthermore, the number of centralized nuclei was increased in both untreated *SMN2*$^{+/+}$ mutants and treated *SMN2*$^{+/+}$ mutants compared to controls. However, the untreated *SMN2*$^{+/+}$ mutants had significantly greater numbers of centralized nuclei fibers compared to treated *SMN2*$^{+/+}$ mutants (Figure 3.6.1A and C). Furthermore, there is also a significant difference between the fiber area size of untreated *SMN2*$^{+/+}$ mutants and treated *SMN2*$^{+/+}$ mutants compared to control. As a result of the morpholino treatment, treated *SMN2*$^{+/+}$ mutants had significantly larger fiber size area than untreated *SMN2*$^{+/+}$ mutants (Figure 3.6.1D).

A.

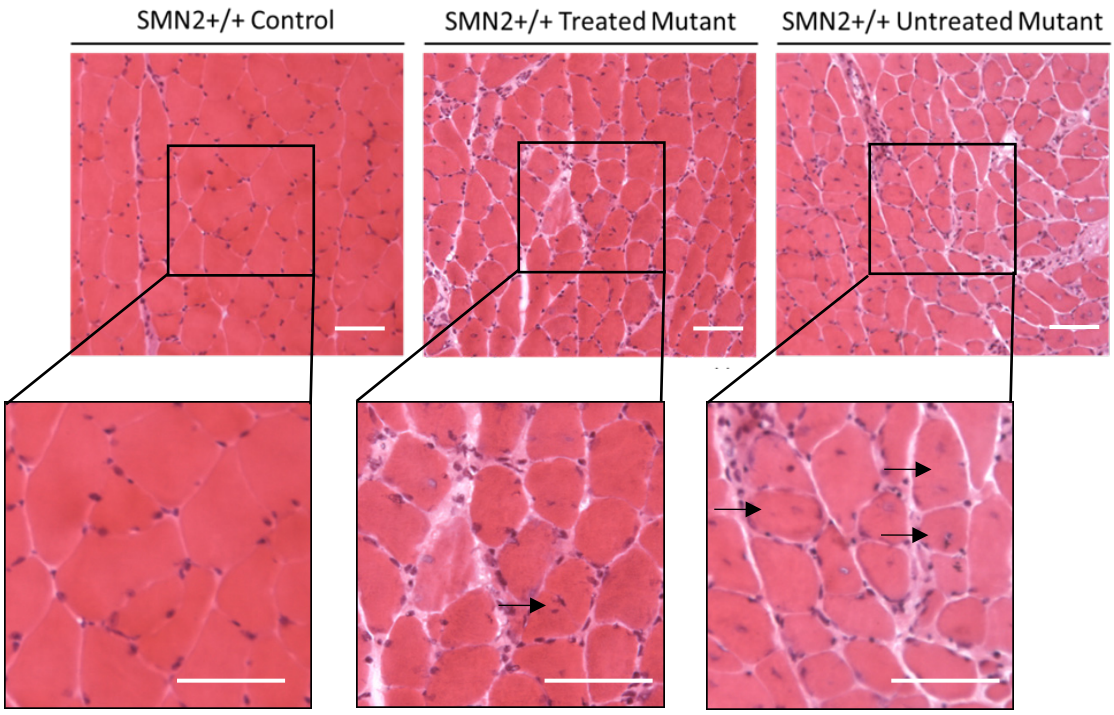
SMN2+/+ Control
SMN2+/+ Treated Mutant
SMN2+/+ Untreated Mutant

B.

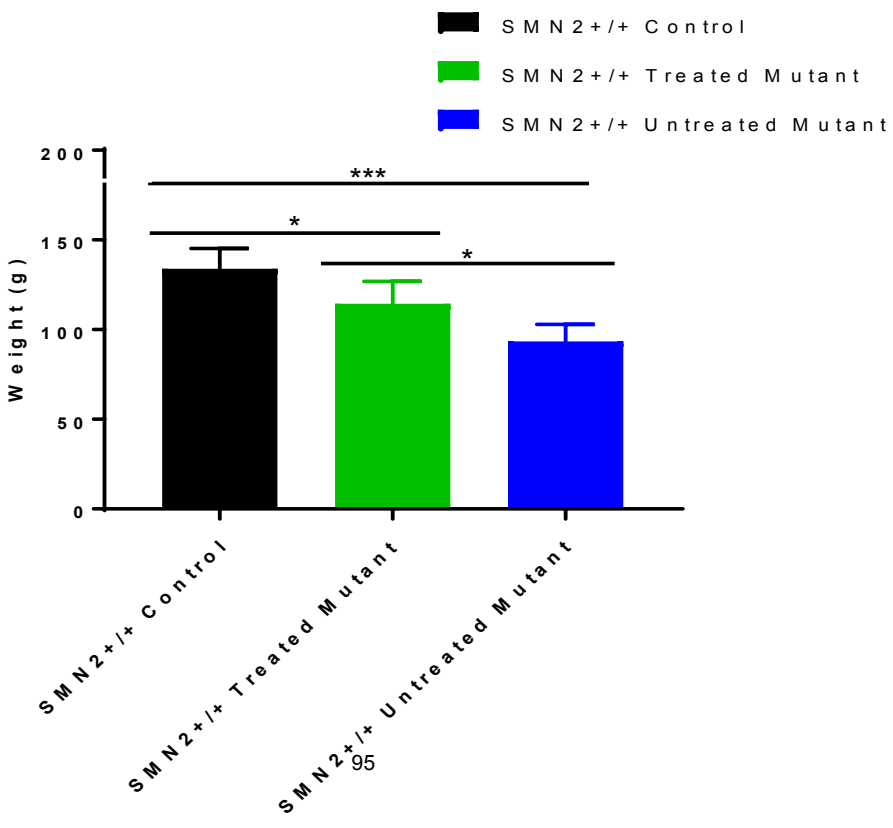
SMN2+/+ Control
SMN2+/+ Treated Mutant
SMN2+/+ Untreated Mutant
***
*
*
200
150
100
50
0
Weight (g)
SMN2+/+ Control
SMN2+/+ Treated Mutant
SMN2+/+ Untreated Mutant

C.

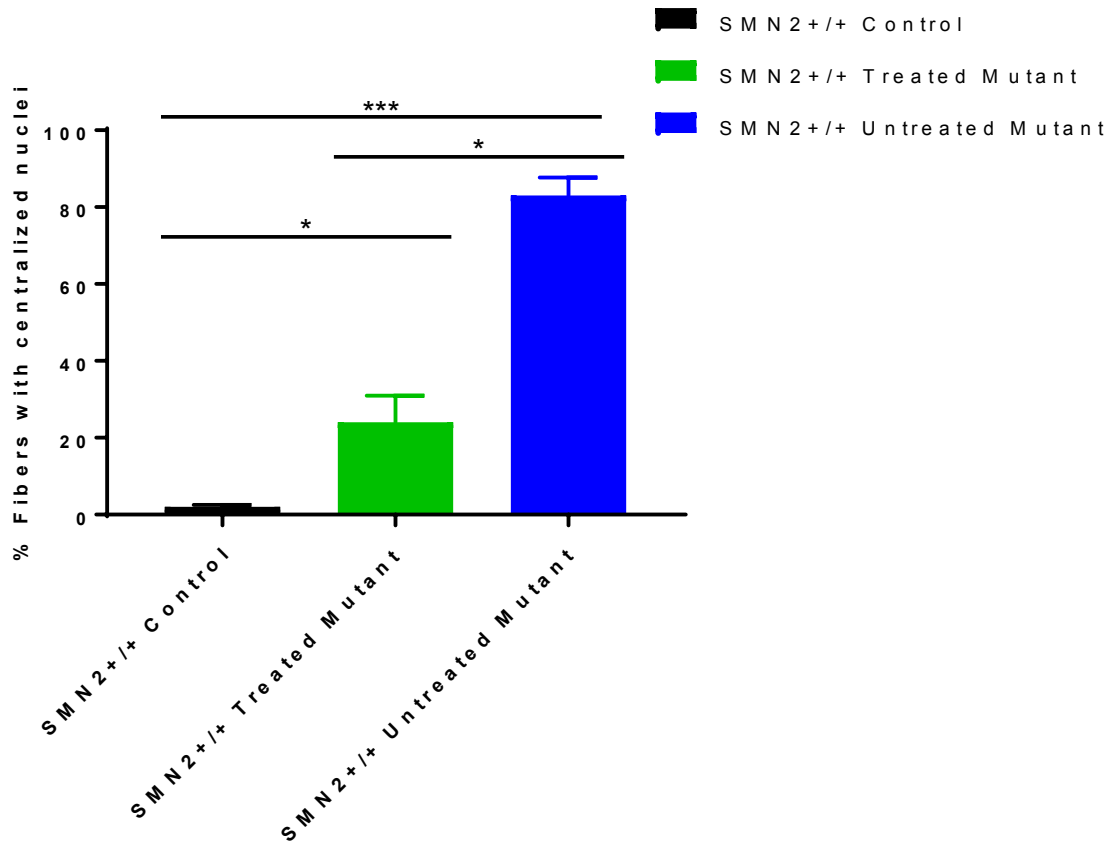
SMN2+/+ Control
SMN2+/+ Treated Mutant
SMN2+/+ Untreated Mutant
% Fibers with centralized nuclei
100
80
60
40
20
0
***
*
*
SMN2+/+ Control
SMN2+/+ Treated Mutant
SMN2+/+ Untreated Mutant

D.

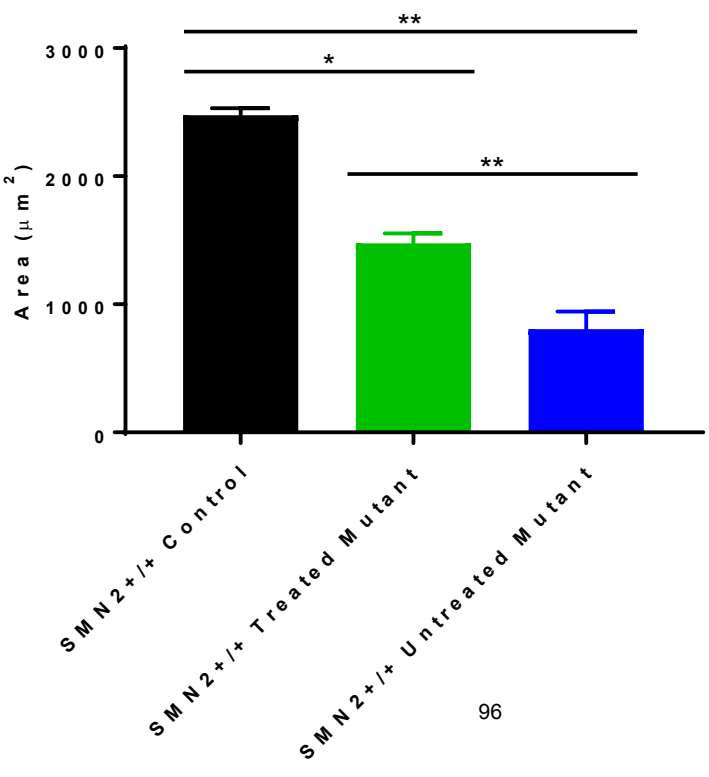
Area (μm²)
3000
2000
1000
0
**
*
**
SMN2+/+ Control
SMN2+/+ Treated Mutant
SMN2+/+ Untreated Mutant

Figure 3.6.1 Muscle pathology mitigated following SMN repletion in symptomatic model mice. **(A)** Representative H&E staining of gastrocnemius of treated and untreated *SMN2*$^{+/+}$ mutants, and controls (Scale bar = 100 μm). **(B)** Weight of gastrocnemius is significantly decreased in both untreated *SMN2*$^{+/+}$ mutants (blue, n=3, ***p<0.001, one-way ANOVA) and treated *SMN2*$^{+/+}$ mutants (green, n=3, *p<0.05, one-way ANOVA) compared to control (black). The weight is significantly increased in treated *SMN2*$^{+/+}$ mutants (green) compared to untreated *SMN2*$^{+/+}$ mutants (blue, n=3, *p<0.05, one-way ANOVA). **(C)** Number of centralized nuclei is increased in both untreated *SMN2*$^{+/+}$ mutants (blue, n=3, ***p<0.001, one-way ANOVA) and treated *SMN2*$^{+/+}$ mutants (green, n=3, *p<0.05, one-way ANOVA). There is a significant difference between untreated *SMN2*$^{+/+}$ mutants (blue) and treated *SMN2*$^{+/+}$ mutants (green, n=3, *p<0.05, one-way ANOVA). **(D)** Furthermore, there is also a significant difference between muscle fiber area of untreated *SMN2*$^{+/+}$ mutants (blue, n=3, **p<0.01, one-way ANOVA) and treated *SMN2*$^{+/+}$ mutants (green, n=3, *p<0.05, one-way ANOVA) compared to control (black). The treated *SMN2*$^{+/+}$ mutants (green) have significantly larger fiber size than untreated *SMN2*$^{+/+}$ mutants (blue, n=3, **p<0.01, one-way ANOVA).

3.6.2 Restoring SMN protein back in skeletal muscle by treating with Morpholino compound mitigates neuromuscular junction defects.

Since the morpholino mitigated the muscle fiber disease phenotype, we looked at the effect it had on the neuromuscular junctions of *SMN2*$^{+/+}$ mutants. There continued to be no significant difference in

the area of the NMJs (Figure 3.6.2A and B), or in the neurofilament accumulation at the nerve terminal among controls, treated and untreated *SMN2*$^{+/+}$ mutant mice (Figure 3.6.2C). None of the groups showed acetylcholine receptors clusters in plaque-like form. There is a significant increase in NMJs with 1-2 perforations in the treated *SMN2*$^{+/+}$ mutant group compared to untreated *SMN2*$^{+/+}$ mutants and controls. The treated *SMN2*$^{+/+}$ mutants also show an increase in NMJs with 3-4 perforations compared untreated *SMN2*$^{+/+}$ mutants and controls. Furthermore, the control group has significantly more NMJs with 4 or more perforations compared to treated *SMN2*$^{+/+}$ mutants and untreated *SMN2*$^{+/+}$ mutants. Treated and untreated *SMN2*$^{+/+}$ mutants have significantly more fragmented NMJs than control. Remarkably, the treated *SMN2*$^{+/+}$ mutants showed fewer fragmented NMJs compared to the untreated *SMN2*$^{+/+}$ mutants (Figure 3.6.2). The significant increase in complexity of NMJs (quantified by the number of perforations in each) in the treated *SMN2*$^{+/+}$ mutants is indicative of newly formed, immature NMJs (Zhonghua *et al*., 2007). Together, these results suggest that after restoring SMN protein to the skeletal muscle of *SMN2*$^{+/+}$ mutants, we were able to mitigate the post-synaptic abnormalities of the NMJs.

A.

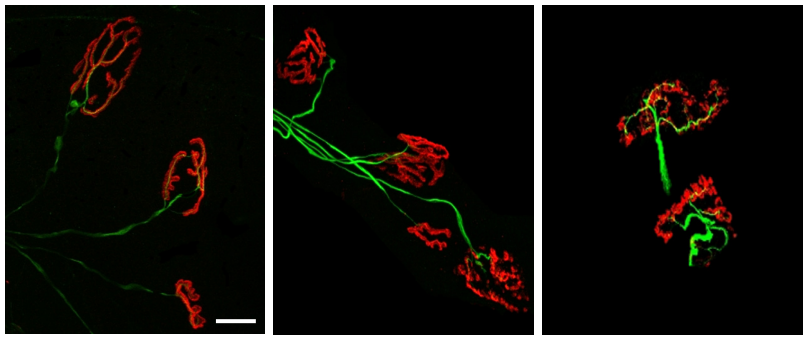
SMN2+/+
SMN2+/+ Treated
SMN2+/+ Untreated

B.

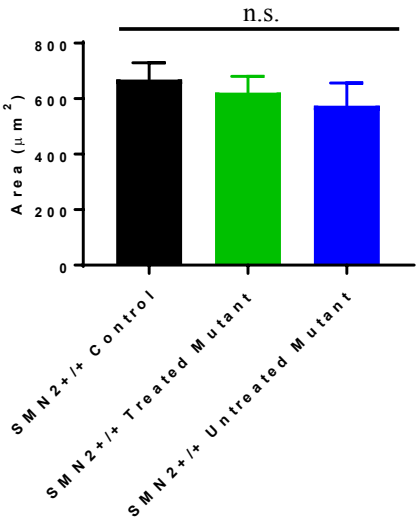
n.s.
Area (μm²)
800
600
400
200
0
SMN2+/+ Control
SMN2+/+ Treated Mutant
SMN2+/+ Untreated Mutant

C.

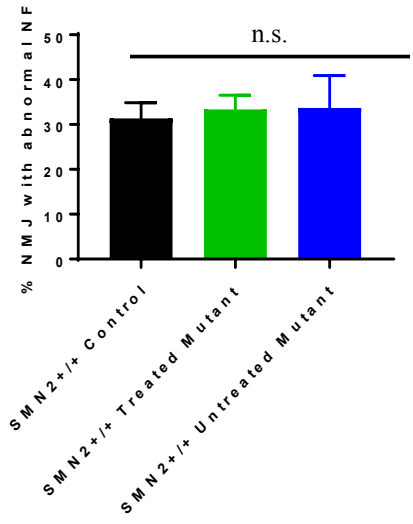
n.s.
% NMJ with abnormal NF
50
40
30
20
10
0
SMN2+/+ Control
SMN2+/+ Treated Mutant
SMN2+/+ Untreated Mutant

D.

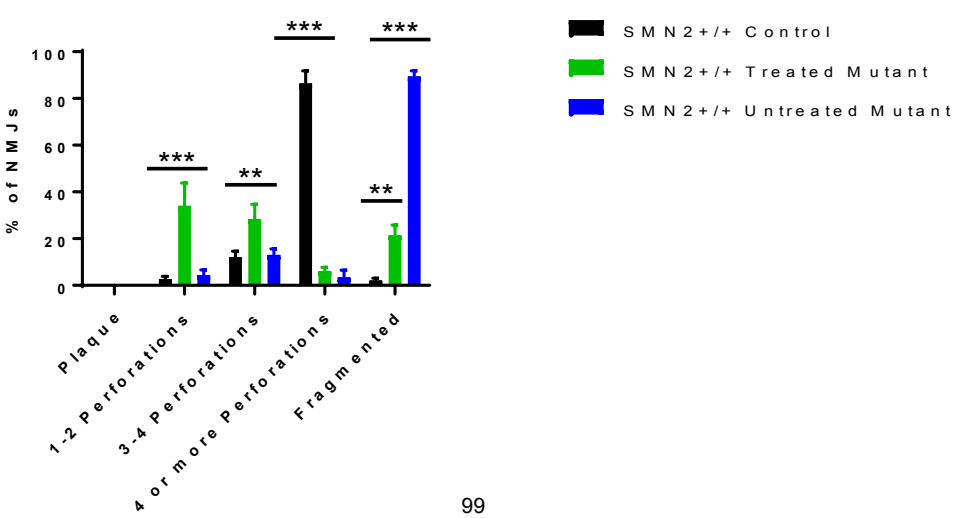
***
***
***
**
**
% of NMJs
100
80
60
40
20
0
Plaque
1-2 Perforations
3-4 Perforations
4 or more Perforations
Fragmented
SMN2+/+ Control
SMN2+/+ Treated Mutant
SMN2+/+ Untreated Mutant

Figure 3.6.2 Restoring SMN protein back in skeletal muscle by treating with Morpholino compound mitigates neuromuscular junction defects **(A)** Representative image of neuromuscular junction of control, treated and untreated *SMN2*$^{+/+}$ mutants. Untreated *SMN2*$^{+/+}$ mutant mice show severe fragmentation of acetylcholine receptor clusters. This fragmentation is mitigated in treated *SMN2*$^{+/+}$ mutants. **(B)** Quantification of NMJ in controls (black), treated (green) and untreated (blue) *SMN2*$^{+/+}$ mutants show no significant difference (n=3, $p>0.05$, one-way ANOVA) among the three groups. **(C)** Although there is a trend in increase of abnormal neurofilament in the nerve terminal between untreated *SMN2*$^{+/+}$ mutants (blue) and control (black), no significant difference was found (n=3, $p>0.05$, one-way ANOVA). **(D)** Quantification of complexity of NMJs shows no NMJs in plaque form. There is a significant increase in NMJs with 1-2 perforations in the treated *SMN2*$^{+/+}$ mutants (green) group compared to untreated *SMN2*$^{+/+}$ mutants (blue) and controls (black, n=3, ***$p<0.001$, one-way ANOVA). The treated *SMN2*$^{+/+}$ mutants (green) also show an increase in NMJs with 3-4 perforations compared untreated *SMN2*$^{+/+}$ mutants (blue) and controls (black, n=3, **$p<0.01$, one-way ANOVA). The control group (black) has significantly more NMJs with 4 or more perforations compared to treated *SMN2*$^{+/+}$ mutants (green) and untreated *SMN2*$^{+/+}$ mutants (blue). Furthermore, untreated *SMN2*$^{+/+}$ mutants (blue) have significantly more fragmented NMJs than control (black, n=3, ***$p<0.001$, one-way ANOVA), and the treated *SMN2*$^{+/+}$ mutants (green) have significantly more fragmented acetylcholine receptors than controls (black, n=3, **$p<0.01$, one-way ANOVA). There is also a significant increase in acetylcholine receptor fragmentation in the untreated *SMN2*$^{+/+}$ mutants (blue) and treated *SMN2*$^{+/+}$ mutants (green, n=3, ***$p<0.001$, one-way ANOVA).

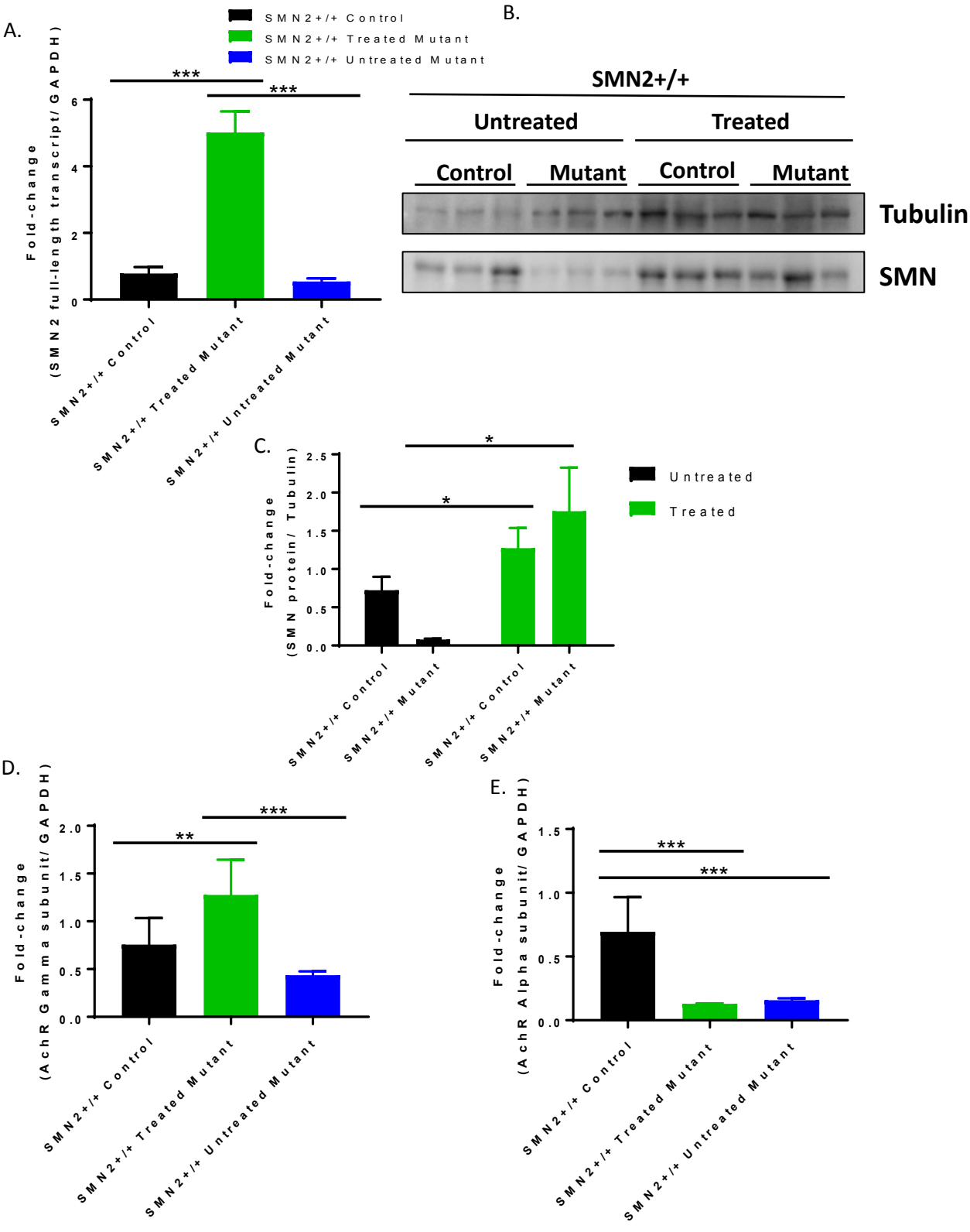
A.
SMN2+/+ Control
SMN2+/+ Treated Mutant
SMN2+/+ Untreated Mutant
***
***
Fold-change
(SMN2 full-length transcript/ GAPDH)
0
2
4
6
SMN2+/+ Control
SMN2+/+ Treated Mutant
SMN2+/+ Untreated Mutant
B.
SMN2+/+
Untreated
Treated
Control
Mutant
Control
Mutant
Tubulin
SMN
C.
*
*
Fold-change
(SMN protein/ Tubulin)
0.0
0.5
1.0
1.5
2.0
2.5
Untreated
Treated
SMN2+/+ Control
SMN2+/+ Mutant
SMN2+/+ Control
SMN2+/+ Mutant
D.
**
***
Fold-change
(AchR Gamma subunit/ GAPDH)
0.0
0.5
1.0
1.5
2.0
SMN2+/+ Control
SMN2+/+ Treated Mutant
SMN2+/+ Untreated Mutant
E.
***
***
Fold-change
(AchR Alpha subunit/ GAPDH)
0.0
0.5
1.0
1.5
SMN2+/+ Control
SMN2+/+ Treated Mutant
SMN2+/+ Untreated Mutant

Figure 3.6.3 Treatment with Morpholino increases *SMN2* full-length transcript but fails to increase number of acetylcholine receptors. **(A)** Through quantitative PCR analyses, we found a significant increase in *SMN2* full-length transcript between treated $SMN2^{+/+}$ mutants (green) and both untreated $SMN2^{+/+}$ mutants (blue) and controls (black, n=3, ***p<0.001, one-way ANOVA). **(B)** Controls (black) have a greater number of acetylcholine receptors than both treated (green) and untreated (blue) $SMN2^{+/+}$ mutants. This was quantified through levels of alpha subunit acetylcholine receptors (n=3, ***p<0.001, one-way ANOVA). **(C)** Treated $SMN2^{+/+}$ mutants (green) show higher expression of gamma subunit acetylcholine receptors than untreated $SMN2^{+/+}$ mutants (blue, n=3, ***p<0.001, one-way ANOVA). Treated $SMN2^{+/+}$ mutants (green) also have a significantly higher expression of gamma subunit than control (black, n=3, **p<0.01, one-way ANOVA).

3.6.3 Treatment with Morpholino (MO) increases *SMN2* full-length transcript and SMN protein, but fails to increase number of acetylcholine receptors.

Studies have shown that utilization of MO targeting ISS-N1 of *SMN2* can modulate splicing mechanics, increase SMN protein and mitigate the SMA disease phenotype (Hua *et al.,* 2010). We felt it was important to conduct an SMN repletion experiments to our skeletal muscle specific SMN-depleted mutant. Additionally, it is therapeutically important to address whether the observed pathology is reversible. Quantitative PCR analyses showed a significant increase in *SMN2* full-length transcript in treated $SMN2^{+/+}$ mutants

compared to both untreated *SMN2*$^{+/+}$ mutants and controls (Figure 3.6.3A). SMN levels in the gastrocnemius of both treated and untreated *SMN2*$^{+/+}$ mutants and controls were determined by western blot analysis (Figure 3.6.3B) There is an increase in SMN protein in both treated *SMN2*$^{+/+}$ mutants and controls compared to untreated *SMN2*$^{+/+}$ mutants and controls (Figure 3.6.3C). This confirms the effectiveness of the MO in increasing the *SMN*2 full-length transcript, and consequently increasing the level of SMN protein in skeletal muscle. Through quantification of the alpha subunit acetylcholine receptor clusters, controls have a higher transcript level of the alpha subunit of the NMJs than both treated and untreated *SMN2*$^{+/+}$ mutants (Figure 3.6.3D). Treated *SMN2*$^{+/+}$ mutants show higher expression of gamma subunit acetylcholine receptor clusters than untreated *SMN2*$^{+/+}$ mutants and controls (Figure 3.6.3E). Remarkably, treated *SMN2*$^{+/+}$ mutants showed a significant increase in gamma subunit acetylcholine receptor clusters, compared to untreated *SMN2*$^{+/+}$ mutants and controls, which is indicative of NMJ remodeling. However, treatment did not rescue the total number of acetylcholine receptor clusters, as treated and untreated *SMN2*$^{+/+}$ had no difference in alpha subunit acetylcholine receptor clusters. This together suggests that the disease phenotype seen in our muscle SMN-depleted mice is caused by insufficient SMN levels. Moreover, increasing the amount of SMN protein to the SMN-depleted muscle proved to mitigate the disease phenotype.

Chapter 4

Discussion

It is known that SMA is caused by insufficient levels of the SMN protein. The decreased level of SMN protein does not only occur in motor neurons, but in every tissue, including skeletal muscle. Previous studies have pointed out that decreased levels of SMN protein in muscle could play a role in the disease phenotype seen in SMA patients.

In 1987, Henderson showed for the first time that low levels of SMN protein in muscle might play a role in the SMA disease phenotype. In his experiments, extracts from SMA patients inhibited neonatal chicken neurite outgrowth (Henderson, 1987). Also, muscle biopsies from Type I and Type II patients when co-cultured with normal rat motor neurons, showed muscle degeneration (Braun, 1995). These results indicate an intrinsic defect in the muscle that only becomes apparent with a connection to a nerve even though the nerve is normal. The aforementioned *in vitro* results suggest that treatment of muscle could have a major influence on the SMA phenotype. However, up to date, no *in vivo* experiments have replicated what has been seen *in vitro* without major caveats.

For instance, to investigate whether a defect of SMN protein in skeletal muscle might have a direct role in the pathology observed in SMA *in vivo*, Cifuentes-Diaz *et al.*, developed a mouse model in which deletion of SMN exon7 was restricted to skeletal muscle. The presumed ablation of SMN led to a severe phenotype characterized by the onset of muscle paralysis after three weeks of age. This ablation of SMN protein culminated in death at a mean age of 33 days. Mononuclear cell infiltration, regenerating myocytes, and necrotic muscle fibers were also observed (Cifuentes-Diaz *et al.*, 2001). In this specific mouse model, the absence of *SMN2* resulted in a complete knockout of skeletal muscle SMN protein, a situation that does not accurately represent human SMA, which is a disease of low SMN. By driving the recombination of the Smn^{F7} allele with the HSA-cre driver, Cifuentes-Diaz *et al*. reported that completely abolishing SMN protein from muscle resulted in a dystrophic phenotype (Cifuentes-Diaz *et al*., 2001). In SMA, some full-length SMN is produced by the *SMN2* gene, and the critical question is whether the low amount of SMN protein is sufficient for normal muscle function. In the *MyoDicre; SMN2;* $Smn^{F7/-}$ mice reported in this current study, the function and structure of skeletal muscle are abnormal upon decreasing SMN in the muscle. The severity of the phenotype induced is dependent on the amount of protein level decrease. *MyoDicre;* $Smn^{F7/-}$ with no copies of *SMN2* are stillborn as they can only rely on $Smn^{\Delta 7}$ for SMN protein.

The Burghes lab made another attempt to investigate the cellular site of action of the SMN protein *in vivo*. Protein levels were selectively restored in severe SMA model. One study restored SMN levels

specifically in skeletal muscle under the human skeletal actin (HSA) promoter, and the other attempted to restore SMN levels specifically in motor neurons under the prion promoter (PrP). Both studies concluded that replacement of SMN in neurons rescues the SMA phenotype and increases the survival of the mice, whereas replacement of SMN levels specifically in muscle fibers had no significant effect on the SMA phenotype or in the survival of the mice (Gavrilina *et al.*, 2008). However, this study did not rule out the possibility that expression of SMN protein in both neurons and muscles is needed for the rescue since the PrP promoter was not completely specific for motor neurons and also showed low levels of expression in muscle.

Additionally, studies have used MyoD and Myf5 (both myogenic regulatory factors) promoters to restore SMN levels *in vivo* specifically in muscle precursor cells and myofibers. The restoration of SMN levels in both satellite cells and myofibers completely rescued myofiber growth, followed by an increase in survival and improved motor behavior. Nevertheless, there was no improvement observed in NMJ morphology (Martinez *et al.*, 2012).

In a recent study published by Iyer *et al.*, it was proposed that low levels of SMN protein are sufficient for normal muscle function in the SMNΔ7 mouse model and that selectively reducing SMN levels in the muscle had no phenotypical effect. They reported no change in the phenotype of their mice upon SMN-reduction in muscle. Moreover, there was no change in body weight, fiber size distribution and survival comparable to healthy controls. In our study, a different

background for the mouse model was used, and it is important to consider that the phenotype of the SMNΔ7 mouse is much less severe than the one seen in the parental *SMN2; Smn*$^{-/-}$ mouse (Le *et al.*, 2005; Monani *et al.*, 2000). The background of the SMNΔ7 may be argued to less accurately mimic the SMA disease than the *SMN2; Smn*$^{-/-}$ background, as it contains an artificial Δ7 cDNA construct that is never found in humans. The mutants in the Iyer *et al.* study may have also been less severe than ours due to the difference in the driver that was used in their study. Although Myf5 is the first skeletal muscle marker, the MyoDicre is an improved Cre (iCre) line that has an improved codon usage for eukaryotic systems which is more efficient than the regular prokaryotic Cre. This increase in efficiency most likely leads to a more efficient MyoDicre driven recombination of the *Smn*^{F7} allele. Our 2 *SMN2* copy mutants develop a progressive phenotype, and Iyer *et al.* conducted most of the histology studies very early on (≤ 8 weeks) with the Myf5-cre mutants. It would have been important to analyze the phenotype of aged Myf5-cre mutants.

In our study, when one copy of *SMN2* is added into the *MyoDicre; Smn*$^{F7/-}$, it is not enough to rescue the phenotype, as they show a decrease in survival, body weight, and deficit in righting reflex. Although the reduction of SMN protein is exclusive to skeletal muscle, the mice have severe muscle weakness, atrophy, and a significant decrease in skeletal muscle fiber number and size.

This study becomes the most interesting when two copies of *SMN2* are added to the *MyoDicre; Smn*$^{F7/-}$ mice. The genetic background of these mice must closely resemble that of severe SMA patients

harboring 2 *SMN2* copies. The 2 copy *SMN2* mutant mice seem to develop normally, as they survive longer than the one copy *SMN2* mice, have similar weights to control, and no defects in the ability to right themselves. However, when these mice reach ~6 months of age, there is a clear progressive disease phenotype mimicking the SMA disease in Type III and Type IV patients. In these patients, there is a late onset of the muscular phenotype and life expectancy is unaffected. Experiments in this study show that the stress of aging causes muscle fibers to degenerate more rapidly in mutants than in controls, and demonstrates the inability of the SMN deficient muscle to undergo repair.

SMA mice and SMA muscle have been studied previously in the situation where SMN is ubiquitously depleted. Abnormalities in myoblast fusion, delayed expression of myogenic proteins, and malformed myotubes have been reported in cell culture studies of SMA muscle (Boyer *et al*., 2014; Bricceno *et al*., 2014; Shafey *et al*., 2005). The results have been reinforced by *in vivo* studies in the muscle of SMA mouse models showing apoptosis of skeletal muscle and defects in the myogenic program (Boyer *et al*., 2014; Fayzullina and Martin, 2014). Likewise, skeletal muscle from SMA Type I fetuses display a decrease in myofiber diameter and fiber size distribution, along with abnormalities in early markers of muscle development.Together these studies have lead to the hypothesis of delayed growth and maturation of skeletal muscle in SMA (Martinez-Hernandez *et al*., 2014; Martinez-Hernandez *et al*., 2009). Overall, muscle appears to show a lack of maturity in the SMA disease, suggesting a delay in myogenesis. In addition, muscle in this state

exhibits a reduced ability to produce force (Boyer *et al*., 2013). The abnormalities in skeletal muscle and at the NMJs observed in our MyoDicre; *SMN2*; $Smn^{F7/-}$ is in agreement with the studies above, even though SMN levels in our mouse model are only depleted in skeletal muscle.

To determine whether these neuromuscular alterations were reversible, we looked into mitigating the pathology seen in our symptomatic $SMN2^{+/+}$ mutant mice by replenishing SMN protein to their skeletal muscle. We accomplished this by administering morpholino IP. The SMN morpholino is an anti-sense oligonucleotide tricking the *SMN2* gene into splicing like the *SMN1* gene. Consequently increasing the production of full-length SMN protein and successfully increasing the life span and improving the phenotype in SMA mice (Hua *et al*., 2011; Passini *et al*., 2011; Porensky *et al*., 2012). In our morpholino study, we have reported an increase in muscle area and myofiber diameter, along with a decrease of fragmentation of the acetylcholine receptor clusters.

Although we have shown that we can mitigate the disease phenotype through restoring SMN protein to the muscle of our mutant mice through the administration of MO, these mice may not have developed any phenotype if they had been treated before the appearance of neuromuscular abnormalities. It would be interesting to see if an earlier administration of the MO could prevent the development of any neuromuscular pathology. It would also be interesting to see if the early administration of MO would increase the survival and the overt phenotype of our $SMN2^{+/-}$ mutants.

As of December of 2016, Nusinersen (Spinraza) became a FDA approved drug to be used in the treatment of spinal muscular atrophy. It is being administered intrathecally, directly to the central nervous system. Nusinersen proved to halt the disease progression during clinical trials in more than half of Type I patients. Like any other antisense drug, Nusinersen comes with risks to the patient, such as abnormalities in coagulation and thrombocytopenia, reduced platelets, renal toxicity, respiratory infections, headaches, back pains, and other side effects that come from the intrathecal injection. There are heightened risks of administering a drug intrathecally. However, to avoid having to cross the blood brain barrier, this is the required route of administration. In our study, we were able to deliver the MO through IP injections, as we did not have to cross the blood brain barrier since SMN protein levels were left intact outside of skeletal muscle.

At this time, Nusinersen is not being administered anywhere outside of the CNS. Muscle protection studies taking place at this time do not address the underlying genetics of SMA or attempt to increase the level of SMN protein in muscle, but instead enhance the muscle's ability to contract, and improve muscle strength (CureSMA.org, 2017).

In 2013, Cure SMA made a drug discovery grant to Cytokinetics, to help fund the study of Tirasemtiv for SMA. Tirasemtiv is a drug that has been examined in clinical trials for individuals with ALS and has laid the foundation for the development of CK-2127107, a skeletal muscle activator. CK-2127107 is a novel fast skeletal muscle

troponin activator being developed as a potential treatment for SMA patients. This first clinical trial of this drug in SMA patients Types II, III, or IV (ages 12 and older) is in Phase 2. It is intended to evaluate the effect of 8 weeks of dosing of CK-2127107 on measures of muscle fatigue and function in both ambulatory and non-ambulatory patients living with SMA (CureSMA.org, 2017).

Increased SMN expression in muscle is an important factor for improvement of the SMA as highlighted by this study. Recently, the importance of high SMN in the peripheral tissues has been indicated (Hua *et al*., 2015). Given our results in the present work where reduction of SMN protein in the muscle contributes to the phenotype seen in SMA patients, we conclude that therapeutically increasing SMN levels in skeletal muscle is necessary for normal muscle function in SMA patients.

REFERENCES

Abbara, C., Estournet, B., Lacomblez, L., Lelièvre, B., Ouslimani, A., Lehmann, B., Viollet, L., Barois, A. and Diquet, B. (2011) 'Riluzole pharmacokinetics in young patients with spinal muscular atrophy', *British Journal of Clinical Pharmacology*, 71(3), pp. 403–410. doi: 10.1111/j.1365-2125.2010.03843.x.

Ackermann, B., Krober, S., Torres-Benito, L., Borgmann, A., Peters, M., Hosseini Barkooie, S. M., Tejero, R., Jakubik, M., Schreml, J., Milbradt, J., Wunderlich, T. F., Riessland, M., Tabares, L. and Wirth, B. (2013) 'Plastin 3 ameliorates spinal muscular atrophy via delayed axon pruning and improves neuromuscular junction functionality', *Human Molecular Genetics*, 22(7), pp. 1328–1347. doi: 10.1093/hmg/dds540.

Andreassi, C., Angelozzi, C., Tiziano, F. D., Vitali, T., De Vincenzi, E., Boninsegna, A., Villanova, M., Bertini, E., Pini, A., Neri, G. and Brahe, C. (2004) 'Phenylbutyrate increases SMN expression in vitro: relevance for treatment of spinal muscular atrophy.', *European journal of human genetics : EJHG*, 12(1), pp. 59–65. doi: 10.1038/sj.ejhg.5201102.

Arnold, A.-S., Gueye, M., Guettier-Sigrist, S., Courdier-Fruh, I., Coupin, G., Poindron, P. and Gies, J.-P. (2004) 'Reduced expression of nicotinic AChRs in myotubes from spinal muscular atrophy I patients', *Laboratory Investigation*, 84(10), pp. 1271–1278. doi: 10.1038/labinvest.3700163.

Avila, A. M., Burnett, B. G., Taye, A. A., Gabanella, F., Knight, M. A., Hartenstein, P., Cizman, Z., Di Prospero, N. A., Pellizzoni, L., Fischbeck, K. H. and Sumner, C. J. (2007) 'Trichostatin A increases SMN expression and survival in a mouse model of spinal muscular atrophy.', *The Journal of clinical investigation*, 117(3), pp. 659–71. doi: 10.1172/JCI29562.

Azzouz, M., Le, T., Ralph, G. S., Walmsley, L., Monani, U. R., Lee, D. C. P., Wilkes, F., Mitrophanous, K. A., Kingsman, S. M., Burghes, A. H. M. and Mazarakis, N. D. (2004) 'Lentivector-mediated SMN replacement in a mouse model of spinal muscular atrophy', *Journal of Clinical Investigation*, 114(12), pp. 1726–1731.

doi: 10.1172/JCI22922.

Bäumer, D., Lee, S., Nicholson, G., Davies, J. L., Parkinson, N. J., Murray, L. M., Gillingwater, T. H., Ansorge, O., Davies, K. E. and Talbot, K. (2009) 'Alternative Splicing Events Are a Late Feature of Pathology in a Mouse Model of Spinal Muscular Atrophy', *PLoS Genetics*. Edited by M. S. Horwitz, 5(12), p. e1000773. doi: 10.1371/journal.pgen.1000773.

Bebee, T. W., Dominguez, C. E. and Chandler, D. S. (2012) 'Mouse models of SMA: tools for disease characterization and therapeutic development', *Human Genetics*, 131(8), pp. 1277–1293. doi: 10.1007/s00439-012-1171-5.

Bernal, S., Also-Rallo, E., Martínez-Hernández, R., Alías, L., Rodríguez-Alvarez, F. J., Millán, J. M., Hernández-Chico, C., Baiget, M. and Tizzano, E. F. (2011) 'Plastin 3 expression in discordant spinal muscular atrophy (SMA) siblings', *Neuromuscular Disorders*, 21(6), pp. 413–419. doi: 10.1016/j.nmd.2011.03.009.

Bosch-Marce, M., Wee, C. D., Martinez, T. L., Lipkes, C. E., Choe, D. W., Kong, L., Van Meerbeke, J. P., Musaro, A. and Sumner, C. J. (2011) 'Increased IGF-1 in muscle modulates the phenotype of severe SMA mice', *Human Molecular Genetics*, 20(9), pp. 1844–1853. doi: 10.1093/hmg/ddr067.

Bowerman, M., Anderson, C. L., Beauvais, A., Boyl, P. P., Witke, W. and Kothary, R. (2009) 'SMN, profilin IIa and plastin 3: a link between the deregulation of actin dynamics and SMA pathogenesis.', *Molecular and cellular neurosciences*, 42(1), pp. 66–74. doi: 10.1016/j.mcn.2009.05.009.

Bowerman, M., Shafey, D. and Kothary, R. (2007) 'Smn depletion alters profilin II expression and leads to upregulation of the RhoA/ROCK pathway and defects in neuronal integrity.', *Journal of molecular neuroscience : MN*, 32(2), pp. 120–31. Available at: http://www.ncbi.nlm.nih.gov/pubmed/17873296 (Accessed: 20 December 2016).

Bowerman, M., Swoboda, K. J., Michalski, J.-P., Wang, G.-S., Reeks, C., Beauvais, A., Murphy, K., Woulfe, J., Screaton, R. A.,

Scott, F. W. and Kothary, R. (2012) ‘Glucose metabolism and pancreatic defects in spinal muscular atrophy.’, *Annals of neurology*, 72(2), pp. 256–68. doi: 10.1002/ana.23582.

Brahe, C., Vitali, T., Tiziano, F. D., Angelozzi, C., Pinto, A. M., Borgo, F., Moscato, U., Bertini, E., Mercuri, E. and Neri, G. (2005) ‘Phenylbutyrate increases SMN gene expression in spinal muscular atrophy patients.’, *European journal of human genetics : EJHG*, 13(2), pp. 256–9. doi: 10.1038/sj.ejhg.5201320.

Brandt, S. (1950) ‘Course and symptoms of progressive infantile muscular atrophy; a follow-up study of 112 cases in Denmark’, *Arch Neurol Psychiat*, 63, pp. 218–228.

Braun, S., Croizat, B., Lagrange, M. C., Poindron, P. and Warter, J. M. (1997) ‘Degeneration of cocultures of spinal muscular atrophy muscle cells and rat spinal cord explants is not due to secreted factors and cannot be prevented by neurotrophins.’, *Muscle & nerve*, 20(8), pp. 953–60. Available at: http://www.ncbi.nlm.nih.gov/pubmed/9236785 (Accessed: 20 December 2016).

Braun, S., Croizat, B., Lagrange, M. C., Warter, J. M. and Poindron, P. (1995) ‘Constitutive muscular abnormalities in culture in spinal muscular atrophy.’, *Lancet (London, England)*, 345(8951), pp. 694–5. Available at: http://www.ncbi.nlm.nih.gov/pubmed/7741893 (Accessed: 20 December 2016).

Brzustowicz, L. M., Lehner, T., Castilla, L. H., Penchaszadeh, G. K., Wilhelmsen, K. C., Daniels, R., Davies, K. E., Leppert, M., Ziter, F., Wood, D., Dubowitz, V., Zerres, K., Hausmanowa-Petrusewicz, I., Ott, J., Munsat, T. L. and Gilliam, T. C. (1990) ‘Genetic mapping of chronic childhood-onset spinal muscular atrophy to chromosome 5q1 1.2–13.3’, *Nature*, 344(6266), pp. 540–541. doi: 10.1038/344540a0.

Buchthal, F. and Olsen, P. Z. (1970) ‘Electromyography and muscle biopsy in infantile spinal muscular atrophy.’, *Brain*, 93, pp. 15–30.

Buchthal and Clemmesen (1941) ‘On the Differentiation of Muscle Atrophy by Electromyography’, *Acta Psych Neurol*, 16, pp. 143–

181.

Burnett, B. G., Crawford, T. O. and Sumner, C. J. (2009) 'Emerging treatment options for spinal muscular atrophy.', *Current treatment options in neurology*, 11(2), pp. 90–101. Available at: http://www.ncbi.nlm.nih.gov/pubmed/19210911 (Accessed: 20 December 2016).

Butchbach, M. E. R., Singh, J., Thorsteinsdottir, M., Saieva, L., Slominski, E., Thurmond, J., Andresson, T., Zhang, J., Edwards, J. D., Simard, L. R., Pellizzoni, L., Jarecki, J., Burghes, A. H. M. and Gurney, M. E. (2010) 'Effects of 2,4-diaminoquinazoline derivatives on SMN expression and phenotype in a mouse model for spinal muscular atrophy', *Human Molecular Genetics*, 19(3), pp. 454–467. doi: 10.1093/hmg/ddp510.

Calder, A. N., Androphy, E. J. and Hodgetts, K. J. (2016) 'Small Molecules in Development for the Treatment of Spinal Muscular Atrophy', *Journal of Medicinal Chemistry*, 59(22), pp. 10067–10083. doi: 10.1021/acs.jmedchem.6b00670.

Cartegni, L., Hastings, M. L., Calarco, J. A., de Stanchina, E. and Krainer, A. R. (2006) 'Determinants of exon 7 splicing in the spinal muscular atrophy genes, SMN1 and SMN2.', *American journal of human genetics*, 78(1), pp. 63–77. doi: 10.1086/498853.

Cauchi, R. J. (2010) 'SMN and Gemins: "We are family" … or are we?', *BioEssays*, 32(12), pp. 1077–1089. doi: 10.1002/bies.201000088.

Chan, Y. B., Miguel-Aliaga, I., Franks, C., Thomas, N., Trülzsch, B., Sattelle, D. B., Davies, K. E. and van den Heuvel, M. (2003) 'Neuromuscular defects in a Drosophila survival motor neuron gene mutant.', *Human molecular genetics*, 12(12), pp. 1367–76. Available at: http://www.ncbi.nlm.nih.gov/pubmed/12783845 (Accessed: 20 December 2016).

Chang, H. C.-H., Dimlich, D. N., Yokokura, T., Mukherjee, A., Kankel, M. W., Sen, A., Sridhar, V., Fulga, T. A., Hart, A. C., Van Vactor, D. and Artavanis-Tsakonas, S. (2008) 'Modeling Spinal Muscular Atrophy in Drosophila', *PLoS ONE*. Edited by A. Lewin, 3(9), p. e3209. doi: 10.1371/journal.pone.0003209.

Chang, J.-G., Hsieh-Li, H.-M., Jong, Y.-J., Wang, N. M., Tsai, C.-H. and Li, H. (2001) 'Treatment of spinal muscular atrophy by sodium butyrate', *Proceedings of the National Academy of Sciences*, 98(17), pp. 9808–9813. doi: 10.1073/pnas.171105098.

Chari, A., Paknia, E. and Fischer, U. (2009) 'The role of RNP biogenesis in spinal muscular atrophy', *Current Opinion in Cell Biology*, 21(3), pp. 387–393. doi: 10.1016/j.ceb.2009.02.004.

Chen, T.-H., Chang, J.-G., Yang, Y.-H., Mai, H.-H., Liang, W.-C., Wu, Y.-C., Wang, H.-Y., Huang, Y.-B., Wu, S.-M., Chen, Y.-C., Yang, S.-N. and Jong, Y.-J. (2010) 'Randomized, double-blind, placebo-controlled trial of hydroxyurea in spinal muscular atrophy', *Neurology*, 75(24), pp. 2190–2197. doi: 10.1212/WNL.0b013e3182020332.

Cifuentes-Diaz, C., Frugier, T., Tiziano, F. D., Lacène, E., Roblot, N., Joshi, V., Moreau, M. H. and Melki, J. (2001) 'Deletion of murine SMN exon 7 directed to skeletal muscle leads to severe muscular dystrophy.', *The Journal of cell biology*, 152(5), pp. 1107–14. Available at: http://www.ncbi.nlm.nih.gov/pubmed/11238465 (Accessed: 20 December 2016).

Corti, S., Locatelli, F., Papadimitriou, D., Del Bo, R., Nizzardo, M., Nardini, M., Donadoni, C., Salani, S., Fortunato, F., Strazzer, S., Bresolin, N. and Comi, G. P. (2007) 'Neural stem cells LewisX + CXCR4 + modify disease progression in an amyotrophic lateral sclerosis model', *Brain*, 130(5), pp. 1289–1305. doi: 10.1093/brain/awm043.

Corti, S., Nizzardo, M., Nardini, M., Donadoni, C., Salani, S., Ronchi, D., Saladino, F., Bordoni, A., Fortunato, F., Del Bo, R., Papadimitriou, D., Locatelli, F., Menozzi, G., Strazzer, S., Bresolin, N. and Comi, G. P. (2008) 'Neural stem cell transplantation can ameliorate the phenotype of a mouse model of spinal muscular atrophy', *Journal of Clinical Investigation*, 118(10), pp. 3316–3330. doi: 10.1172/JCI35432.

Corti, S., Nizzardo, M., Nardini, M., Donadoni, C., Salani, S., Simone, C., Falcone, M., Riboldi, G., Govoni, A., Bresolin, N. and

Comi, G. P. (2010) 'Systemic transplantation of c-kit+ cells exerts a therapeutic effect in a model of amyotrophic lateral sclerosis', *Human Molecular Genetics*, 19(19), pp. 3782–3796. doi: 10.1093/hmg/ddq293.

Crawford, T. O. and Pardo, C. A. (1996) 'The neurobiology of childhood spinal muscular atrophy.', *Neurobiology of disease*, 3(2), pp. 97–110. doi: 10.1006/nbdi.1996.0010.

Dachs, E., Hereu, M., Piedrafita, L., Casanovas, A., Calderó, J. and Esquerda, J. E. (2011) 'Defective neuromuscular junction organization and postnatal myogenesis in mice with severe spinal muscular atrophy.', *Journal of neuropathology and experimental neurology*, 70(6), pp. 444–61. doi: 10.1097/NEN.0b013e31821cbd8b.

Darbar, I. A., Plaggert, P. G., Resende, M. B. D., Zanoteli, E. and Reed, U. C. (2011) 'Evaluation of muscle strength and motor abilities in children with type II and III spinal muscle atrophy treated with valproic acid', *BMC Neurology*, 11(1), p. 36. doi: 10.1186/1471-2377-11-36.

Dimitriadi, M., Derdowski, A., Kalloo, G., Maginnis, M. S., O'Hern, P., Bliska, B., Sorkaç, A., Nguyen, K. C. Q., Cook, S. J., Poulogiannis, G., Atwood, W. J., Hall, D. H. and Hart, A. C. (2016) 'Decreased function of survival motor neuron protein impairs endocytic pathways', *Proceedings of the National Academy of Sciences*, 113(30), pp. E4377–E4386. doi: 10.1073/pnas.1600015113.

Dimitriadi, M., Sleigh, J. N., Walker, A., Chang, H. C., Sen, A., Kalloo, G., Harris, J., Barsby, T., Walsh, M. B., Satterlee, J. S., Li, C., Van Vactor, D., Artavanis-Tsakonas, S. and Hart, A. C. (2010) 'Conserved Genes Act as Modifiers of Invertebrate SMN Loss of Function Defects', *PLoS Genetics*. Edited by G. S. Barsh, 6(10), p. e1001172. doi: 10.1371/journal.pgen.1001172.

Doktor, T. K., Hua, Y., Andersen, H. S., Brøner, S., Liu, Y. H., Wieckowska, A., Dembic, M., Bruun, G. H., Krainer, A. R. and Andresen, B. S. (2016) 'RNA-sequencing of a mouse-model of spinal muscular atrophy reveals tissue-wide changes in splicing of

U12-dependent introns.', *Nucleic acids research*, p. gkw731. doi: 10.1093/nar/gkw731.

Dombert, B., Sivadasan, R., Simon, C. M., Jablonka, S., Sendtner, M., Battle, D., Kasim, M., Yong, J., Lotti, F., Lau, C., Lotti, F., Imlach, W., Saieva, L., Beck, E., Hao, lT, Kong, L., Wang, X., Choe, D., Polley, M., Burnett, B., Ling, K., Lin, M., Zingg, B., Feng, Z., Ko, C., Ling, K., Gibbs, R., Feng, Z., Ko, C., Martinez-Hernandez, R., Bernal, S., Also-Rallo, E., Alias, L., Barcelo, M., Kariya, S., Obis, T., Garone, C., Akay, T., Sera, F., Swoboda, K., Prior, T., Scott, C., McNaught, T., Wride, M., Kariya, S., Park, G., Maeno-Hikichi, Y., Leykekhman, O., Lutz, C., Martinez, T., Kong, L., Wang, X., Osborne, M., Crowder, M., Ruiz, R., Casanas, J., Torres-Benito, L., Cano, R., Tabares, L., Torres-Benito, L., Ruiz, R., Tabares, L., Torres-Benito, L., Neher, M., Cano, R., Ruiz, R., Tabares, L., Jablonka, S., Beck, M., Lechner, B., Mayer, C., Sendtner, M., Liu, Q., Dreyfuss, G., Carvalho, T., Almeida, F., Calapez, A., Lafarga, M., Berciano, M., Rossoll, W., Kroning, A., Ohndorf, U., Steegborn, C., Jablonka, S., Rossoll, W., Jablonka, S., Andreassi, C., Kroning, A., Karle, K., Zhang, H., Xing, L., Rossoll, W., Wichterle, H., Singer, R., Grimmler, M., Otter, S., Peter, C., Muller, F., Chari, A., Otter, S., Grimmler, M., Neuenkirchen, N., Chari, A., Sickmann, A., Gubitz, A., Feng, W., Dreyfuss, G., Chari, A., Paknia, E., Fischer, U., Pellizzoni, L., Yong, J., Dreyfuss, G., Kolb, S., Battle, D., Dreyfuss, G., Schrank, B., Gotz, R., Gunnersen, J., Ure, J., Toyka, K., Burghes, A., Beattie, C., Glinka, M., Herrmann, T., Funk, N., Havlicek, S., Rossoll, W., Piazzon, N., Rage, F., Schlotter, F., Moine, H., Branlant, C., Yamazaki, T., Chen, S., Yu, Y., Yan, B., Haertlein, T., Turner, B., Baumer, D., Parkinson, N., Scaber, J., Ansorge, O., Shan, X., Chiang, P., Price, D., Wong, P., Bose, J., Wang, I., Hung, L., Tarn, W., Shen, C., Rossoll, W., Bassell, G., Fallini, C., Zhang, H., Su, Y., Silani, V., Singer, R., McWhorter, M., Monani, U., Burghes, A., Beattie, C., Sleeman, J., Chaudhury, A., Chander, P., Howe, P., Han, S., Tang, Y., Smith, R., Mourelatos, Z., Abel, L., Yong, J., Kataoka, N., Dreyfuss, G., Mizutani, A., Fukuda, M., Ibata, K., Shiraishi, Y., Mikoshiba, K., Dunn, K., Kamocka, M., McDonald, J., Porter, B., Weis, J., Sanes, J., Nishimune, H., Sanes, J., Carlson, S., Kim, J., Hahm, B., Kim, Y., Choi, M., Jang, S., Renvoise, B., Querol, G., Verrier, E., Burlet, P., Lefebvre, S., Grimmler, M., Bauer, L., Nousiainen, M., Korner, R., Meister, G., Petri, S., Grimmler, M.,

Over, S., Fischer, U., Gruss, O., Husedzinovic, A., Oppermann, F., Draeger-Meurer, S., Chari, A., Fischer, U., Carnegie, G., Sleeman, J., Morrice, N., Hastie, C., Peggie, M., Jablonka, S., Schrank, B., Kralewski, M., Rossoll, W., Sendtner, M., Williams, B., Vinnakota, S., Sawyer, C., Waldrep, J., Hamilton, S., Walker, M., Rajendra, T., Saieva, L., Fuentes, J., Pellizzoni, L., Fayzullina, S., Martin, L., Tadesse, H., Deschênes-Furry, J., Boisvenue, S., Côte, J., Tsuiji, H., Iguchi, Y., Furuya, A., Kataoka, A., Hatsuta, H., Hubers, L., Valderrama-Carvajal, H., Laframboise, J., Timbers, J., Sanchez, G., Akten, B., Kye, M., Hao, lT, Wertz, M., Singh, S., Jablonka, S., Dombert, B., Asan, E., Sendtner, M., Noakes, P., Gautam, M., Mudd, J., Sanes, J., Merlie, J., Le, T., McGovern, V., Alwine, I., Wang, X., Massoni-Laporte, A., Gogliotti, R., Cardona, H., Singh, J., Bail, S., Emery, C., Groen, E., Fumoto, K., Blokhuis, A., Engelen-Lee, J., Zhou, Y., Gerbino, V., Carri, M., Cozzolino, M., Achsel, T., Yamazaki, T., Chen, S., Yu, Y., Yan, B., Haertlein, T., Armstrong, G., Drapeau, P., Shahidullah, M., Marchand, S. Le, Fei, H., Zhang, J., Pandey, U., Achsel, T., Barabino, S., Cozzolino, M., Carri, M., Alami, N., Smith, R., Carrasco, M., Williams, L., Winborn, C., Dale, J., Shen, H., Barry, D., Garcia, V., Rose, F., Chen, H., Chang, J., Lu, R., Peng, T., Tarn, W., Cho, S., Moon, H., Loh, T., Oh, H., Cho, S., Harahap, I., Saito, T., San, L., Sasaki, N., al Gunadi, et, Hofmann, Y., Wirth, B., Hua, Y., Vickers, T., Okunola, H., Bennett, C., Krainer, A., Kashima, T., Rao, N., David, C., Manley, J., Sanchez, G., Dury, A., Murray, L., Biondi, O., Tadesse, H., Kim, H., Kim, N., Wang, Y., Scarborough, E., Moore, J., Rage, F., Boulisfane, N., Rihan, K., Neel, H., Gostan, T., Zhang, Z., Pinto, A., Wan, L., Wang, W., Berg, M., Wiese, S., Herrmann, T., Drepper, C., Jablonka, S., Funk, N., Subramanian, N., Wetzel, A., Dombert, B., Yadav, P., Havlicek, S., Lois, C., Hong, E., Pease, S., Brown, E., Baltimore, D., Simon, C., Jablonka, S., Ruiz, R., Tabares, L. and Sendtner, M. (2014) 'Presynaptic Localization of Smn and hnRNP R in Axon Terminals of Embryonic and Postnatal Mouse Motoneurons', *PLoS ONE*. Edited by M. A. Fox. Public Library of Science, 9(10), p. e110846. doi: 10.1371/journal.pone.0110846.

Dominguez, E., Marais, T., Chatauret, N., Benkhelifa-Ziyyat, S., Duque, S., Ravassard, P., Carcenac, R., Astord, S., de Moura, A. P., Voit, T. and Barkats, M. (2011) 'Intravenous scAAV9 delivery of a codon-optimized SMN1 sequence rescues SMA mice', *Human*

Molecular Genetics, 20(4), pp. 681–693. doi: 10.1093/hmg/ddq514.

Dubowitz, V., Sewry, C. A. and Fitzsimons, R. B. (1985) *Muscle biopsy : a practical approach*. 2nd ed., *London ; Philadelphia : Baillière Tindall*. 2nd ed. Available at: http://www.ncbi.nlm.nih.gov/pubmed/8707811.

Evans, M. C., Cherry, J. J. and Androphy, E. J. (2011) 'Differential regulation of the SMN2 gene by individual HDAC proteins', *Biochemical and Biophysical Research Communications*, 414(1), pp. 25–30. doi: 10.1016/j.bbrc.2011.09.011.

Fallini, C., Bassell, G. and Rossoll, W. (2012) 'Spinal muscular atrophy: The role of SMN in axonal mRNA regulation', *Brain Research*, 1462, pp. 81–92. doi: 10.1016/j.brainres.2012.01.044.

Fallini, C., Zhang, H., Su, Y., Silani, V., Singer, R. H., Rossoll, W. and Bassell, G. J. (2011) 'The Survival of Motor Neuron (SMN) Protein Interacts with the mRNA-Binding Protein HuD and Regulates Localization of Poly(A) mRNA in Primary Motor Neuron Axons', *Journal of Neuroscience*, 31(10), pp. 3914–3925. doi: 10.1523/JNEUROSCI.3631-10.2011.

Farooq, F., Molina, F. A., Hadwen, J., MacKenzie, D., Witherspoon, L., Osmond, M., Holcik, M. and MacKenzie, A. (2011) 'Prolactin increases SMN expression and survival in a mouse model of severe spinal muscular atrophy via the STAT5 pathway', *Journal of Clinical Investigation*, 121(8), pp. 3042–3050. doi: 10.1172/JCI46276.

Finkel, R. S. *et al*. (2016) 'Treatment of infantile-onset spinal muscular atrophy with nusinersen: a phase 2, open-label, dose-escalation study', *The Lancet*, 388(10063), pp. 3017–3026.

Fischer, U., Liu, Q. and Dreyfuss, G. (1997) 'The SMN-SIP1 complex has an essential role in spliceosomal snRNP biogenesis.', *Cell*, 90(6), pp. 1023–9. Available at: http://www.ncbi.nlm.nih.gov/pubmed/9323130 (Accessed: 20 December 2016).

Foust, K. D., Wang, X., McGovern, V. L., Braun, L., Bevan, A. K., Haidet, A. M., Le, T. T., Morales, P. R., Rich, M. M., Burghes, A.

H. M. and Kaspar, B. K. (2010) ‘Rescue of the spinal muscular atrophy phenotype in a mouse model by early postnatal delivery of SMN.’, *Nature biotechnology*. NIH Public Access, 28(3), pp. 271–4. doi: 10.1038/nbt.1610.

Gabanella, F., Butchbach, M. E. R., Saieva, L., Carissimi, C., Burghes, A. H. M. and Pellizzoni, L. (2007) ‘Ribonucleoprotein assembly defects correlate with spinal muscular atrophy severity and preferentially affect a subset of spliceosomal snRNPs.’, *PloS one*. Public Library of Science, 2(9), p. e921. doi: 10.1371/journal.pone.0000921.

Garbes, L., Riessland, M., Hölker, I., Heller, R., Hauke, J., Tränkle, C., Coras, R., Blümcke, I., Hahnen, E. and Wirth, B. (2009) ‘LBH589 induces up to 10-fold SMN protein levels by several independent mechanisms and is effective even in cells from SMA patients non-responsive to valproate.’, *Human molecular genetics*, 18(19), pp. 3645–58. doi: 10.1093/hmg/ddp313.

Garcia, E. L., Lu, Z., Meers, M. P., Praveen, K. and Matera, A. G. (2013) ‘Developmental arrest of Drosophila survival motor neuron (Smn) mutants accounts for differences in expression of minor intron-containing genes.’, *RNA (New York, N.Y.)*. Cold Spring Harbor Laboratory Press, 19(11), pp. 1510–6. doi: 10.1261/rna.038919.113.

Gavrilina, T. O., McGovern, V. L., Workman, E., Crawford, T. O., Gogliotti, R. G., DiDonato, C. J., Monani, U. R., Morris, G. E. and Burghes, A. H. M. (2008) ‘Neuronal SMN expression corrects spinal muscular atrophy in severe SMA mice while muscle-specific SMN expression has no phenotypic effect’, *Human Molecular Genetics*, 17(8), pp. 1063–1075. doi: 10.1093/hmg/ddm379.

Giesemann, T., Rathke-Hartlieb, S., Rothkegel, M., Bartsch, J. W., Buchmeier, S., Jockusch, B. M. and Jockusch, H. (1999) ‘A role for polyproline motifs in the spinal muscular atrophy protein SMN. Profilins bind to and colocalize with smn in nuclear gems.’, *The Journal of biological chemistry*, 274(53), pp. 37908–14. Available at: http://www.ncbi.nlm.nih.gov/pubmed/10608857 (Accessed: 20 December 2016).

Gogliotti, R. G., Hammond, S. M., Lutz, C. and DiDonato, C. J. (2010) 'Molecular and phenotypic reassessment of an infrequently used mouse model for spinal muscular atrophy', *Biochemical and Biophysical Research Communications*, 391(1), pp. 517–522. doi: 10.1016/j.bbrc.2009.11.090.

Greensmith, L. and Vrbová, G. (1997) 'Disturbances of neuromuscular interaction may contribute to muscle weakness in spinal muscular atrophy.', *Neuromuscular disorders : NMD*, 7(6–7), pp. 369–72. Available at: http://www.ncbi.nlm.nih.gov/pubmed/9327400 (Accessed: 20 December 2016).

Grunstein, M. (1997) 'Histone acetylation in chromatin structure and transcription.', *Nature*, 389(6649), pp. 349–352. doi: 10.1038/38664.

Grzeschik, S. M., Ganta, M., Prior, T. W., Heavlin, W. D. and Wang, C. H. (2005) 'Hydroxyurea enhances SMN2 gene expression in spinal muscular atrophy cells.', *Annals of neurology*, 58(2), pp. 194–202. doi: 10.1002/ana.20548.

Guettier-Sigrist, S., Coupin, G., Braun, S., Warter, J. M. and Poindron, P. (1998) 'Muscle could be the therapeutic target in SMA treatment.', *Journal of neuroscience research*, 53(6), pp. 663–9. doi: 10.1002/(SICI)1097-4547(19980915)53:6<663::AID-JNR4>3.0.CO;2-3.

Haddad, H., Cifuentes-Diaz, C., Miroglio, A., Roblot, N., Joshi, V. and Melki, J. (2003) 'Riluzole attenuates spinal muscular atrophy disease progression in a mouse model.', *Muscle & nerve*, 28(4), pp. 432–7. doi: 10.1002/mus.10455.

Hahnen, E., Eyupoglu, I. Y., Brichta, L., Haastert, K., Trankle, C., Siebzehnrubl, F. A., Riessland, M., Holker, I., Claus, P., Romstock, J., Buslei, R., Wirth, B. and Blumcke, I. (2006) 'In vitro and ex vivo evaluation of second-generation histone deacetylase inhibitors for the treatment of spinal muscular atrophy', *Journal of Neurochemistry*, 98(1), pp. 193–202. doi: 10.1111/j.1471-4159.2006.03868.x.

Hamilton, G. and Gillingwater, T. H. (2013) 'Spinal muscular

atrophy: going beyond the motor neuron', *Trends in Molecular Medicine*, 19(1), pp. 40–50. doi: 10.1016/j.molmed.2012.11.002.

Hao, L. T., Wolman, M., Granato, M. and Beattie, C. E. (2012) 'Survival motor neuron affects plastin 3 protein levels leading to motor defects.', *The Journal of neuroscience : the official journal of the Society for Neuroscience*. NIH Public Access, 32(15), pp. 5074–84. doi: 10.1523/JNEUROSCI.5808-11.2012.

Hastings, M. L., Berniac, J., Liu, Y. H., Abato, P., Jodelka, F. M., Barthel, L., Kumar, S., Dudley, C., Nelson, M., Larson, K., Edmonds, J., Bowser, T., Draper, M., Higgins, P. and Krainer, A. R. (2009) 'Tetracyclines that promote SMN2 exon 7 splicing as therapeutics for spinal muscular atrophy.', *Science translational medicine*, 1(5), p. 5ra12. doi: 10.1126/scitranslmed.3000208.

Hayhurst, M., Wagner, A. K., Cerletti, M., Wagers, A. J. and Rubin, L. L. (2012) 'A cell-autonomous defect in skeletal muscle satellite cells expressing low levels of survival of motor neuron protein', *Developmental Biology*, 368(2), pp. 323–334. doi: 10.1016/j.ydbio.2012.05.037.

Hegedus, J., Putman, C. T. and Gordon, T. (2007) 'Time course of preferential motor unit loss in the SOD1G93A mouse model of amyotrophic lateral sclerosis', *Neurobiology of Disease*, 28(2), pp. 154–164. doi: 10.1016/j.nbd.2007.07.003.

Heier, C. R. and DiDonato, C. J. (2009) 'Translational readthrough by the aminoglycoside geneticin (G418) modulates SMN stability in vitro and improves motor function in SMA mice in vivo.', *Human molecular genetics*. Oxford University Press, 18(7), pp. 1310–22. doi: 10.1093/hmg/ddp030.

Heier, C. R., Satta, R., Lutz, C. and DiDonato, C. J. (2010) 'Arrhythmia and cardiac defects are a feature of spinal muscular atrophy model mice.', *Human molecular genetics*, 19(20), pp. 3906–18. doi: 10.1093/hmg/ddq330.

Henderson, C. E., Hauser, S. L., Huchet, M., Dessi, F., Hentati, F., Taguchi, T., Changeux, J. P. and Fardeau, M. (1987) 'Extracts of muscle biopsies from patients with spinal muscular atrophies inhibit neurite outgrowth from spinal neurons.', *Neurology*, 37(8), pp.

1361–4. Available at: http://www.ncbi.nlm.nih.gov/pubmed/3614658 (Accessed: 20 December 2016).

Hosseinibarkooie, S., Peters, M., Torres-Benito, L., Rastetter, R. H., Hupperich, K., Hoffmann, A., Mendoza-Ferreira, N., Kaczmarek, A., Janzen, E., Milbradt, J., Lamkemeyer, T., Rigo, F., Bennett, C. F., Guschlbauer, C., Büschges, A., Hammerschmidt, M., Riessland, M., Kye, M. J., Clemen, C. S. and Wirth, B. (2016) 'The Power of Human Protective Modifiers: PLS3 and CORO1C Unravel Impaired Endocytosis in Spinal Muscular Atrophy and Rescue SMA Phenotype', *The American Journal of Human Genetics*, 99(3), pp. 647–665. doi: 10.1016/j.ajhg.2016.07.014.

Hua, Y., Sahashi, K., Hung, G., Rigo, F., Passini, M. A., Bennett, C. F. and Krainer, A. R. (2010) 'Antisense correction of SMN2 splicing in the CNS rescues necrosis in a type III SMA mouse model', *Genes & Development*, 24(15), pp. 1634–1644. doi: 10.1101/gad.1941310.

Hua, Y., Sahashi, K., Rigo, F., Hung, G., Horev, G., Bennett, C. F. and Krainer, A. R. (2011) 'Peripheral SMN restoration is essential for long-term rescue of a severe spinal muscular atrophy mouse model', *Nature*, 478(7367), pp. 123–126. doi: 10.1038/nature10485.

Hubers, L., Valderrama-Carvajal, H., Laframboise, J., Timbers, J., Sanchez, G. and Côté, J. (2011) 'HuD interacts with survival motor neuron protein and can rescue spinal muscular atrophy-like neuronal defects.', *Human molecular genetics*, 20(3), pp. 553–79. doi: 10.1093/hmg/ddq500.

Imlach, W. L., Beck, E. S., Choi, B. J., Lotti, F., Pellizzoni, L. and McCabe, B. D. (2012) 'SMN Is Required for Sensory-Motor Circuit Function in Drosophila', *Cell*, 151(2), pp. 427–439. doi: 10.1016/j.cell.2012.09.011.

Jablonka, S. and Sendtner, M. (2003) 'Molecular and cellular basis of spinal muscular atrophy.', *Amyotrophic lateral sclerosis and other motor neuron disorders : official publication of the World Federation of Neurology, Research Group on Motor Neuron Diseases*, 4(3), pp. 144–9. Available at:

http://www.ncbi.nlm.nih.gov/pubmed/13129800 (Accessed: 20 December 2016).

Kadosh, D. and Struhl, K. (no date) 'Histone deacetylase activity of Rpd3 is important for transcriptional repression in vivo'.

Kariya, S., Park, G.-H., Maeno-Hikichi, Y., Leykekhman, O., Lutz, C., Arkovitz, M. S., Landmesser, L. T. and Monani, U. R. (2008) 'Reduced SMN protein impairs maturation of the neuromuscular junctions in mouse models of spinal muscular atrophy', *Human Molecular Genetics*, 17(16), pp. 2552–2569. doi: 10.1093/hmg/ddn156.

Kashima, T., Rao, N. and Manley, J. L. (2007) 'An intronic element contributes to splicing repression in spinal muscular atrophy.', *Proceedings of the National Academy of Sciences of the United States of America*. National Academy of Sciences, 104(9), pp. 3426–31. doi: 10.1073/pnas.0700343104.

Katoh-Semba, R., Asano, T., Ueda, H., Morishita, R., Takeuchi, I. K., Inaguma, Y. and Kato, K. (2002) 'Riluzole enhances expression of brain-derived neurotrophic factor with consequent proliferation of granule precursor cells in the rat hippocampus', *The FASEB Journal*, 16(10), pp. 1328–30. doi: 10.1096/fj.02-0143fje.

Kong, L., Wang, X., Choe, D. W., Polley, M., Burnett, B. G., Bosch-Marce, M., Griffin, J. W., Rich, M. M. and Sumner, C. J. (2009) 'Impaired Synaptic Vesicle Release and Immaturity of Neuromuscular Junctions in Spinal Muscular Atrophy Mice', *Journal of Neuroscience*, 29(3), pp. 842–851. doi: 10.1523/JNEUROSCI.4434-08.2009.

Le, T. T., Pham, L. T., Butchbach, M. E. R., Zhang, H. L., Monani, U. R., Coovert, D. D., Gavrilina, T. O., Xing, L., Bassell, G. J. and Burghes, A. H. M. (2005) 'SMN 7, the major product of the centromeric survival motor neuron (SMN2) gene, extends survival in mice with spinal muscular atrophy and associates with full-length SMN', *Human Molecular Genetics*, 14(6), pp. 845–857. doi: 10.1093/hmg/ddi078.

Lefebvre, S., Bürglen, L., Reboullet, S., Clermont, O., Burlet, P., Viollet, L., Benichou, B., Cruaud, C., Millasseau, P. and Zeviani,

M. (1995) ‘Identification and characterization of a spinal muscular atrophy-determining gene.’, *Cell*, 80(1), pp. 155–65. Available at: http://www.ncbi.nlm.nih.gov/pubmed/7813012 (Accessed: 20 December 2016).

Li, H., Hsieh-Li, H. M., Chang, J.-G., Jong, Y.-J., Wu, M.-H., Wang, N. M. and Tsai, C. H. (2000) ‘A mouse model for spinal muscular atrophy.’, *Nature Genetics*, 24(1), pp. 66–70. doi: 10.1038/71709.

Lim, S. R. and Hertel, K. J. (2001) ‘Modulation of survival motor neuron pre-mRNA splicing by inhibition of alternative 3’ splice site pairing.’, *The Journal of biological chemistry*, 276(48), pp. 45476–83. doi: 10.1074/jbc.M107632200.

Ling, K. K. Y., Gibbs, R. M., Feng, Z. and Ko, C.-P. (2012) ‘Severe neuromuscular denervation of clinically relevant muscles in a mouse model of spinal muscular atrophy’, *Human Molecular Genetics*, 21(1), pp. 185–195. doi: 10.1093/hmg/ddr453.

Liu, Q. and Dreyfuss, G. (1996) ‘A novel nuclear structure containing the survival of motor neurons protein.’, *The EMBO journal*. European Molecular Biology Organization, 15(14), pp. 3555–65. Available at: http://www.ncbi.nlm.nih.gov/pubmed/8670859 (Accessed: 20 December 2016).

Lorson, C. L., Hahnen, E., Androphy, E. J. and Wirth, B. (1999) ‘A single nucleotide in the SMN gene regulates splicing and is responsible for spinal muscular atrophy.’, *Proceedings of the National Academy of Sciences of the United States of America*, 96(11), pp. 6307–11. doi: 10.1073/pnas.96.11.6307.

Lotti, F., Imlach, W. L., Saieva, L., Beck, E. S., Hao, L. T., Li, D. K., Jiao, W., Mentis, G. Z., Beattie, C. E., McCabe, B. D. and Pellizzoni, L. (2012) ‘An SMN-Dependent U12 Splicing Event Essential for Motor Circuit Function’, *Cell*, 151(2), pp. 440–454. doi: 10.1016/j.cell.2012.09.012.

Markowitz, J. A., Tinkle, M. B., Fischbeck, K. H., Andreassi, C., Jarecki, J., Zhou, J., Coovert, D. D., Monani, U. R., Chen, X., Battaglia, G., Princivalle, A., Forti, F., Lizier, C., Zeviani, M.,

Bingham, P., Shen, N., Rennert, H., Rorke, L. B., Black, A. W., Padilla, M., Brahe, C., Burglen, L., Lefebvre, S., Clermont, O., Burlet, P., Viollet, L., Cruaud, C., Burlet, P., Huber, C., Bertrandy, S., Ludosky, M. A., Zwaenepoel, I., Clermont, O., Chang, J. G., Hsieh -Li, H., Jong, Y.
D., Le, T., McAndrew, P., Strasswimmer, J., Crawford, T., Mendell, J., Crawford, T. O., Cusco, I., Barcelo, M. J., Soler, C., Parra, J., Baiget, M., Tizzano, E., Daniels, G., Pettigrew, R., Thornhill, A., Abbs, S., Lashwood, A., O'Mahoney, F., DeVriendt, K., Lammens, M., Schollen, E., Hole, C. Van, Dom, R., Devlieger, H., Dreesen, J. C., Bras, M., Die -Smulders, C. de
Evers, J. L., Emery, A. E. H., Falsaperla, R., Romeo, G., Giorgio, A. Di, Pavone, P., Parano, E., Connolly, A. M., Feldkotter, M., Schwarzer, V., Wirth, R., Wienker, T. F., Wirth, B., Fidzianska, A., Rafalowska, J., Field, M. J., Behrmen, R. E., Hsieh -Li, H. M.,
Chang, J. G., Jong, Y. I., Wu, M. H., Wang, N., Tsai, C. H., Iannaccone, S. T., Jones, S. L., Fallon, L. A., Knebel, A., Hudgings, C., Lorson, C., Androphy, E., Lorson, C., Hahnen, E., Androphy, E., Wirth, B., MacLeod, M. J., Taylor, J. E., Lunt, P. W., Mathew, C. G., Robb, S. A., Miller, R. G., Moore, D. H., Dronsky, V., Bradley, W., Barohn, R., Bryan, W., Milunsky, J. M., Cheney, S. M., Monani, U., Sendtner, M., Coovert, D., Parsons, D. W., Andreassi, C., Le, T., Munsat, T., Davies, K., Nicole, S., Diaz, C. C., Frugier, T., Melki, J., Ogino, S., Leonard, D. G. B., Rennert, H., Ewens, W. J., Wilson, R. B., Parker, D., Maddocks, I., Stern, L. M., Pellizzoni, L., Kataoka, N., Charroux, B., Dreyfuss, G. A., Scheffer, H., Cobben, J. M., Matthijs, G., Wirth, B., Schmalbruch, H., Hasse, G., Semprini, S., Tacconelli, A., Capon, F., Brancati, F., Dallapiccola, B., Novelli, G., Terns, M., Terns, R. M., Stiller, R. J., Lieberson, D., Herzlinger, R., Siddiqui, D., Laifer, S. A., Whetham, C. G., Volpe, J., Wirth, B., Wirth, B., Herz, M., Wetter, A., Moskau, S., Hahnen, E., Rudnik -Schoneborn, S
Schmidt, T., Hahnen, E., Rudnik -Schoneborn, S.
and Muller -Myhosk, B. (20
Neonate', *Journal of Obstetric, Gynecologic & Neonatal Nursing*. Elsevier, 33(1), pp. 12–20. doi: 10.1177/0884217503261125.

Martínez-Hernández, R., Bernal, S., Also-Rallo, E., Alías, L., Barceló, M., Hereu, M., Esquerda, J. E. and Tizzano, E. F. (2013) 'Synaptic defects in type I spinal muscular atrophy in human development', *The Journal of Pathology*, 229(1), pp. 49–61. doi:

10.1002/path.4080.

Martinez, T. L., Kong, L., Wang, X., Osborne, M. A., Crowder, M. E., Van Meerbeke, J. P., Xu, X., Davis, C., Wooley, J., Goldhamer, D. J., Lutz, C. M., Rich, M. M. and Sumner, C. J. (2012) 'Survival Motor Neuron Protein in Motor Neurons Determines Synaptic Integrity in Spinal Muscular Atrophy', *Journal of Neuroscience*, 32(25), pp. 8703–8715. doi: 10.1523/JNEUROSCI.0204-12.2012.

Mattis, V. B., Bowerman, M., Kothary, R. and Lorson, C. L. (2008) 'A SMNΔ7 read-through product confers functionality to the SMNΔ7 protein', *Neuroscience Letters*, 442(1), pp. 54–58. doi: 10.1016/j.neulet.2008.06.059.

McWhorter, M. L., Monani, U. R., Burghes, A. H. M. and Beattie, C. E. (2003) 'Knockdown of the survival motor neuron (Smn) protein in zebrafish causes defects in motor axon outgrowth and pathfinding', *The Journal of Cell Biology*, 162(5), pp. 919–932. doi: 10.1083/jcb.200303168.

Melki, J., Sheth, P., Abdelhak, S., Burlet, P., Bachelot, M. F., Lathrop, M. G., Frezal, J. and Munnich, A. (1990) 'Mapping of acute (type I) spinal muscular atrophy to chromosome 5q12-q14. The French Spinal Muscular Atrophy Investigators.', *Lancet (London, England)*, 336(8710), pp. 271–3. Available at: http://www.ncbi.nlm.nih.gov/pubmed/1973971 (Accessed: 20 December 2016).

Mercuri, E., Bertini, E., Messina, S., Solari, A., D'Amico, A., Angelozzi, C., Battini, R., Berardinelli, A., Boffi, P., Bruno, C., Cini, C., Colitto, F., Kinali, M., Minetti, C., Mongini, T., Morandi, L., Neri, G., Orcesi, S., Pane, M., Pelliccioni, M., Pini, A., Tiziano, F. D., Villanova, M., Vita, G. and Brahe, C. (2007) 'Randomized, double-blind, placebo-controlled trial of phenylbutyrate in spinal muscular atrophy', *Neurology*, 68(1), pp. 51–55. doi: 10.1212/01.wnl.0000249142.82285.d6.

Miguel-Aliaga, I., Culetto, E., Walker, D. S., Baylis, H. A., Sattelle, D. B. and Davies, K. E. (1999) 'The Caenorhabditis elegans orthologue of the human gene responsible for spinal muscular atrophy is a maternal product critical for germline maturation and

embryonic viability.', *Human molecular genetics*, 8(12), pp. 2133–43. Available at: http://www.ncbi.nlm.nih.gov/pubmed/10545592 (Accessed: 20 December 2016).

Monani, U. R., Coovert, D. D. and Burghes, A. H. (2000) 'Animal models of spinal muscular atrophy.', *Human molecular genetics*, 9(16), pp. 2451–7. Available at: http://www.ncbi.nlm.nih.gov/pubmed/11005801 (Accessed: 20 December 2016).

Monani, U. R., Lorson, C. L., Parsons, D. W., Prior, T. W., Androphy, E. J., Burghes, A. H. and McPherson, J. D. (1999) 'A single nucleotide difference that alters splicing patterns distinguishes the SMA gene SMN1 from the copy gene SMN2.', *Human molecular genetics*, 8(7), pp. 1177–83. Available at: http://www.ncbi.nlm.nih.gov/pubmed/10369862 (Accessed: 20 December 2016).

Murray, L. M., Comley, L. H., Thomson, D., Parkinson, N., Talbot, K. and Gillingwater, T. H. (2007) 'Selective vulnerability of motor neurons and dissociation of pre- and post-synaptic pathology at the neuromuscular junction in mouse models of spinal muscular atrophy', *Human Molecular Genetics*, 17(7), pp. 949–962. doi: 10.1093/hmg/ddm367.

Narver, H. L., Kong, L., Burnett, B. G., Choe, D. W., Bosch-Marcé, M., Taye, A. A., Eckhaus, M. A. and Sumner, C. J. (2008) 'Sustained improvement of spinal muscular atrophy mice treated with trichostatin a plus nutrition', *Annals of Neurology*, 64(4), pp. 465–470. doi: 10.1002/ana.21449.

Oprea, G. E., Krober, S., McWhorter, M. L., Rossoll, W., Muller, S., Krawczak, M., Bassell, G. J., Beattie, C. E. and Wirth, B. (2008) 'Plastin 3 Is a Protective Modifier of Autosomal Recessive Spinal Muscular Atrophy', *Science*, 320(5875), pp. 524–527. doi: 10.1126/science.1155085.

Otter, S., Grimmler, M., Neuenkirchen, N., Chari, A., Sickmann, A. and Fischer, U. (2007) 'A comprehensive interaction map of the human survival of motor neuron (SMN) complex.', *The Journal of biological chemistry*, 282(8), pp. 5825–33. doi:

10.1074/jbc.M608528200.

Park, G.-H., Maeno-Hikichi, Y., Awano, T., Landmesser, L. T. and Monani, U. R. (2010) 'Reduced Survival of Motor Neuron (SMN) Protein in Motor Neuronal Progenitors Functions Cell Autonomously to Cause Spinal Muscular Atrophy in Model Mice Expressing the Human Centromeric (SMN2) Gene', *Journal of Neuroscience*, 30(36), pp. 12005–12019. doi: 10.1523/JNEUROSCI.2208-10.2010.

Passini, M. A., Bu, J., Richards, A. M., Kinnecom, C., Sardi, S. P., Stanek, L. M., Hua, Y., Rigo, F., Matson, J., Hung, G., Kaye, E. M., Shihabuddin, L. S., Krainer, A. R., Bennett, C. F. and Cheng, S. H. (2011) 'Antisense Oligonucleotides Delivered to the Mouse CNS Ameliorate Symptoms of Severe Spinal Muscular Atrophy', *Science Translational Medicine*, 3(72), p. 72ra18-72ra18. doi: 10.1126/scitranslmed.3001777.

Passini, M. A., Bu, J., Roskelley, E. M., Richards, A. M., Sardi, S. P., O'Riordan, C. R., Klinger, K. W., Shihabuddin, L. S. and Cheng, S. H. (2010) 'CNS-targeted gene therapy improves survival and motor function in a mouse model of spinal muscular atrophy', *Journal of Clinical Investigation*, 120(4), pp. 1253–1264. doi: 10.1172/JCI41615.

Pearn, J. (1978) 'Incidence, prevalence, and gene frequency studies of chronic childhood spinal muscular atrophy.', *Journal of medical genetics*, 15(6), pp. 409–13. doi: 10.1136/jmg.15.6.409.

Piazzon, N., Rage, F., Schlotter, F., Moine, H., Branlant, C. and Massenet, S. (2008) 'In vitro and in cellulo evidences for association of the survival of motor neuron complex with the fragile X mental retardation protein.', *The Journal of biological chemistry*. American Society for Biochemistry and Molecular Biology, 283(9), pp. 5598–610. doi: 10.1074/jbc.M707304200.

Prior, T. W., Snyder, P. J., Rink, B. D., Pearl, D. K., Pyatt, R. E., Mihal, D. C., Conlan, T., Schmalz, B., Montgomery, L., Ziegler, K., Noonan, C., Hashimoto, S. and Garner, S. (2010) 'Newborn and carrier screening for spinal muscular atrophy', *American Journal of Medical Genetics, Part A*, 152(7), pp. 1608–1616. doi:

10.1002/ajmg.a.33474.

Rage, F., Boulisfane, N., Rihan, K., Neel, H., Gostan, T., Bertrand, E., Bordonne, R. and Soret, J. (2013) 'Genome-wide identification of mRNAs associated with the protein SMN whose depletion decreases their axonal localization', *RNA*, 19(12), pp. 1755–1766. doi: 10.1261/rna.040204.113.

Rajendra, T. K., Gonsalvez, G. B., Walker, M. P., Shpargel, K. B., Salz, H. K. and Matera, A. G. (2007) 'A Drosophila melanogaster model of spinal muscular atrophy reveals a function for SMN in striated muscle.', *The Journal of cell biology*, 176(6), pp. 831–41. doi: 10.1083/jcb.200610053.

Rezania, K. and Roos, R. (2013) 'Spinal cord: motor neuron diseases.', *Neurol Clin.*, Feb;31((1)), pp. 219–39. Available at: https://www.ncbi.nlm.nih.gov/pubmed/23186902.

Riessland, M., Ackermann, B., Forster, A., Jakubik, M., Hauke, J., Garbes, L., Fritzsche, I., Mende, Y., Blumcke, I., Hahnen, E. and Wirth, B. (2010) 'SAHA ameliorates the SMA phenotype in two mouse models for spinal muscular atrophy', *Human Molecular Genetics*, 19(8), pp. 1492–1506. doi: 10.1093/hmg/ddq023.

Riessland, M., Brichta, L., Hahnen, E. and Wirth, B. (2006) 'The benzamide M344, a novel histone deacetylase inhibitor, significantly increases SMN2 RNA/protein levels in spinal muscular atrophy cells', *Human Genetics*, 120(1), pp. 101–110. doi: 10.1007/s00439-006-0186-1.

Rose, F. F., Mattis, V. B., Rindt, H. and Lorson, C. L. (2009) 'Delivery of recombinant follistatin lessens disease severity in a mouse model of spinal muscular atrophy', *Human Molecular Genetics*, 18(6), pp. 997–1005. doi: 10.1093/hmg/ddn426.

Rossoll, W., Jablonka, S., Andreassi, C., Kröning, A.-K., Karle, K., Monani, U. R. and Sendtner, M. (2003) 'Smn, the spinal muscular atrophy-determining gene product, modulates axon growth and localization of beta-actin mRNA in growth cones of motoneurons.', *The Journal of cell biology*. The Rockefeller University Press, 163(4), pp. 801–12. doi: 10.1083/jcb.200304128.

Rossoll, W., Kröning, A.-K., Ohndorf, U.-M., Steegborn, C., Jablonka, S. and Sendtner, M. (2002) 'Specific interaction of Smn, the spinal muscular atrophy determining gene product, with hnRNP-R and gry-rbp/hnRNP-Q: a role for Smn in RNA processing in motor axons?', *Human molecular genetics*, 11(1), pp. 93–105. Available at: http://www.ncbi.nlm.nih.gov/pubmed/11773003 (Accessed: 20 December 2016).

Rudnik-Schoneborn, S., Heller, R., Berg, C., Betzler, C., Grimm, T., Eggermann, T., Eggermann, K., Wirth, R., Wirth, B. and Zerres, K. (2008) 'Congenital heart disease is a feature of severe infantile spinal muscular atrophy', *Journal of Medical Genetics*, 45(10), pp. 635–638. doi: 10.1136/jmg.2008.057950.

de Ruijter, A. J. M., van Gennip, A. H., Caron, H. N., Kemp, S. and van Kuilenburg, A. B. P. (2003) 'Histone deacetylases (HDACs): characterization of the classical HDAC family.', *The Biochemical journal*, 370(Pt 3), pp. 737–49. doi: 10.1042/BJ20021321.

Sanchez, G., Dury, A. Y., Murray, L. M., Biondi, O., Tadesse, H., El Fatimy, R., Kothary, R., Charbonnier, F., Khandjian, E. W. and Cote, J. (2013) 'A novel function for the survival motoneuron protein as a translational regulator', *Human Molecular Genetics*, 22(4), pp. 668–684. doi: 10.1093/hmg/dds474.

Schrank, B., Götz, R., Gunnersen, J. M., Ure, J. M., Toyka, K. V, Smith, A. G. and Sendtner, M. (1997) 'Inactivation of the survival motor neuron gene, a candidate gene for human spinal muscular atrophy, leads to massive cell death in early mouse embryos.', *Proceedings of the National Academy of Sciences of the United States of America*, 94(18), pp. 9920–5. Available at: http://www.ncbi.nlm.nih.gov/pubmed/9275227 (Accessed: 20 December 2016).

Schreml, J., Riessland, M., Paterno, M., Garbes, L., Roßbach, K., Ackermann, B., Krämer, J., Somers, E., Parson, S. H., Heller, R., Berkessel, A., Sterner-Kock, A. and Wirth, B. (2013) 'Severe SMA mice show organ impairment that cannot be rescued by therapy with the HDACi JNJ-26481585', *European Journal of Human Genetics*, 21(6), pp. 643–652. doi: 10.1038/ejhg.2012.222.

Shababi, M., Habibi, J., Yang, H. T., Vale, S. M., Sewell, W. A. and Lorson, C. L. (2010) 'Cardiac defects contribute to the pathology of spinal muscular atrophy models', *Human Molecular Genetics*, 19(20), pp. 4059–4071. doi: 10.1093/hmg/ddq329.

Somers, E., Lees, R. D., Hoban, K., Sleigh, J. N., Zhou, H., Muntoni, F., Talbot, K., Gillingwater, T. H. and Parson, S. H. (2016) 'Vascular Defects and Spinal Cord Hypoxia in Spinal Muscular Atrophy', *Annals of Neurology*, 79(2), pp. 217–230. doi: 10.1002/ana.24549.

Strahl, B. D. and Allis, C. D. (2000) 'The language of covalent histone modifications', *Nature*, 403(6765), pp. 41–45. doi: 10.1038/47412.

Stratigopoulos, G., Lanzano, P., Deng, L., Guo, J., Kaufmann, P., Darras, B., Finkel, R., Tawil, R., McDermott, M. P., Martens, W., Devivo, D. C. and Chung, W. K. (2010) 'Association of plastin 3 expression with disease severity in spinal muscular atrophy only in postpubertal females.', *Archives of neurology*, 67(10), pp. 1252–6. doi: 10.1001/archneurol.2010.239.

Sugarman, E. A., Nagan, N., Zhu, H., Akmaev, V. R., Zhou, Z., Rohlfs, E. M., Flynn, K., Hendrickson, B. C., Scholl, T., Sirko-Osadsa, D. A. and Allitto, B. A. (2012) 'Pan-ethnic carrier screening and prenatal diagnosis for spinal muscular atrophy: clinical laboratory analysis of >72,400 specimens.', *European journal of human genetics : EJHG*. Nature Publishing Group, 20(1), pp. 27–32. doi: 10.1038/ejhg.2011.134.

Sumner, C. J., Huynh, T., Markowitz, J., Perhac, J. S., Hill, B., Coovert, D., Chen, X., Jarecki, J., Burghes, A., Taylor, J. P. and Fischbeck, K. (2003) 'Valproic acid increases SMN levels in spinal muscular atrophy patient cells.', *Annals of neurology*, 54(5), pp. 647–54. doi: 10.1002/ana.10743.

Sumner, C. J., Wee, C. D., Warsing, L. C., Choe, D. W., Ng, A. S., Lutz, C. and Wagner, K. R. (2009) 'Inhibition of myostatin does not ameliorate disease features of severe spinal muscular atrophy mice', *Human Molecular Genetics*, 18(17), pp. 3145–3152. doi: 10.1093/hmg/ddp253.

Swoboda, K. J., Kissel, J. T., Crawford, T. O., Bromberg, M. B., Acsadi, G., D'Anjou, G., Krosschell, K. J., Reyna, S. P., Schroth, M. K., Scott, C. B. and Simard, L. R. (2007) 'Perspectives on clinical trials in spinal muscular atrophy.', *Journal of child neurology*. NIH Public Access, 22(8), pp. 957–66. doi: 10.1177/0883073807305665.

Swoboda, K. J., Scott, C. B., Crawford, T. O., Simard, L. R., Reyna, S. P., Krosschell, K. J., Acsadi, G., Elsheik, B., Schroth, M. K., D'Anjou, G., LaSalle, B., Prior, T. W., Sorenson, S. L., Maczulski, J. A., Bromberg, M. B., Chan, G. M. and Kissel, J. T. (2010) 'SMA CARNI-VAL Trial Part I: Double-Blind, Randomized, Placebo-Controlled Trial of L-Carnitine and Valproic Acid in Spinal Muscular Atrophy', *PLoS ONE*. Edited by I. Boutron, 5(8), p. e12140. doi: 10.1371/journal.pone.0012140.

Thomson, S. R., Nahon, J. E., Mutsaers, C. A., Thomson, D., Hamilton, G., Parson, S. H. and Gillingwater, T. H. (2012) 'Morphological Characteristics of Motor Neurons Do Not Determine Their Relative Susceptibility to Degeneration in a Mouse Model of Severe Spinal Muscular Atrophy', *PLoS ONE*. Edited by H. Cai, 7(12), p. e52605. doi: 10.1371/journal.pone.0052605.

Thurmond, J., Butchbach, M. E. R., Palomo, M., Pease, B., Rao, M., Bedell, L., Keyvan, M., Pai, G., Mishra, R., Haraldsson, M., Andresson, T., Bragason, G., Thosteinsdottir, M., Bjornsson, J. M., Coovert, D. D., Burghes, A. H. M., Gurney, M. E. and Singh, J. (2008) 'Synthesis and Biological Evaluation of Novel 2,4-Diaminoquinazoline Derivatives as *SMN2* Promoter Activators for the Potential Treatment of Spinal Muscular Atrophy', *Journal of Medicinal Chemistry*, 51(3), pp. 449–469. doi: 10.1021/jm061475p.

Tiziano, F. D., Lomastro, R., Pinto, A. M., Messina, S., D'Amico, A., Fiori, S., Angelozzi, C., Pane, M., Mercuri, E., Bertini, E., Neri, G. and Brahe, C. (2010a) 'Salbutamol increases survival motor neuron (SMN) transcript levels in leucocytes of spinal muscular atrophy (SMA) patients: relevance for clinical trial design', *Journal of Medical Genetics*, 47(12), pp. 856–858. doi: 10.1136/jmg.2010.080366.

Tiziano, F. D., Lomastro, R., Pinto, A. M., Messina, S., D'Amico,

A., Fiori, S., Angelozzi, C., Pane, M., Mercuri, E., Bertini, E., Neri, G. and Brahe, C. (2010b) 'Salbutamol increases survival motor neuron (SMN) transcript levels in leucocytes of spinal muscular atrophy (SMA) patients: relevance for clinical trial design', *Journal of Medical Genetics*, 47(12), pp. 856–858. doi: 10.1136/jmg.2010.080366.

Tsai, L.-K., Tsai, M.-S., Ting, C.-H. and Li, H. (2008) 'Multiple therapeutic effects of valproic acid in spinal muscular atrophy model mice', *Journal of Molecular Medicine*, 86(11), pp. 1243–1254. doi: 10.1007/s00109-008-0388-1.

Tsuiji, H., Iguchi, Y., Furuya, A., Kataoka, A., Hatsuta, H., Atsuta, N., Tanaka, F., Hashizume, Y., Akatsu, H., Murayama, S., Sobue, G. and Yamanaka, K. (2013) 'Spliceosome integrity is defective in the motor neuron diseases ALS and SMA', *EMBO Molecular Medicine*, 5(2), pp. 221–234. doi: 10.1002/emmm.201202303.

Valori, C. F., Ning, K., Wyles, M., Mead, R. J., Grierson, A. J., Shaw, P. J. and Azzouz, M. (2010) 'Systemic Delivery of scAAV9 Expressing SMN Prolongs Survival in a Model of Spinal Muscular Atrophy', *Science Translational Medicine*, 2(35), p. 35ra42-35ra42. doi: 10.1126/scitranslmed.3000830.

Vrbova, G. (2008) 'Spinal muscular atrophy: motoneurone or muscle disease?', *Neuromuscular disorders : NMD*, 18(1), pp. 81–2. Available at: http://www.ncbi.nlm.nih.gov/pubmed/18365338 (Accessed: 20 December 2016).

Walker, M. P., Rajendra, T. K., Saieva, L., Fuentes, J. L., Pellizzoni, L. and Matera, A. G. (2008) 'SMN complex localizes to the sarcomeric Z-disc and is a proteolytic target of calpain', *Human Molecular Genetics*, 17(21), pp. 3399–3410. doi: 10.1093/hmg/ddn234.

Wang, C. H. and Lunn, M. R. (2008) 'Spinal muscular atrophy: advances in research and consensus on care of patients.', *Current treatment options in neurology*, 10(6), pp. 420–8. Available at: http://www.ncbi.nlm.nih.gov/pubmed/18990310 (Accessed: 20 December 2016).

Wen, H. L., Lin, Y. T., Ting, C. H., Lin-Chao, S., Li, H. and Hsieh-

Li, H. M. (2010) 'Stathmin, a microtubule-destabilizing protein, is dysregulated in spinal muscular atrophy', *Human Molecular Genetics*, 19(9), pp. 1766–1778. doi: 10.1093/hmg/ddq058.

Williams, J. H., Schray, R. C., Patterson, C. A., Ayitey, S. O., Tallent, M. K. and Lutz, G. J. (2009) 'Oligonucleotide-Mediated Survival of Motor Neuron Protein Expression in CNS Improves Phenotype in a Mouse Model of Spinal Muscular Atrophy', *Journal of Neuroscience*, 29(24), pp. 7633–7638. doi: 10.1523/JNEUROSCI.0950-09.2009.

Wirth, B., Brichta, L. and Hahnen, E. (2006) 'Spinal muscular atrophy and therapeutic prospects.', *Progress in molecular and subcellular biology*, 44, pp. 109–32. Available at: http://www.ncbi.nlm.nih.gov/pubmed/17076267 (Accessed: 20 December 2016).

Wu, Y., Sun, H., Yakar, S. and LeRoith, D. (2009) 'Elevated levels of insulin-like growth factor (IGF)-I in serum rescue the severe growth retardation of IGF-I null mice.', *Endocrinology*. The Endocrine Society, 150(9), pp. 4395–403. doi: 10.1210/en.2009-0272.

Wyatt, T. J. and Keirstead, H. S. (2010) 'Stem cell-derived neurotrophic support for the neuromuscular junction in spinal muscular atrophy', *Expert Opinion on Biological Therapy*, 10(11), pp. 1587–1594. doi: 10.1517/14712598.2010.529895.

Yamazaki, T., Chen, S., Yu, Y., Yan, B., Haertlein, T. C., Carrasco, M. A., Tapia, J. C., Zhai, B., Das, R., Lalancette-Hebert, M., Sharma, A., Chandran, S., Sullivan, G., Nishimura, A. L., Shaw, C. E., Gygi, S. P., Shneider, N. A., Maniatis, T. and Reed, R. (2012) 'FUS-SMN Protein Interactions Link the Motor Neuron Diseases ALS and SMA', *Cell Reports*, 2(4), pp. 799–806. doi: 10.1016/j.celrep.2012.08.025.

Zerres, K. and Rudnik-Schöneborn, S. (1995) 'Natural history in proximal spinal muscular atrophy. Clinical analysis of 445 patients and suggestions for a modification of existing classifications.', *Archives of neurology*, 52(5), pp. 518–23. Available at: http://www.ncbi.nlm.nih.gov/pubmed/7733848 (Accessed: 20

December 2016).

Zhang, H. L., Pan, F., Hong, D., Shenoy, S. M., Singer, R. H. and Bassell, G. J. (2003) 'Active transport of the survival motor neuron protein and the role of exon-7 in cytoplasmic localization.', *The Journal of neuroscience : the official journal of the Society for Neuroscience*, 23(16), pp. 6627–37. Available at: http://www.ncbi.nlm.nih.gov/pubmed/12878704 (Accessed: 20 December 2016).

Zhang, H., Xing, L., Rossoll, W., Wichterle, H., Singer, R. H. and Bassell, G. J. (2006) 'Multiprotein complexes of the survival of motor neuron protein SMN with Gemins traffic to neuronal processes and growth cones of motor neurons.', *The Journal of neuroscience : the official journal of the Society for Neuroscience*. NIH Public Access, 26(33), pp. 8622–32. doi: 10.1523/JNEUROSCI.3967-05.2006.

Zhang, Z., Lotti, F., Dittmar, K., Younis, I., Wan, L., Kasim, M. and Dreyfuss, G. (2008) 'SMN Deficiency Causes Tissue-Specific Perturbations in the Repertoire of snRNAs and Widespread Defects in Splicing', *Cell*, 133(4), pp. 585–600. doi: 10.1016/j.cell.2008.03.031.